LABORATORIA
N.V. PHILIPS' GLOEILAMPENFABRIEKEN
EINDHOVEN (HOLLAND)

THERMIONIC EMISSION

BY

A. VENEMA

Reprinted from: Handbook of Vacuum Physics, Vol. 2.
Physical Electronics, p. 179-298, 1966.

HANDBOOK OF VACUUM PHYSICS

VOLUME 2

PHYSICAL ELECTRONICS

PARTS 2 and 3

HANDBOOK OF VACUUM PHYSICS

VOLUME 2

PHYSICAL ELECTRONICS

EDITED BY

A. H. BECK
Engineering Laboratory, Cambridge

Part 2

A. VENEMA—Thermionic Emission

Part 3

D. J. GIBBONS—Secondary Electron Emission

PERGAMON PRESS

OXFORD · LONDON · EDINBURGH · NEW YORK
TORONTO · PARIS · BRAUNSCHWEIG

Pergamon Press Ltd., Headington Hill Hall, Oxford
4 & 5 Fitzroy Square, London, W.1
Pergamon Press (Scotland) Ltd., 2 & 3 Teviot Place, Edinburgh 1
Pergamon Press Inc., 44–01 21st Street, Long Island City, New York 11101
Pergamon of Canada, Ltd., 6 Adelaide Street East, Toronto, Ontario
Pergamon Press S.A.R.L., 24 rue des Écoles, Paris 5e
Friedr. Vieweg und Sohn Verlag, Postfach 185, 33 Braunschweig, West Germany

First edition 1966

Library of Congress Catalog Card No. 63–21443

Set in Monotype Times 10 on 12 pt.
and printed in Great Britain by
Bell and Bain Ltd., Glasgow

(2469/66)

CONTENTS

PART 2

THERMIONIC EMISSION

A. VENEMA

Philips Research Laboratories,
N.V. Philips' Gloeilampenfabrieken, Eindhoven, Netherlands

PART 2

THERMIONIC EMISSION

A. VENEMA

Philips Research Laboratories,
N.V. Philips' Gloeilampenfabrieken, Eindhoven, Netherlands

GLOSSARY OF SYMBOLS

a	Thermionic constant (eq. 20, p. 222)
A	Universal thermionic constant $= 1.2 \times 10^6$ A/m^2 °K^2 (p. 202)
A^*	Apparent thermionic constant (p. 224)
A_R	Richardson value of thermionic constant (eq. 21, p. 223)
C_{ci}	Cathode interface capacitance (p. 237)
d	Cathode–anode distance in a plane-parallel diode (p. 208)
D	Transmission coefficient of the surface potential barrier for an electron $= 1 - r$ (p. 204)
e	Electronic charge $= 1.602 \times 10^{-19}$C (p. 198)
E	Total electron energy (p. 184)
E	Electric field (p. 199)
E_a	Electron affinity (p. 203)
$-E_d$	Donor energy (p. 191)
E_F	Fermi energy (p. 187)
f	Frequency (p. 215)
$f(E)$	Fermi–Dirac distribution function (p. 187)
F	Electrical force (p. 197)
g_m	Transconductance $= \left(\frac{\partial I_a}{\partial V_{g1}}\right)_{V_a}$ (p. 234)
G	Thermodynamic potential, Gibbs function, Gibbs free energy (p. 188)
h	Planck's constant $= 6.625 \times 10^{-34}$Ws^2 (p. 184)
I_c	Cathode current (p. 234)
I_a	Anode current (p. 234)
J	Current density (p. 192)
J_{ret}	Retarding field current density (p. 207)

J_{sat} Saturated current density (p. 202)
J_{sp} Space charge current density (p. 207)
$\boldsymbol{k}$ Wave vector (p. 184)
k Boltzmann constant = 1.380×10^{-23} Ws/°K (p. 187)
m Electron rest mass = 9.108×10^{-31} kg (p. 190)
m_n^* Effective electron mass (p. 186)
m_p^* Effective hole mass (p. 186)
n Number density (p. 190)
n_n Number density of electrons (p. 193)
n_p Number density of holes (p. 193)
n_a Number density of donors (p. 191)
p Electric dipole moment (p. 194)
$\boldsymbol{p}$ Electron momentum
$= \frac{h}{2\pi} \boldsymbol{k}$ (p. 184)
p Pressure (p. 188)
P Power (p. 205)
Q Electric charge (p. 188)
r Reflection coefficient of the surface potential barrier for an electron (p. 201)
R Gas constant = 8.31 J/mole °K
R_c Cathode resistance (p. 234)
R_{ci} Cathode interface resistance (p. 237)
S Entropy (p. 188)
T Absolute temperature (p. 187)
$u_p(\boldsymbol{r})$ Periodic function of p, with the same periodicity as the crystal lattice (p. 184)
U Internal energy (p. 188)
v Velocity (p. 192)
V Volume (p. 188)
V_a Anode voltage (p. 207)
V_m Voltage of the space charge minimum (p. 207)
Γ^2 Mean square smoothing factor (p. 216)
δ Dipole distance (p. 194)
ε_0 Permittivity of vacuum = 8.854×10^{-12} F/m
ε Permittivity (p. 195)
μ_n Mobility of electrons (p. 193)
μ_p Mobility of holes (p. 193)
μ Chemical potential (p. 189)
μ_e Electrochemical potential (p. 189)

ρ Charge density (p. 195)
σ Electrical conductivity (p. 193)
σ Surface charge density (p. 194)
φ Work function (p. 198)
φ_0 Work function at $T = 0°K$ (p. 221)
φ^0 Work function in the absence of an externally applied electric field (p. 200)
φ_a Anode work function (p. 207)
φ_E Effective work function (eq. 22, p. 224)
φ_c Cathode work function (p. 207)
φ_R Richardson value of the work function (eq. 21, p. 223)
ϕ Work factor (eq. 20, p. 222)
ϕ Electrical potential (p. 188)
ψ Wave function (p. 184)

A. THEORY OF THERMIONIC CATHODES

1. The band theory of solids

The behaviour of an electron in an ideal crystal of limited size is described quantum-mechanically by means of its wave function $\psi\,(x, y, z, t)$*. In the Bloch scheme, which is based on a one-electron approximation, this function is a solution of the wave equation or Schrödinger equation in which the potential energy is a periodic function of the coordinates x, y, z, with a period corresponding to that of the crystal lattice. It appears that the solution ψ represents an electron wave with wavelength $h/\boldsymbol{p}$, h = Planck's constant, $\boldsymbol{p}$ = crystal momentum, and frequency E/h, E = total energy, modulated by a function $u_p(\boldsymbol{r})$ which is periodic in space, with the same periodicity as the lattice:

$$\psi = u_p(\boldsymbol{r}) \exp\left[2\pi i \left(\frac{\boldsymbol{p}}{h} \boldsymbol{r} - \frac{E}{h} t \right) \right]$$

In principle $u_p(\boldsymbol{r})$ can be expressed as a function of the coordinates x, y, z, of the momentum $\boldsymbol{p}$ or the wave vector $\boldsymbol{k} = 2\pi\boldsymbol{p}/h$ and of the energy E.

It can be shown that k can take a fixed number of different values, related to the interatomic distances and to the dimensions of the crystal. It further appears that physically significant solutions of $u_p(\boldsymbol{r})$ exist only in certain ranges of E values, called " allowed energy bands ". These bands can be considered as being the result of the co-operation of all atoms present in the crystal in their action on the electrons. In isolated atoms the allowed electron energies appear in discrete levels. When the atoms are brought together forming the ideal crystal, the electrons no longer belong to one particular atom, but to the whole crystal. Their possible energies, which are the same when the atoms are isolated, now combine to form energy bands. It may happen that particular values of allowed energies belong to different bands; the bands are then said to overlap. Figure 1 gives a schematic picture of the splitting of the electron energy levels of the free atoms into the energy bands of the crystal.

* Literature and references are found on pp. 291 *et sqq.*

So far only the possible quantum states for electrons have been considered. Whether these states are really occupied by electrons depends on various factors, e.g. the number of available electrons and the temperature. A particular quantum state can be occupied by two electrons because of the electron spin. In the absence of current flow through the crystal the movement of the electrons is such that the net flow of all electrons together is zero. If all quantum states of an energy band are occupied by electrons, the application of a small electric field cannot cause a change in energy and velocity of the ensemble of electrons. Therefore no electrical conduction is

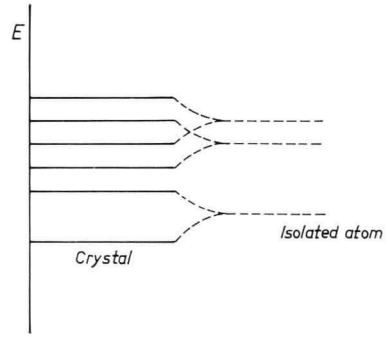

FIG. 1. The energy levels in the isolated atoms split into bands when the atoms combine to form a crystal.

observed under these circumstances. Electrical conduction is observed however, if the possible energy levels in a band are only partly occupied by electrons.

Regarding the occupation of the quantum states of the energy bands, one can distinguish between the following possibilities:

(*a*) The highest filled energy band is located at an appreciable distance from the next higher band. Even at high temperatures the number of electrons which have been raised into the empty band is so small that the conductivity remains negligible. The crystal is an insulator.

(*b*) The highest filled band is close to the next higher band. In this case semiconducting behaviour is observed. At very low temperatures the crystal behaves as an insulator but at higher temperatures electrons are raised from the filled band into the originally empty band, leaving a partly filled band. Now

conduction can take place. How great the conductivity will be depends among other things on the width of the band gap and the temperature.

(*c*) The highest energy band is not completely filled or several bands overlap. In this case the crystal shows metallic behaviour.

In the theory which describes the movement of an electron in an ideal crystal lattice the average velocity of the electron can be expressed in terms of the properties of the wave functions. Also the effect of an applied electrical field can be treated in this way and it can be shown that the electron behaves as a particle with an effective mass m_n^* which is generally different from the rest mass of the electron. Physically an electron with a large mass m_n^* can be interpreted as an electron which interacts strongly with the lattice and which hardly reacts to an applied electric field.

If a band is not completely filled, which is equivalent to saying that holes are present in the upper part of the band, electrical conductivity due to these holes will be observed. Although also in this case the electrons are responsible for the conduction, a detailed analysis shows that this conductivity can be described as due to the movement of the holes which act as particles with a positive charge e and an effective mass m_p^*. The electrical conductivity observed under these circumstances is called p-type conductivity, in contradistinction to n-type conductivity, found with negatively charged carriers.

So far only pure ideal single crystals have been considered. Electrical conductivity in semiconducting crystals of this kind, called intrinsic conductivity, can only be obtained by lifting electrons from the highest filled band, the valency band, into the next empty one, the conduction band. This can be done by a temperature increase. However, conductivity can be strongly influenced by the presence of impurities, e.g. foreign atoms built into the lattice, an excess of one of the constituents, interstitials, etc. The impurities may give rise to possible electronic states with energy levels situated in the forbidden gap. When such a level is occupied by an electron at absolute zero temperature and is located close to the conduction band, a temperature increase may raise the electron into this band. In this case the impurity atom is said to be a donor. It is also possible that the impurity level is unoccupied at absolute zero and is located close to the filled band. At higher temperatures it may then be occupied by an electron from the filled band which leaves a hole

behind. This impurity centre is called an acceptor. Both donor and acceptor become ionized and the ionization energies may be estimated using a Bohr model. In order that the impurities should give rise to a reasonable conductivity at room temperature the ionization energy must be of the order of kT at 300°K, which is 2.6×10^{-2} eV.

2. Fermi–Dirac statistics

It has already been noted that a possible quantum state need not be occupied by an electron. Whether this is the case depends upon the number of electrons which are available and on the temperature. The law which governs the distribution of the electrons over the available states is the Fermi–Dirac distribution law. It is derived in books on statistical mechanics and it answers the question what must be the most probable population of the energy levels, given the total number of available electrons and their total energy.

The result is:

$$f(E) = 1 \Big/ \exp\left[\left(\frac{E - E_F}{kT}\right) + 1\right] \tag{1}$$

where $f(E)$ = the probability that an electron has the energy E, E_F = Fermi energy, k = Boltzmann's constant, and T = absolute temperature.

The value of the Fermi energy E_F is derived from the consideration that

$$\int_{-\infty}^{+\infty} N(E)f(E)\mathrm{d}E = N_{\text{tot}} = \text{total number of electrons}$$

in which $N(E)$ represents the number of possible states with energies between E and $E + \mathrm{d}E$. The value of E_F is completely determined by the density distribution of states $N(E)$ and the temperature. The function $f(E)$ is represented in Fig. 2 for various values of E_F/kT. Mathematically E_F represents the energy level for which the probability of being occupied is $\frac{1}{2}$. For metals, this energy E_F has also a physical meaning because electrons with this energy are really present. In semiconductors, however, the Fermi energy usually lies in the forbidden gap, so that there are no electrons with this energy. In impure semiconductors the impurity levels contribute to fixing the Fermi energy.

Another aspect of the Fermi energy, which is of great importance, is its equivalence to the thermodynamic potential per electron or the

electrochemical potential of the ensemble of electrons under consideration. This relation is also derived from statistical mechanics. The thermodynamic potential of a closed system of uncharged particles is given by the expression:

$$G = U - TS + pV$$

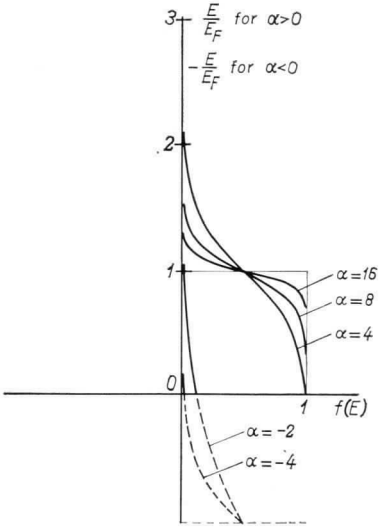

FIG. 2. The Fermi distribution function $f(E)$ as a function of E/E_F for various values of $\alpha = E_F/KT$.

in which

G = thermodynamic potential or Gibbs free energy
U = internal energy
S = entropy
p = pressure of the system
V = volume of the system.

The equivalent expression for a system of charged particles reads:

$$G = U - TS + pV + Q\phi$$

with Q = total charge = $-Ne$ for electrons
ϕ = electrical potential of the system.

If now dN electrons are added, while keeping the temperature, the pressure and the potential constant, the change in thermodynamic potential can be written as:

$$dG = \mu dN - e\phi dN$$

The quantity

$$\left(\frac{\partial G}{\partial N}\right)_{p,T,\phi} = \mu - e\phi = \mu_e$$

is called the electrochemical potential while the quantity μ, which is of importance for systems of uncharged particles, is referred to as the chemical potential. For a system of charged particles the important relation holds:

$$\mu_e = E_F$$

In thermodynamics it is shown that the thermodynamic potential for a closed system always tends to a minimum. If, therefore, two systems with electrons are brought into contact and we transfer, after equilibrium has been reached, electrons from one system to the other, the change $dG = dG_1 + dG_2$ must be zero. (dG_1 represents the change in thermodynamical potential of system 1, dG_2 the same for system 2.) As $dN_1 = -dN_2$ it follows immediately that

$$\mu_{e_1} = \mu_{e_2}$$

So two systems of electrons are in equilibrium if the Fermi levels E_F are the same. Also, in a single system in which potential differences occur, for example in a conductor with space charge, the equilibrium situation is characterized by the same level of the Fermi energy throughout the system. The importance of the Fermi energy level for practical thermionic emitters is due to the fact that the ability of these cathodes to emit electrons is directly related to the position of the Fermi energy as will be explained in section 4. In section 3 it will be shown that the electrical conductivity of semiconductors is also governed by the Fermi energy.

The value of the Fermi energy E_F with reference to the bottom of the conduction band can be calculated fairly easily for metals in which the electrons that contribute to electrical conductivity may be considered as free. In phase space the volume occupied by a quantum state can be shown to be h^3. Therefore the number of quantum states is given by the expression:

$$\frac{1}{h^3}\int_{xyz}\int_{p_x p_y p_z} dx\,dy\,dz\,dp_x\,dp_y\,dp_z$$

The number of possible states for free electrons can be written as:

$$\frac{2}{h^3} \times V \int_p 4\pi p^2 \mathrm{d}p = \frac{V}{h^3} \times 4\pi(2m)^{3/2} \int_E E^{\frac{1}{2}} \mathrm{d}E = \int_E N(E)\mathrm{d}E$$

The number of possible states per unit volume in the energy interval E, $E + \mathrm{d}E$ will be denoted by $n(E)\mathrm{d}E$ and the total number of electrons per unit volume by n. Then the following relationship must hold:

$$n = \int n(E)f(E)\mathrm{d}E = \frac{1}{h^3} \times 4\pi(2m)^{3/2} \int_0^\infty \frac{E^{\frac{1}{2}}}{\exp\left[\left(\frac{E - E_F}{kT}\right) + 1\right]} \mathrm{d}E$$

At absolute zero temperature $f(E) = 1$ for $E < E_F$

$$f(E) = 0 \text{ for } E > E_F$$

So neglecting the influence of temperature:

$$n = \frac{4\pi}{h^3} (2m)^{3/2} \int^{(E_F)_0} E^{\frac{1}{2}} \mathrm{d}E$$

$(E_F)_0$ is the Fermi energy at zero temperature from which it follows that:

$$(E_F)_0 = \frac{h^2}{2m} \left(\frac{3n}{8\pi}\right)^{2/3}$$

At not too high temperatures, the calculation leads to:

$$E_F = (E_F)_0 \left[1 - \frac{\pi^2}{12} \left\{\frac{kT}{(E_F)_0}\right\}^2\right] \tag{2}$$

The calculation of the Fermi level in a semiconductor usually starts with the assumption of a certain model. If an intrinsic semiconductor is considered, i.e. a semiconductor in which impurities do not influence the electric conductivity, so that this conductivity can only be caused by thermal excitation of electrons from the valency band into the conduction band, the Fermi energy can be calculated to lie exactly halfway between the bands at zero absolute temperature.

In general, both acceptor and donor levels will be present between the valency and the conduction band, some of which will be ionized

at temperatures above zero. Again, given the total number of electrons in the valency band and in the impurity levels, the value of the Fermi energy can be calculated from the Fermi–Dirac distribution function[1].

The simple model, proposed by A. H. Wilson[2], consisting of the conduction band and a donor level situated at a depth E_d below the band, will be discussed here in some detail as it has been used very extensively to interpret thermionic data. It is assumed in this model that the band gap is wide, so that the contribution of electrons excited from the valency band into the conduction band is negligible. The density of the donor levels is taken n_d per unit volume and their energy as $-E_d$. Strictly speaking, the impurity levels will occupy a small energy band at $-E_d$, but the width of this band will be neglected as this simplification does not alter the result significantly. At absolute zero temperature each donor level is occupied by one electron which at higher temperatures may be raised into the conduction band and will then be considered free. At zero temperature the conduction band is empty.

The number of electrons per unit volume, present at the donor energy level is given by:

$$\frac{n_d}{\exp\left(\dfrac{-E_d - E_F}{kT}\right) + 1}$$

The number of electrons per unit volume in the conduction band is given by (see p. 190):

$$\frac{1}{h^3}\, 4\pi(2m)^{3/2} \int_0^\infty \frac{E^{\frac{1}{2}}}{\exp\left(\dfrac{E - E_F}{kT}\right) + 1}\, \mathrm{d}E$$

Consequently the following relationship must hold:

$$\frac{n_d}{\exp\left(\dfrac{-E_d - E_F}{kT}\right) + 1} + \frac{4\pi}{h^3}\,(2m)^{3/2} \int_0^\infty \frac{E^{\frac{1}{2}}}{\exp\left(\dfrac{E - E_F}{kT}\right) + 1}\, \mathrm{d}E = n_d$$

From this equation the position of the Fermi level E_F can be calculated as a function of temperature.

If it is assumed that the Fermi level is located many times kT below the bottom of the conduction band, the integral can be written explicitly with the result:

$$n_d \left\{1 - \left[\exp\left(\frac{-E_d - E_F}{kT}\right) + 1\right]^{-1}\right\} = \frac{2}{h^3}(2\pi mkT)^{3/2} \exp\left(\frac{E_F}{kT}\right)$$

A further approximation is possible if it is assumed also that the distance from the Fermi level to the donor level is many times kT. It follows then that:

$$n_d \exp\left(\frac{-E_d - E_F}{kT}\right) = \frac{2}{h^3}(2\pi mkT)^{3/2} \exp\left(\frac{E_F}{kT}\right)$$

and

$$E_F = -\frac{E_d}{2} + \frac{kT}{2} \ln n_d \frac{h^3}{2(2\pi mkT)^{3/2}} \tag{3}$$

At zero temperature the Fermi energy level is situated exactly halfway between the conduction band and the donor level. It decreases continuously with increasing temperature except for a very small increase at very low temperatures.

3. The electrical conductivity

Electrical conductivity through solids can be caused by electrons in a partly filled energy band. The sign, which must be attributed to the charge carriers, may be positive or negative (see p. 186). In an ideal periodic crystal the electrons move without disturbance and the application of an electric field would result in a current which would increase indefinitely. As the result of the interaction of the charge carriers with certain lattice imperfections, which may be, for example, chemical impurities, dislocations or deviations from the perfect lattice structure due to the thermal movement of the atoms, the current reaches a certain finite value.

The current density J caused by charge carriers moving with a velocity v is given by:

$$\boldsymbol{J} = nev \tag{4}$$

n = number density.

The problem of determining the current density in a solid, flowing under the influence of an electric field E, with charge carriers moving

with different velocities in different directions, consists in the calculation of the average velocity or drift velocity $\bar{v}$. A rigorous treatment of the determination of the current density and the conductivity is beyond the scope of this treatise.

Often the conductivity is expressed by means of the mobility μ of the charge carriers, which is the drift velocity per unit field:

$$\mu = \frac{\bar{v}}{E}$$

The conductivity can now be written as:

$$\sigma = \frac{J}{E} = \frac{ne\bar{v}}{E} = ne\mu \tag{5}$$

As both electrons and holes can act as charge carriers the final expression becomes for semiconductors:

$$\sigma = n_n e\mu_n + n_p e\mu_p \tag{5a}$$

with n_n = number density of electrons
μ_n = mobility of electrons
n_p = number density of holes
μ_p = mobility of holes.

The determination of the mobility of the charge carriers in single crystals of barium oxide[3] and in alkaline earth oxide cathodes[4] contributes to a better understanding of the mechanism of operation of these cathodes. The values of n_n and n_p which appear in eq. (5a) are determined by the Fermi–Dirac distribution function. In the case of the Wilson model n_n is given by the expression:

$$n_n = n_d^{\frac{1}{2}} \frac{2^{\frac{1}{4}}(2\pi mkT)^{3/4}}{h^{3/2}} \exp\left(-\frac{E_d}{2kT}\right) \tag{6}$$

$$n_p = 0$$

4. Surface phenomena and work function

Under the influence of an applied potential gradient an electron current will flow through the lattice of a conductor, but potential gradients or jumps can also exist close to or at the surface without any current flow. These may be due to charges present or to an external electric field at the surface. In the same way that charges in the interior of the crystal are described as ionized donors or

acceptors and electrons or holes, it is usual to speak of surface donors and acceptors, which under appropriate conditions may become ionized.

These donor and acceptor levels related to the surface states may be purely an end effect of the lattice. Such states, called Tamm states, have been the subject of several theoretical studies[5], which have shown that the density would be about 10^{19} per m^2. From experiments on pure surfaces it can be unambiguously concluded that surface energy levels between the bands exist, but it is not certain that the density has the value mentioned above. Surface states may also arise from the presence of adsorbed atoms or molecules. Well-known examples are the adsorption of caesium and barium on tungsten, where part of the caesium or barium is present in the form of positive ions.

Charges at the surface are screened from the interior by a charge of opposite sign located in the interior close to the surface. In the case of a metal the charges of opposite sign constitute a layer which is extremely thin, due to the great number of charge carriers present in the interior. The result is a surface dipole layer which gives a potential jump at the surface given by:

$$\Delta\phi = \frac{\sigma\delta}{\varepsilon_0} = \frac{p}{\varepsilon_0}$$

in which σ = surface charge density
δ = distance between the layers of opposite sign
ε_0 = permittivity of vacuum
p = dipole moment value per unit area.

Also, in the case of adsorbed molecules or atoms a surface dipole layer may be formed due to polarization effects or to the presence of a permanent dipole in the adsorbed species.

At the surface of a semiconductor the situation is a little more complicated because the density of the carriers is much less than in a metal[6]. Therefore the space charge layer may have an appreciable thickness. If the density of the mobile charge carriers in the interior is equal to 10^{21} per m^3 and the surface charge density is 10^{15} per m^2, which is only about 0.01 per cent of a monolayer, the neutralization takes place over a distance of the order of 10^{-6} m. In this region the macroscopic electrical potential varies with the distance from the surface. An electron in the conduction band at a certain place far inside the crystal, with a particular kinetic and

macroscopic potential energy will now be compared with an electron at another place close to the surface with the same kinetic energy but with a different potential energy. In the band scheme the distances from the energy levels of the electrons at the two places to the bottom of the conduction band will be the same, because the kinetic energy of the two electrons is the same. The distances from the energy levels to the Fermi level will be different, however, as the Fermi energy (equal to the electrochemical potential) includes the potential energy, as explained in section 2, p. 189. Since, in equilibrium, the Fermi energy is the same throughout the crystal it is, evident that in the band scheme the energy levels of the electrons at the two places will be located at a different height, the difference being the difference in potential energy. Also the bottom of the conduction band at different places in the crystal will be located at different heights. Obviously a variation in macroscopic potential inside the crystal is reflected in a curvature of the energy bands in the band scheme. This band bending has a great influence on the ability of the crystal to emit electrons to the outside.

The calculation of the bending of the bands near the surface starts from Poisson's equation[7]:

$$\Delta\phi = -\frac{\rho}{\varepsilon\varepsilon_0} = -\frac{e}{\varepsilon\varepsilon_0}(n_+ - n_-) \tag{7}$$

in which ε = permittivity, ρ = charge density. It is assumed that the potential varies only in the direction perpendicular to the surface. The values of n_+ and n_- are calculated in exactly the same way as in the interior using the Fermi–Dirac statistics and expressed as a function of ϕ and E_F. The integration of eq. (7) then leads to the desired relationship between the field E, the potential ϕ and the distance from the surface.

Three important cases of band bending will be mentioned; they are represented schematically in Fig. 3. If, on an n-type material the bands bend downwards, due to ionized donor levels at the surface, the concentration of electrons in the conduction band at the surface will be greater than in the interior. An enrichment region exists near the surface. In a p-type material an enrichment region will be found if ionized acceptor levels exist at the surface (Fig. 3*a*). This region is of a more pronounced n-type or p-type than is the interior. With decreasing charge density at the surface the enrichment region becomes less important and finally vanishes. If the surface charge

changes its sign, i.e. if on an *n*-type crystal ionized surface acceptor levels exist causing the bands to bend upwards, the concentration of electrons in the conduction band at the surface will be smaller than in the interior, and an exhaustion region exists near the surface. In

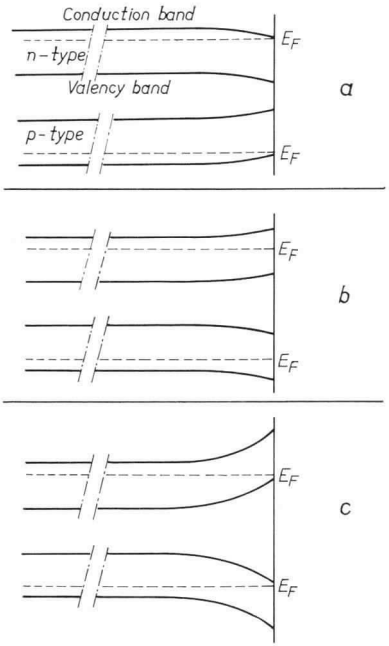

FIG. 3. Band bending at the surface of a semiconductor.
(*a*) Enrichment layer, due to ionized donors at the surface of an *n*-type material or to ionized acceptors at the surface of a *p*-type material.
(*b*) Exhaustion layer near the surface, due to ionized acceptors at the surface of an *n*-type material or to ionized donors at the surface of a *p*-type material.
(*c*) Inversion layer near the surface.

a *p*-type crystal an exhaustion region is found if ionized donor levels exist at the surface (Fig. 3*b*). If now the charge density at the surface is increased the exhaustion region may change to an inversion region, i.e. in this region the dominant carriers are of opposite sign to those in the interior. In an *n*-type crystal the surface layer becomes *p*-type and in a *p*-type crystal it becomes *n*-type (Fig. 3*c*). The effect

of band bending not only appears if surface charge is present, but also when a field is applied externally. This field penetrates the crystal and causes an internal space charge. The field effect, the influence of the applied field on the conductivity, is an important tool in the study of semiconductor surfaces. In thermionically emitting semiconductors the field penetration must be considered if saturated emission is drawn. Due to a surface charge a *p*-type material may show *n*-type conduction if the measurement is carried out on finely powdered material where surface conduction predominates.

An electron, present in a semiconducting crystal at a distance of some tens of interatomic spacings from the surface, is under the influence of the space charge region just described. Closer to the surface at a distance of the order of one or two interatomic distances, the electron meets with the irregularities in the microscopic potential field connected with the lattice boundary. Around the surface atoms, which have no neighbours at the outside, the potential must be different in different directions. The electron distribution at the outside will be different from that in the interior. A negative dipole will be formed when the electrons are pulled out. At a metal surface the surface dipole layer is of the same order of thickness as the space charge region. In this case it is difficult to distinguish between these layers as has been done for semiconductors. It is to be expected that the short range forces resulting from this boundary effect will vary for different crystal orientations and that they will be influenced by the adsorption of foreign molecules, atoms or ions. The result is that a potential barrier exists over a few interatomic distances at the surface, which may be different for different crystal planes. This barrier prevents an electron from escaping from the crystal, if its kinetic energy is too small.

If an electron with sufficient kinetic energy has passed the barrier due to the short range forces a long range force is still active. This is the image force, the result of the interaction between the electron and the positive charge induced in the crystal[8]. If the surface is considered as perfectly conducting and flat, the force F is equal to

$$F = \frac{e^2}{16\pi\varepsilon_0 x^2}$$

in which x = distance of the electron from the surface. The electron behaves as if it moves in an electric field with potential:

$$\phi = \frac{e}{16\pi\varepsilon_0 x} + \text{constant} \tag{8}$$

The distance x_0 at which the force on the electron changes from the image force into a short range force is not well defined. The potential (8) has to be added to the pure electrostatic potential. The total potential is called the " motive " as suggested by Langmuir[9]. It is defined as the scalar quantity whose gradient at any point and in any direction is equal to the force per unit charge exerted on an

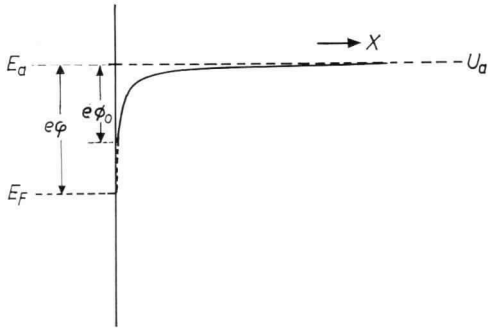

FIG. 4. Electron energy as a function of the distance from the surface in the absence of an externally applied electric field.

electron at the chosen point in the chosen direction. To remove the electron from the distance x_0 to infinity the potential energy $e\phi_0$ must be provided:

$$\phi_0 = \frac{e}{16\pi\varepsilon_0 x_0} \tag{9}$$

In Fig. 4 a schematic picture is given of the energy of the electron near the surface.

The difference between the electrochemical potential μ_e inside the crystal and the potential energy of an electron outside the crystal at an infinite distance in the absence of external electric fields, divided by the electronic charge e, is called the work function φ of the crystal surface. If individual crystal planes have different surface dipole moments, then the work functions of those planes will also be different.

In the older British and American literature the work function, also usually indicated by φ, was defined as the energy difference $e\varphi$ in our notation. In Herring and Nichols' paper[10] either definition

is used, whereas in the more recent literature φ is usually a potential[11]. In practice the difference appears in expressing the work function in volts or in electron volts. In several other languages different expressions are used which indicate the concept of potential or energy.

The work function will generally be a function of the temperature. As has been discussed in section 2 the electrochemical potential, i.e. the Fermi level, is a function of the temperature. Moreover, the surface dipole may be influenced by a temperature change, although this effect will probably be small when compared to the first. For metals, the value of the Fermi energy generally decreases with increasing temperature. The temperature coefficient of the work

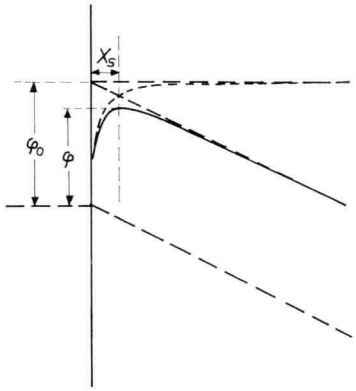

FIG. 5. The potential in the neighbourhood of the surface as a function of the distance in the presence of an externally applied electric field.

function of metals is thus positive, as it is for semiconductors of the Wilson type.

Not only the temperature, but also any external electric field will influence the potential barrier at the surface. The motive must include this field. If the field E is homogeneous the potential ϕ will be given by (see Fig. 5):

$$\phi = \frac{e}{16\pi\varepsilon_0 x} + Ex + \text{constant}$$

This potential has its minimum at:

$$x_s = \frac{1}{4}\sqrt{\frac{e}{\pi\varepsilon_0 E}}$$

The difference between the potential minimum and the potential at infinity in the absence of the field is given by:

$$\frac{1}{2}\sqrt{\frac{eE}{\pi\varepsilon_0}}$$

Consequently, the work function φ in the presence of an electric field E can be written as:

$$\varphi = \varphi^0 - \frac{1}{2}\sqrt{\frac{eE}{\pi\varepsilon_0}}$$

$$\varphi = \varphi^0 - 3.79 \times 10^{-5}\sqrt{E} \qquad (10)$$

where φ^0 is the work function in the absence of an externally applied electric field. The numerical constant 3.79×10^{-5} holds for φ expressed in V and E expressed in V/m.

It has been assumed so far that the crystal surface was perfectly flat. The problem of the influence of an external electric field in the case of surface roughness on a micro scale has been treated by Lewis[12] and by Morant and House[13]. An important effect on the work function, as calculated by Lewis, is, according to the last authors however, greatly reduced by the field existing between the areas of different work functions, the so-called patch field.

5. The emission equation and the velocity distribution of the emitted electrons

(*a*) THE EMISSION EQUATION

The calculation of the number of electrons emitted at a certain temperature T from an ideal crystal plane per second and per unit area may in principle be carried out in two ways which must yield the same result:

(α) Directly, by considering the electrons inside the crystal and calculation of the number which go from inside to outside, or

(β) Indirectly, assuming an equilibrium between the whole of electrons inside and outside the crystal. The number of electrons coming from the outside and passing the surface may now be calculated and equated with the number of emitted electrons.

The first, direct method is not easy because the movement of the electrons in the periodic field of the crystal lattice must be considered. The much more simple indirect method will be used here,

because the electrons outside the crystal may be considered free and classical mechanics with the Fermi–Dirac distribution law can be applied.

The number of possible quantum states for the electrons is given by the expression:

$$\frac{1}{h^3} \int_{xyz} \int_{p_x p_y p_z} \mathrm{d}x\mathrm{d}y\mathrm{d}z\mathrm{d}p_x\mathrm{d}p_y\mathrm{d}p_z$$

The number of electrons with energy E occupying these states is given by:

$$N(E) = \frac{2}{h^3} \int_{xyz} \int_{p_x p_y p_z} \frac{1}{\exp\left(\dfrac{E - E_F}{kT}\right) + 1} \mathrm{d}x\mathrm{d}y\mathrm{d}z\mathrm{d}p_x\mathrm{d}p_y\mathrm{d}p_z$$

Assuming the crystal plane to coincide with the yz plane, the number of electrons impinging per second on this plane is given by:

$$\frac{2}{h^3} \int_{yz} \int_{p_x p_y p_z} \frac{|v_x|}{\exp\left(\dfrac{E - E_F}{kT}\right) + 1} \mathrm{d}y\mathrm{d}z\mathrm{d}p_x\mathrm{d}p_y\mathrm{d}p_z$$

Furthermore,

$$v_x = \frac{\partial E_x}{\partial p_x}$$

To obtain the number of electrons impinging from the outside on the surface region, which is assumed to extend a short distance in the x-direction, to exclude the irregularities in the immediate vicinity of the actual crystal surface, the integration must be carried out with respect to p_y and p_z taking into account only the kinetic part of the total energy E. The potential energy, which is constant along the planes parallel to the yz plane, is given by $E_F + e\varphi$. Consequently, the number of electrons with energy E_x in the interval $\mathrm{d}E_x$ impinging from the outside per second and per unit area is found to be:

$$n(E_x)\mathrm{d}E_x = \frac{2}{h^3} \cdot 2\pi mkT \ln \left\{1 + \exp\left(-\frac{E_x + e\varphi}{kT}\right)\right\} \mathrm{d}E_x \qquad (11)$$

The electron has a certain probability r of being reflected at the energy barrier, so the $(1 - r)$ times the number of electrons can pass. In general r, the reflection coefficient, will be a function of the

energy E_x and will also depend upon the structure of the potential barrier. The number of electrons entering the crystal per unit area and per second is consequently given by:

$$n_e = \int_o^\infty \frac{2}{h^3} \cdot 2\pi mkT(1 - r) \ln \left\{1 + \exp\left(-\frac{E_x + e\varphi}{kT}\right)\right\} \mathrm{d}E_x$$

Assuming $e\varphi/kT$ to be large, the integration leads to the expression:

$$n_e = \frac{4\pi mk^2T^2}{h^3}(1 - \bar{r}) \exp\left(-\frac{e\varphi}{kT}\right)$$

in which $\bar{r}$ is the mean reflection coefficient. The emitted current density, being equal to the current density entering the crystal, is consequently:

$$J_{\text{sat}} = \frac{4\pi emk^2T^2}{h^3}(1 - \bar{r}) \exp\left(-\frac{e\varphi}{kT}\right) \qquad (12)$$

which is the well-known Richardson–Laue–Dushman equation. For a refinement to this equation see Ollendorf[14]. The equation has been derived without any reference to the nature of the crystal. It may either be a metal or a semiconductor, and only the free electron mass m appears in the final eq. (12). The constant

$$\frac{4\pi emk^2}{h^3} = A = 1.2 \times 10^6 \text{ A/m}^2 \text{ °K}^2 \qquad (12a)$$

is the universal thermionic constant.

The work function is generally a function of temperature. For metals the temperature dependence of the work function has been discussed in section 4. A correction for the temperature dependence can easily be inserted in eq. (12).

Dealing with semiconductors, the position of the Fermi level at the surface is the determining factor. As has also been explained in section 4 the presence of surface states may fix the Fermi energy at the surface at a value with respect to the bottom of the conduction band which is quite different from its position with respect to the same reference level in the interior. If it is assumed that the position of the bottom of the conduction band is the same throughout the whole specimen, and if a Wilson model is used, then the formula

(12) may be written in another way which has been usual in the literature on oxide-coated cathodes.

According to formula (3) the position of the Fermi level is given by the expression:

$$E_F = -\frac{E_d}{2} + \frac{kT}{2} \ln n_d \frac{h^3}{2(2\pi mkT)^{3/2}} \tag{3}$$

Denoting the energy of an electron at infinity outside the specimen in the absence of an external field by E_a, see Fig. 6, the work function is given by:

$$\varphi = \frac{-E_F + E_a}{e}$$

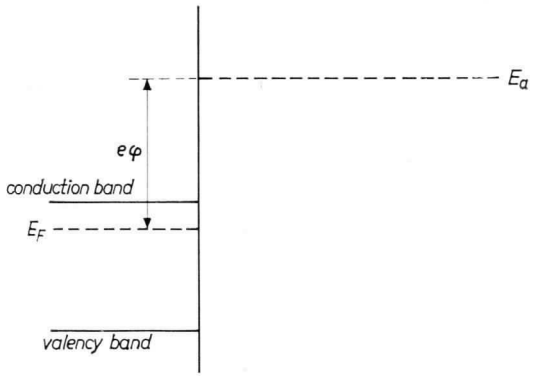

FIG. 6. The energy diagram at the surface of a semiconductor in the absence of band bending.

Insertion of this expression for φ in the emission eq. (12) leads to:

$$J_{\text{sat}} = (1 - \bar{r}) n_d^{1/2} \frac{2^{1/2} e \,.\, (2\pi m)^{1/4} k^{5/4}}{h^{3/2}} T^{5/4} \exp\left(-\frac{E_a + (E_d/2)}{kT}\right) \tag{13}$$

This equation is known as the Fowler emission equation[15]. It takes into account, under certain appropriate conditions, the temperature dependence of the work function. It must be remarked, however, that the validity of (3) and consequently of (13) is limited to low temperatures, even below the normal operating temperature of alkaline earth oxide cathodes. Moreover E_a will generally be a function of temperature.

(*b*) THE ENERGY DISTRIBUTION OF THE EMITTED ELECTRONS

The energy distribution of the electrons passing any plane in the immediate vicinity of the crystal plane and parallel to it, is calculated easily using eq. (11). The number density of electrons emitted with a velocity v_x in the interval v_x, $v_x + \mathrm{d}v_x$ is obviously:

$$n(v_x)\mathrm{d}v_x = \frac{4\pi m^2 kT}{h^3}(1 - r_{v_x}) \exp\left(-\frac{e\varphi + \frac{1}{2}mv_x^2}{kT}\right) v_x \mathrm{d}v_x$$

The distribution is given by:

$$f(v_x)\mathrm{d}v_x = \frac{1 - r_{v_x}}{1 - \bar{r}} \frac{mv_x}{kT} \exp\left(-\tfrac{1}{2}\frac{mv_x^2}{kT}\right) \mathrm{d}v_x$$

If r is independent of the normal velocity this represents a Maxwellian distribution of the normal velocities.

The determination of the value of the transmission coefficient $D = 1 - r$ has been the subject of both theoretical and experimental studies. The theoretical studies indicate that the value of D cannot be very different from 1[16]. The interpretation of the results of the experiments is controversial. According to Nottingham[17] and Hutson[18], whose measurements of the velocity distribution of the emitted electrons showed a deficiency of slow electrons, the results can be explained by a transmission coefficient for these electrons which is strongly energy-dependent. Their work has, however, been criticized by Herring and Nichols[19] and by Smith[20]. It is usually assumed that r can be neglected.

It can easily be shown that the emitted electrons carry in the normal direction a mean energy equal to kT if $\bar{r}$ is independent of the normal velocity. The velocities in the y and z directions do not change so that in these directions an energy of $\frac{1}{2}kT$ is carried. The average kinetic energy of the emitted electrons is consequently given by:

$$\bar{E}_k = 2kT$$

In addition to this mean kinetic energy a potential energy $e\varphi$ has to be supplied to the emitted electrons, so that on the average the total energy needed per emitted electron is equal to:

$$\bar{E} = e\varphi + 2kT$$

The power loss of the emitter from which the current density J_{sat} is drawn is:

$$P = J_{sat}\left(\varphi + \frac{2kT}{e}\right)$$

In this calculation a small thermoelectric term has been neglected.

6. The emitting crystal surface in an external electric field

It will still be assumed that the emitter is ideal, which means that the emitting surface is atomically flat, that the work function is

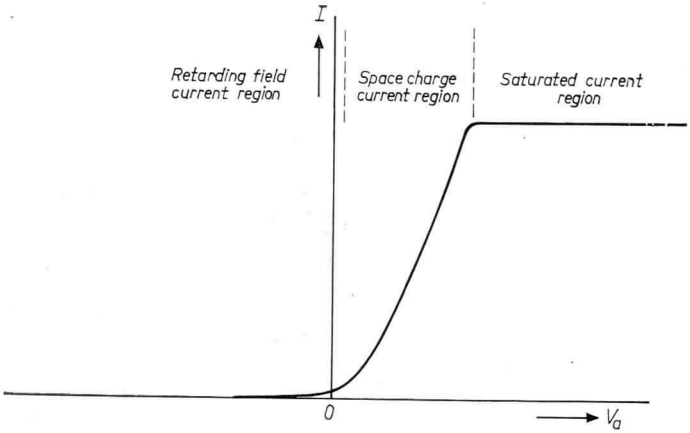

FIG. 7. The $I-V_a$ characteristic of a diode (schematic).

constant along the surface and that no resistance is present. Information about the emitted current can only be obtained by collecting the electrons, or a certain part of the electrons, on a second electrode. The current–voltage characteristic of the diode which is so formed can be divided into three regions. The currents flowing in these regions are referred to as:

(*a*) the retarding field current
(*b*) the space charge-limited current
(*c*) the saturated current.

These regions are represented in Fig. 7, while the distribution of the field between a flat parallel cathode and anode is given schematically in Fig. 8a. Note the direction of positive anode voltage! If the

temperature of the emitter is chosen very low the saturated emission current is low and the space charge in front of the cathode is very small. The space charge region is practically absent and the

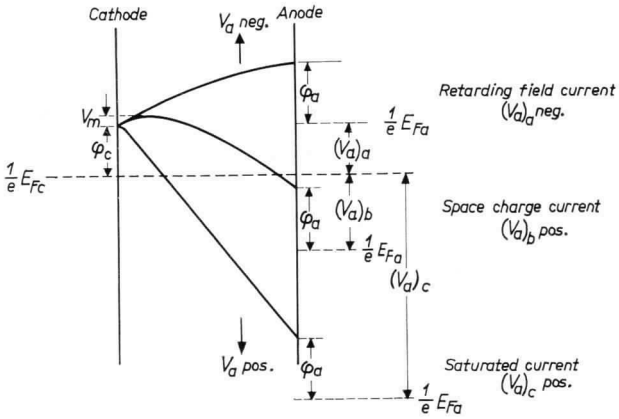

FIG. 8(*a*). The electric potential in a diode for the three current regions as a function of the place between cathode and anode (schematic).

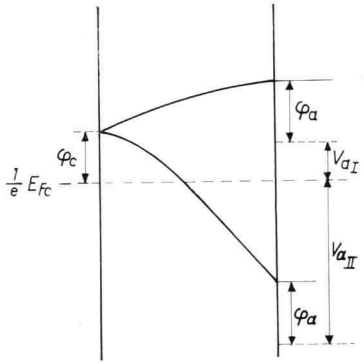

FIG. 8(*b*) The electric potential in a diode with the values V_{aI} and V_{aII} of the anode voltage, bounding the space charge region (schematic).

saturated region immediately follows the retarding field region. It will be assumed in the following treatment of the I–V_a relationship in these regions, that the reflection coefficient $\bar{r}$ in eq. (12) is zero,

and that the geometry is plane parallel. The reflection coefficient of the anode, which is also assumed to be ideal, is taken as zero.

(*a*) THE RETARDING FIELD REGION

The potential barrier which must be passed by the electrons flowing from cathode to anode is equal to $(V_a)_a + \varphi_a$ (see Fig. 8*a*). It follows then from eq. (12) that the current density is given by:

$$J_{\text{ret}} = \frac{4\pi emk^2T^2}{h^3} \exp\left\{-\frac{e(-V_a + \varphi_a)}{kT}\right\} = J_{\text{sat}} \exp\left\{\frac{e}{kT}(V_a - \varphi_a + \varphi_c)\right\} \tag{14}$$

V_a = anode voltage = potential difference between the Fermi energy level of the cathode and the anode
φ_c = work function of the cathode
φ_a = work function of the anode.

The $\log J_{\text{ret}}$ versus V_a curve must be a straight line, the slope of which is a measure of the temperature of the cathode. See Fig. 9 (p. 208). The work function of the anode is of immediate importance for the retarding field current but that of the cathode work function is immaterial. The measurement of J_{ret} as a function of V_a represents in fact a determination of the energy distribution of the emitted electrons. If plotting of $\log J_{\text{ret}}$ versus V_a results in a straight line the distribution of the electron velocities is Maxwellian.

(*b*) THE SPACE CHARGE REGION

In this region a space charge exists in front of the cathode owing to the fact that more electrons are emitted than are transported to the anode. Combined with this space charge is a potential minimum. The current density to the anode is now (see Fig. 8*a*):

$$J_{\text{sp}} = \frac{4\pi emk^2T^2}{h^3} \exp\left\{-\frac{e(\varphi_c - V_m)}{kT}\right\} = J_{\text{sat}} \exp\left(\frac{eV_m}{kT}\right) \tag{15}$$

The calculation of J_{sp} is complicated because V_m is a function of J_{sp}. The solution has been given by Epstein[21], Fry[22] and Langmuir[23]. The problem breaks up in two parts. First the electron density is calculated as a function of the potential, then this density is introduced in Poisson's equation, which can be integrated once explicitly and is integrated for the second time numerically (compare the similar problem in section 4). The solution is obtained

by introducing two dimensionless variables η and ξ which measure the potential and the distance with respect to the space charge minimum. The rather concise table of Langmuir has been extended by Kleynen[24], whereas Rittner[25] has given expressions for ξ in terms of η and vice versa, over the complete range of these variables. In these calculations the potentials in the vacuum just outside cathode and anode are used. To obtain the external voltage difference

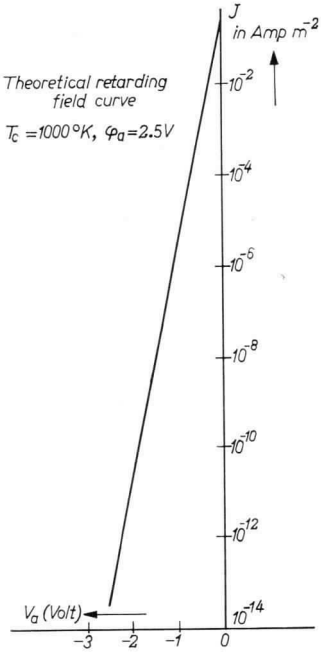

FIG. 9. The retarding field current as a function of anode voltage with $T_c = 1000°\text{K}$ and $\varphi_a = 2.5$ V.

between cathode and anode the work function difference $\varphi_a - \varphi_c$ must be added.

For a quick calculation the Child formula[26] may be used, which is derived under the assumption of zero kinetic energy of the electrons at the cathode surface. The Child formula is:

$$J_{sp} = \frac{4\varepsilon_0}{9}\left(\frac{2e}{m}\right)^{1/2}\frac{1}{d^2}(V_a + \varphi_c - \varphi_a)^{3/2} \tag{16}$$

d = cathode–anode distance.

If the current is measured in A/m^2, the anode voltage in V and the distance in m, the value of the constant

$$\frac{4\varepsilon_0}{9}\left(\frac{2e}{m}\right)^{\frac{1}{2}}$$

is equal to 2.334×10^{-6}. Formula (16) gives reasonable results when the anode voltages are not low and when the cathode–anode

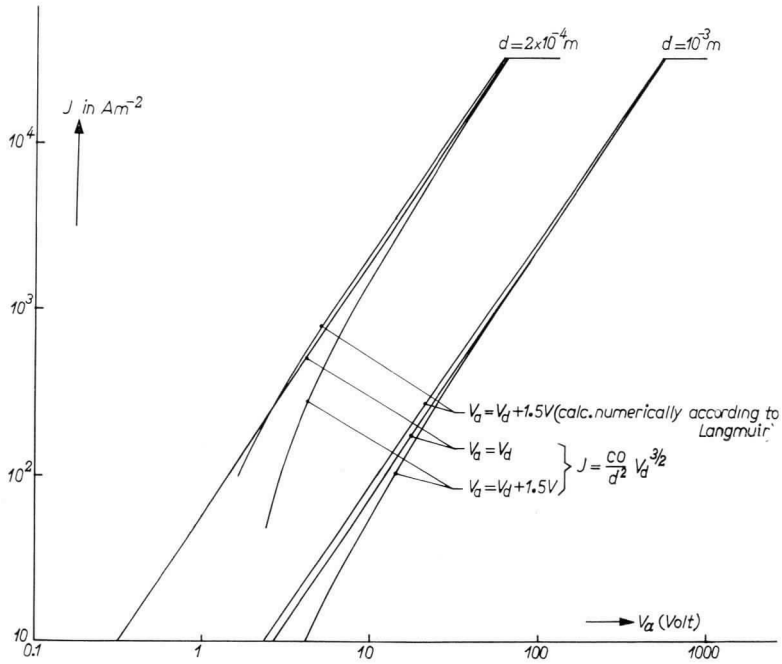

FIG. 10. The space charge current density in a plane-parallel diode as a function of anode voltage for different values of the cathode–anode distance calculated in different ways. V_d = potential difference in vacuum just outside cathode and anode, V_a = anode voltage

$$V_d = V_a + \varphi_c - \varphi_a$$
$$\varphi_a - \varphi_c = 1.5 \text{ V}.$$

distance is large compared to the distance between cathode and space charge minimum. See Fig. 10.

Other expressions and charts which allow the calculation of J_{sp}, also for the cylindrical arrangement, are given in the literature[27].

Note that under space charge conditions the work function of the cathode is of very minor importance, if $V_a \gg \varphi_a - \varphi_c$.

(c) THE SATURATED CURRENT REGION

Under the influence of a sufficiently high anode voltage all electrons emitted by the cathode are collected at the anode. The saturated current is given by:

$$J_{\text{sat}} = \frac{4\pi emk^2}{h^3} T^2 \exp\left(-\frac{e\varphi}{kT}\right) \tag{12}$$

$$\frac{4\pi emk^2}{h^3} = 1.2 \times 10^6 \text{ A/m}^2 \text{ °K}^2 \tag{12a}$$

At high field strength at the cathode surface the decrease of the work function under influence of the field, the Schottky effect[8], may be appreciable (cf. eq. (10)).

$$J_{\text{sat}} = \frac{4\pi emk^2}{h^3} T^2 \exp\left\{-\frac{e}{kT}(\varphi - \Delta\varphi)\right\}$$

$$\Delta\varphi = \frac{1}{2}\left(\frac{eE}{\pi\varepsilon_0}\right)^{\frac{1}{2}} = \frac{1}{2}\left(\frac{eV_a}{\pi\varepsilon_0 d}\right)^{\frac{1}{2}} \tag{17}$$

If $\log J_{\text{sat}}$ is plotted against $V_a^{\frac{1}{2}}$ a straight line with a slope, determined by the cathode temperature and the cathode–anode distance, must be obtained.

Accurate measurements of the current emitted by a metal cathode under saturated conditions as a function of the accelerating voltage have shown that small periodic deviations exist from the straight line $\log J_{\text{sat}} - V_a^{\frac{1}{2}}$[28]. The explanation of this interesting phenomenon, although of negligible importance for practical cathodes, is sought in the reflection of the electron waves at the surface barriers, the first located at the surface proper of the crystal, the second in the vacuum outside, as explained on p. 197[29]. The net number of reflected electrons is influenced by the reflection at both barriers, which depends upon their distance. Consequently the number of transmitted electrons must also be a function of this distance and hence of the value of the field strength.

In semiconductors the applied field penetrates the crystal and influences the band structure near the surface, as mentioned in section A4. This phenomenon will be discussed together with

problems related to the measurement of cathode properties. See p. 228.

The three regions of diode voltages just described are separated by two values of the voltage which are given in Fig. 8b as $V_{a\mathrm{I}}$ and $V_{a\mathrm{II}}$. At $V_{a\mathrm{I}}$ the field strength is zero at the collector, at $V_{a\mathrm{II}}$ it is zero at the emitter. At these values the space charge minimum enters the mirror image force region at the electrodes. It can be shown that at $V_{a\mathrm{I}}$ where the retarding field current passes into the space charge current the value of J is given by:

$$J = 7.7 \times 10^{-12} \frac{T^{3/2}}{d^2} \tag{18}$$

Here J is measured in A/m^2 and d in m.

The numerical factor is valid for sufficiently high values of the saturated current density. At lower values of J_{sat} the numerical factor decreases. It can easily be calculated from the ξ, η tables. At $V_{a\mathrm{II}}$ the current density at the cathode is given by J_{sat}.

In case of a geometry different from plane parallel the formulae (14), (15), (16), (17) and (18) change. For the coaxial cylindrical arrangement, see ref. (30).

7. Influence of patches

In the theory so far presented it has been assumed that the emitting surface is uniform, which means that the work function is constant over the surface. Only in very few cases have experiments on thermionically emitting surfaces of this kind been made. Usually the emitters have a quite inhomogeneously emitting surface. The question arises how this inhomogeneity is reflected in the results of the measurements which are made on such a surface. The influence of patches has been the subject of various studies; Becker[30a] and Herring and Nichols[10] especially have given it an elaborate treatment.

Before considering the influence of the patch effect in the various regions of applied external voltage, the case of zero external voltage will be dealt with.

(*a*) ZERO APPLIED FIELD

Suppose that the surface is composed of a number of patches of type i which have a work function φ_i and that f_i represents the

fraction of the surface occupied by this type of patch. Immediately in front of each patch the electrostatic potential is given by:

$$\phi_i = -\frac{\mu_e}{e} - \varphi_i$$

The potential at small distances from the surface varies along the surface in accordance with the work function. At a large distance from the surface the potential becomes constant. The influences of all patches combine to a certain mean value. This value is given by the expression:

$$\bar{\phi} = -\frac{\mu_e}{e} - \bar{\varphi}$$

in which $\bar{\varphi}$ has the value:

$$\bar{\varphi} = \sum_i f_i \varphi_i$$

It is evident that two conductors I and II with patchy surfaces, for example a cathode and an anode, placed at a distance which is large compared with the dimensions of the patches, will show in equilibrium a potential difference equal to:

$$\bar{\varphi}_{\mathrm{I}} - \bar{\varphi}_{\mathrm{II}}$$

(*b*) THE RETARDING FIELD REGION

The collector will be assumed to be uniform. The trajectories of the electrons in the neighbourhood of the patches will be very complicated as the patch field in front of the surface influences the tangential velocities. If it is assumed that the effect of the tangential velocities is averaged out so that only the normal kinetic energy needs to be considered, then the calculation of the contribution of the various patches is rather simple. If a sufficiently large retarding field is used the emission from all patches is governed by the expression (14), and the work function differences have no influence on the current. Increasing the anode voltage causes the high work function patches to pass from the retarding field region into the accelerating field region. As the saturated current of these high work function patches is low, the space charge minimum will hardly exist and hence the current will quickly become saturated. The $\log J$ versus V_a curve will deviate from the straight line. How marked

this deviation will be depends evidently on the current contribution of the high work function patches, on the configuration of the patchy surface and on the geometry of the diode. If the work function differences of the various patches are small the saturated emission part of the high work function areas will be preceded by a space charge-limited emission and the log J versus V_a curve will likewise deviate usually to a smaller extent.

(*c*) SPACE CHARGE REGION

As the current in this region is almost independent of the cathode work function for anode voltages which are not very small, a patchy surface will show nearly the same J–V_a characteristic as does the ideal homogeneous cathode. However, deviation will occur as soon as the high work function patches tend to saturate. Then the slope of the J–V_a curve will decrease with increasing contribution to the number of saturated patches.

(*d*) HIGH ACCELERATING FIELD REGION

The potential distribution near the cathode for a not unduly high accelerating field is sketched in Fig. 11 (p. 214). The cathode behaves as having a work function $\bar{\varphi}$ lowered by a small amount due to the Schottky effect. Patches, however, with higher work function than $\bar{\varphi}$ contribute with a current corresponding to their work function. For high collecting fields, such that the fields between individual patches are of minor importance, all patches will contribute with their particular saturation current. The Schottky correction to the work function applies to each contribution equally.

Summarizing, the following picture may be given:

In the intermediate region of space charge-limited emission for all patches—a region which may be quite small in practice—the J–V_a curve has almost the same shape as the J–V_a curve of a homogeneous emitter. Going to higher accelerating fields the regions of high work functions become saturated, the slope of the curve becomes smaller and, depending on the kind of inhomogeneity, the current becomes saturated. A more or less broad transition region develops between space charge and saturated region. A further slow increase with increasing voltage demonstrates the Schottky effect. Going to lower accelerating voltage and to retarding voltages the slope of the J–V_a curve will change more or

less regularly, depending on the particular combination of patches of different work functions. Here, too, a transition region is found. At sufficiently high negative values of the applied voltage the slope of the log J_{sat}–V_a curve equals the theoretical one which is determined only by the temperature of the emitter.

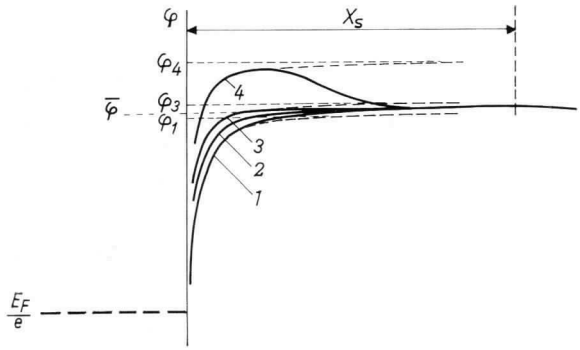

FIG. 11. The potential distribution in the presence of a not unduly high accelerating field in front of a patchy cathode. X_s = distance between Schottky minimum and the cathode.
The potential distributions 1, 2, 3, 4 belong to patches with work functions increasing in value in this sequence. The value of $\bar{\varphi}$ depends on the configuration, on the areas and on the values of the work function of the different patches.

8. Noise from thermionic cathodes

Noise is the statistical fluctuation in electric current, related to the special character of electricity—the existence of electrons—and to the thermal energy of these electrons. A change in the current density $J = nev$ can be expressed by:

$$\Delta J = ev\Delta n + ne\Delta v$$

of which the first part is due to a change in the number of electrons, giving rise to the shot noise, and the second part is due to a change in the velocity of the electrons, resulting in thermal noise.

The random fluctuations of the current are measured in terms of its mean square deviation from the mean current value:

$$\overline{\Delta I^2} = \overline{(I - \bar{I})^2} = \overline{I^2} - (\bar{I})^2$$

Usually one is not only interested in the total noise, but even more in its frequency dependence given by the contribution $\overline{\Delta I^2_{df}}$ in the frequency interval df.

The thermionic emission from an ideal cathode is believed to be a Poisson process, which means that the probability of emission of one electron in an infinitesimal time interval dt is a constant, and that the probability of emission of two or more electrons in this interval is proportional to dt or to a corresponding higher power of dt. In general, a large number of electrons are emitted per unit time, but it may be expected that this number will not be completely constant in time. The small variations around the mean number are the origin of the shot noise and can be measured in a saturated diode. $(\overline{\Delta I^2_{df}})_s$, due to the shot noise, is independent of the frequency and has the value[31]:

$$(\overline{\Delta I^2_{df}})_s = 2Ie\mathrm{d}f$$

The thermal noise plays an important part in current flow in circuits, composed of resistors, self-inductors and capacitors. Calculation shows that [32]:

$$(\overline{\Delta I^2_{df}})_{\mathrm{th}} = \frac{4kT}{R}\,\mathrm{d}f$$

in which R is the resistance of the circuit. The thermal noise is related to the random thermal movement of the electrons due to the interactions with the crystal lattice of the conductors, at the temperature T.

If the electrons flowing in a diode were emitted from the cathode in a completely regular manner, so that originally no fluctuations in number per unit time exist, the anode current would still show variations, because the different velocities of the electrons would result in a different arrival rate. If the noise of this diode is measured at relatively low frequency (in the Mc/s range), where the time of flight of the electrons between cathode and anode is short compared to the period of vibration, it can be treated completely as shot noise. If, however, the measuring frequency becomes so high that the transit time becomes comparable with the time of vibration, the influence of the velocity distribution must be considered separately. This influence is smaller the higher the accelerating anode voltage, the ratio of thermal energy to the kinetic energy due to the anode voltage being the determining factor.

In a diode, with temperature-limited emission, where the number of electrons flowing between cathode and anode is determined by the almost fixed potential barrier at the cathode, and in a diode in the retarding field region, where the current is determined by the fixed potential barrier at the anode, the shot noise is given by:

$$(\overline{\Delta I_{df}^2})_s = 2Ie\mathrm{d}f$$

In the space charge-controlled diode where the space charge barrier is a function of the current, the situation is different. If the electrons were emitted with zero energy and if the work functions of cathode and anode are assumed to be constant, the anode current would only depend upon the anode voltage and would be independent of the total number of electrons emitted by the cathode. It is given by formula (16):

$$J_{\mathrm{sp}} = \frac{4\varepsilon_0}{9}\left(\frac{2e}{m}\right)^{1/2}\frac{1}{d^2}(V_a + \varphi_c - \varphi_a)^{3/2}$$

In this case no shot noise would be expected. The noise found, however, in a diode under space charge conditions is due to the energy distribution of the emitted electrons and can be considered as a thermal noise. It is usually expressed as a reduced shot noise:

$$(\overline{\Delta I_{df}^2})_{\mathrm{sp}} = 2\Gamma^2 Ie\mathrm{d}f$$

where Γ^2 is the mean square smoothing factor. From what has been said before, it is not surprising that Γ^2 is a function of the ratio of the kinetic energy, gained from the potential difference between anode and cathode, and the thermal energy, related to the cathode temperature. Its value may be quite small, of the order of a few per cent. The smoothing of the shot noise under space charge conditions is considerable.

In addition to the sources of noise which have been discussed so far, other sources must be present to explain the additional noise found at low frequencies, below a few kc/s. This additional noise increases with decreasing frequency, usually being about inversely proportional to it. Various kinds of low frequency noise have been established[33].

(*a*) True flicker noise, seen as fluctuations in emission found under temperature-limited conditions and reduced by space charge. Its magnitude is proportional to the square of the mean

current and inversely proportional to the frequency. Study of the flicker noise contributes to an understanding of practical cathodes.

(*b*) Anomalous flicker noise, which is due to the influence of positive ions on the space charge potential distribution. It is only found under space charge conditions.

(*c*) Interface noise, which is caused by the presence of an interface resistance. The resistance usually present in the cathode is so small that it does not give rise to extra noise, but the interface resistance, sometimes found in oxide-coated cathodes, can have a considerable value. The interface resistance is caused by poorly conducting compounds formed by chemical reactions between the alkaline earth oxides and certain elements present in the base material. The noise due to this resistance is also proportional to the square of the current and about inversely proportional to the frequency. It is only found under space charge conditions because the additional voltage fluctuations across the resistance do not influence the diode current under saturated conditions.

B. MEASUREMENTS ON THERMIONIC CATHODES

1. Introduction

In studying thermionic cathodes the essential measurements are of the emitting area of the cathode, of its temperature, and of electric currents and voltages. The instruments for carrying out these measurements will not be discussed here, but attention will be paid to the underlying principles.

A difference will exist in the way in which measurements are carried out on ideal cathodes—to which pure single crystal surfaces represent the closest approach, the theory of which has been outlined above—and on non-ideal cathodes which are used in practice. In the first case the utmost care is taken to make and keep the surface in a clean state and the most refined vacuum techniques are used. Scrupulous attention must be paid to influences of other electrodes in the structure, in particular to the anode. Usually, a diode structure is used since this is simple and provides ample information. Unfortunately, products which are released from the anode, for example by electron bombardment, have a much greater chance of reaching the cathode than a suitable gettering device. A thorough outgassing of all components present in the structure is needed to prevent contamination of the cathode afterwards.

For a practical cathode, e.g. the alkaline earth oxide cathode, it is not *a priori* evident that the structure must be given the same careful attention. Under practical conditions, such as exist in a radio valve, the situation is extremely complex and the cathode is influenced by a great number of different factors. A measurement of the properties of the emitter under these conditions will be of great value as these properties determine the actual performance of the device. To obtain knowledge of the properties of the cathode as such, however, measurements under much better conditions will be needed. The aim is then to introduce the various disturbing factors one by one and finally together, in order to explain the peculiarities found under practical conditions.

Modern vacuum techniques, in particular the ultra high vacuum technique, enable the experimental physicist to carry out his experiments at pressure levels so low that no fears need be entertained of disturbances from outside the cathode. Pressures down to 10^{-10} torr and lower can be maintained over long periods by the use of getter-ion pumps attached to the system. In the measurement of thermionic emission it is fortunate that the cathode is at a high temperature since the sticking time—the time an adsorbed atom or molecule stays on the surface before desorption—is usually short so that a clean surface is much more easily achieved and maintained. The application of small mass spectrometers, such as the omegatron[34], permits the analysis of the gas composition down to partial pressures of about 10^{-11} torr. The use of these new techniques has already led to a better comprehension of the gas reactions occurring in the systems which are under consideration here. The influence of the temperature is of especially great importance in connection with the gas composition. Another question is whether the residual gas in practical systems has an unfavourable or beneficial effect on the properties of the cathodes used. It does not seem always to be the best policy in systems where oxide-coated cathodes are used to try to keep the pressure of a gas such as hydrogen as low as possible[122].

In order to reduce unwanted interference from other components in the structure to the lowest possible level the materials which are to be used must be chosen with great care. A thorough degassing treatment at high temperature must be possible. This limits the choice of the metals used for construction purposes usually to tungsten, molybdenum, tantalum, the platinum metals, and nickel.

These introductory remarks are meant to stress the importance of

taking the utmost care both in the construction of devices used for measurements of certain emission properties and in the interpretation of the results of the measurements, especially if they are obtained under circumstances which are not accurately known. In section 2 measurements will be treated which are made with specially designed apparatus, whereas section 3 deals with some measurements carried out in practical tubes.

2. Measurements in special devices

(*a*) SINGLE CRYSTAL METAL CATHODES

The Richardson–Laue–Dushman equation (12) contains two quantities $\bar{r}$ and φ which determine at a certain temperature the maximum current density to be delivered by an ideal thermionic

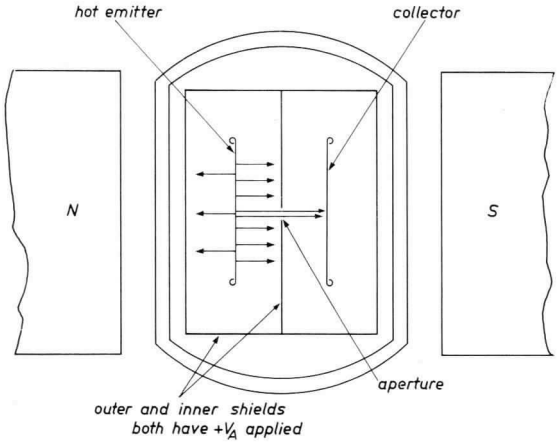

FIG. 12. Schematic picture of the experimental tube, used by Shelton. The magnetic field and the single aperture collimate the electrons, thereby defining the emitting area of the sampled current. From Shelton, H., *Phys. Rev.* **107**, 1553 (1957).

cathode. It has been remarked already that no unanimity exists about the value of $\bar{r}$, more specifically about its dependence on energy. The problem may be solved either by measuring the energy distribution under the most ideal conditions possible or by directly determining the reflection coefficient of slow electrons impinging on the crystal from outside.

The first experiment has been carried out by Shelton[35] who built a plane-parallel diode with cathode and anode of single

crystals of tantalum. Great care was taken to prevent any contamination. Between cathode and anode a diaphragm was placed and a magnetic field in the direction of the electric field was used. See Figs. 12 and 13.

The I–V_a characteristic was measured in the retarding and

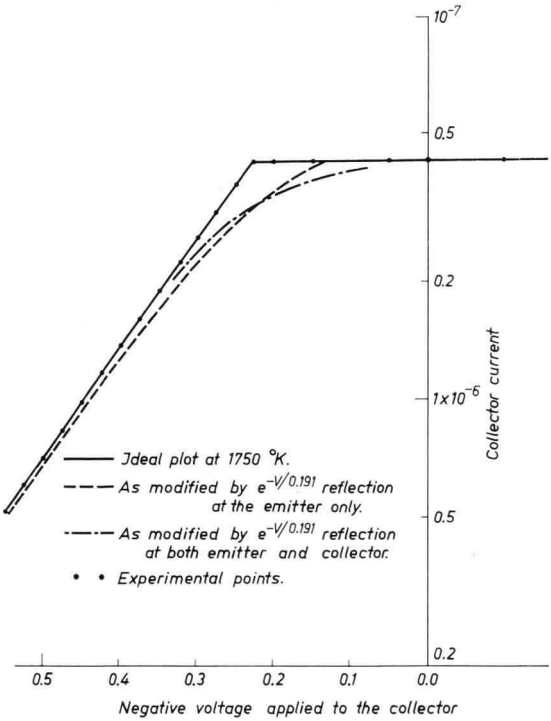

FIG. 13. Upper part of the retarding potential plot measured by Shelton. The left-hand part remains straight down to 10^{-12}A. The experiment confirms the ideal Maxwellian energy distribution. From Shelton, H., *Phys. Rev.* **107**, 1553 (1957).

accelerating field region. The results did not show a dependence of $D = 1 - \bar{r}$ on the energy as suggested by Nottingham[17]. The possible interference of the magnetic field has been the subject of a study by Greenburg[36]. His measurements do not show any influence of the magnetic field on the saturation emission of molybdenum.

The second type of experiments, the direct determination of the

reflection of slow electrons, has been carried out by Lange also on a tantalum crystal and by Hobson[37]. Lange's work does not seem to have been published so far, but it is mentioned by Nottingham[38] that at room temperature no indication of reflection has been found. Hobson also finds a small reflection ($\bar{r} < 0.05$) for electron energies approaching zero and an increase of $\bar{r}$ at higher energies which is in contrast with the relation suggested by Nottingham.

The diode structure of Shelton can also be used for the determination of the work function φ. At sufficiently high accelerating fields (depending on the temperature of the cathode) saturated emission can be drawn. It might be necessary under these conditions to apply the Schottky correction and to evaluate the saturation current at zero field at the emitter.

The disadvantage of a fixed structure, which enables the determination of the reflection coefficient and the work function for one orientation of the crystal only, can be overcome by using a structure in which the crystal can be rotated. This has been done by Nichols[39] who used a tungsten wire containing a sufficiently large single crystal orientated with the [110] direction along the axis of the filament. The crystal was surrounded by a coaxial cylindrical anode with a slit. Electrons emitted from a certain part of the crystal passed this slit to be received by a collector. This arrangement permitted the exact measurement of the work function of various crystallographic orientations. A similar construction was used by Smith[40]. Hutson[18] perfected this type of instrument by the addition of a magnetic analyser which enabled him to determine the energy distribution of the emitted electrons.

When the saturated emission density is measured at different temperatures a calculation of the temperature coefficient of the work function can be made if it is assumed that the reflection coefficient may be omitted. Writing $\varphi = \varphi_0 + (\partial\varphi/\partial T)_0\, T$, thus neglecting higher terms in the series, the Richardson equation (12) becomes:

$$J_{\text{sat}} = \frac{4\pi emk^2}{h^3} \exp\left\{-\frac{e}{k}\left(\frac{\partial\varphi}{\partial T}\right)_0\right\}(1-\bar{r})\,T^2 \exp\left(-\frac{e\varphi_0}{kT}\right) =$$

$$A_T(1-\bar{r})\,T^2 \exp\left(-\frac{e\varphi_0}{kT}\right)$$

$$A_T = A \exp\left\{-\frac{e}{k}\left(\frac{\partial\varphi}{\partial T}\right)_0\right\}$$

Plotting $\ln (I_{sat}/T^2)$ as a function of $1/T$ must yield a straight line with the slope $-(e\varphi_0/kT)$ and an intercept with the $\ln (I_{sat}/T^2)$ axis proportional to

$$\ln A(1 - \bar{r}) - \frac{e}{k}\left(\frac{\partial \varphi}{\partial T}\right)_0 .$$

From this intercept $(\partial\varphi/\partial T)_0$ may be calculated, if $\bar{r} = 0$.

(*b*) POLYCRYSTALLINE METAL CATHODES

In many cases single crystals of sufficient size for emission measurements are not available, and frequently one is interested in the emission properties of a certain piece of wire or of a plate of a certain metal, available in polycrystalline form. Under these conditions an inhomogeneous emission is to be expected and great care is needed when the experimental results have to be interpreted. If the field strength at the cathode surface is made sufficiently large all areas emit with their saturation current. The total current is the sum of the currents of the individual patches and is consequently determined by the area and the work function of the patches:

$$J_{sat} = \sum_i f_i J_{i_{sat}} \tag{19}$$

For this type of emitter the use of the Richardson equation for describing the emission of the whole specimen is arbitrary. Therefore in the case of polycrystalline metal cathodes, and even more in the case of composite surfaces, it might be better to describe the saturated current density of such cathodes as a function of temperature by means of an empirical equation, as has been suggested by Nottingham[41]. He suggested the form:

$$J_{sat} = a \exp\left(-\frac{e\phi}{kT}\right) \tag{20}$$

which fits well with the experimental results.

Both constants a and ϕ, the latter called work factor, are dependent on the material of the cathode, and on its crystallographic configuration. No certainty exists that the same material used by two experimenters under different conditions will show the same values of a and ϕ. The determination of a and ϕ must obviously be done from the saturated emission current.

On the other hand, realising the arbitrariness of the Richardson formula to describe the electron emission as a function of temperature, no great objections can be made if this formula is maintained with the necessary indication that the emission constant and the work function are not the universal emission constant multiplied by $1 - \bar{r}$ and the true work function. The emission density of a non-ideal surface, calculated from the current obtained at a sufficiently high field at the surface and the geometrical area, is therefore described by the equation:

$$J_{\text{sat}} = A_R T^2 \exp\left(-\frac{e\varphi_R}{kT}\right) \tag{21}$$

where A_R is the apparent value of the emission constant which has been called Richardson emission constant to distinguish it from the "apparent" emission constant A^* which will be defined later. The quantity φ_R is likewise called the Richardson work function (see E. B. Hensley[42]). The constants A_R and φ_R are determined from the Richardson plot $\ln (I_{\text{sat}}/T^2) \sim 1/T$. Referring to eq. (19) it is evident that it is generally impossible to relate these constants to the physical picture of the cathode surface under investigation. It is also impossible to draw any further conclusion about the temperature coefficient of the work function, as the A_R value contains strongly the influence of the patches. Assuming a certain configuration of patches a calculation of the resulting A_R and φ_R values can easily be made. The knowledge of these values alone, however, does not allow one to draw a conclusion about the configuration of the patchy surface. Measurements about the homogeneity of practical cathodes, to be discussed later, have shown that the deviation of A_R from the theoretical value 1.2×10^6 A/m^2 °K^2 is mainly due to the fact that only part of the cathode surface actually contributes to the emission. The use of the two constants φ_R and A_R is therefore advantageous, because it allows one to distinguish more or less between two factors which determine the emission of a practical cathode: (*a*) the potential barrier at the cathode surface and (*b*) the actual emitting area.

The emission characteristic of a practical cathode can also be described accurately enough by one constant, a kind of average work function also called effective work function[42]. Starting from eq. (19) one can write:

$$J_{\text{sat}} = \sum_i f_i J_{i_{\text{sat}}} = AT^2 \sum_i f_i \exp\left(-\frac{e\varphi_i}{kT}\right) = AT^2 \exp\left(-\frac{e\varphi_E}{kT}\right)$$

$$\varphi_E = -\frac{kT}{e} \ln \sum_i f_i \exp\left(-\frac{e\varphi_i}{kT}\right) \tag{22}$$

This constant φ_E however, bears no relation to the potential barrier at the cathode surface.

Quite often a Richardson curve is constructed using saturated currents which have been corrected for the influence of the accelerating field (the Schottky effect). The work function and the emission constant obtained in this way are usually called the apparent work function, φ^*, and the apparent emission constant, $A^{*(10)}$. Unfortunately these same constants have also been called Richardson work

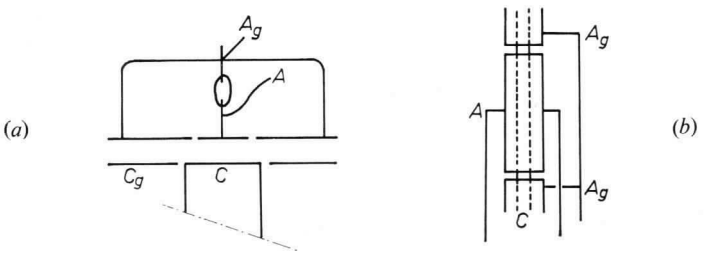

FIG. 14. (*a*) Schematic drawing of a plane-parallel diode with guard rings C_g and A_g around cathode C and anode A.
(*b*) Schematic drawing of a cylindrical diode with guard electrode A_g. C—cathode, A—anode.

function and Richardson emission constant[11]. Difficulties arise when the slope of the Schottky line—ln I_a versus $V_a^{\frac{1}{2}}$—deviates from the theoretical one, a phenomenon which often occurs. The problems related to this deviation will be discussed below.

The measurements of the constants A_R and φ_R are carried out in a plane-parallel configuration if the cathode is available in a flat form and in a coaxial cylindrical one in the case of a cylindrical cathode. Care must be taken to prevent spurious currents from reaching the anode. Suitable constructions for a plane-parallel diode and the cylindrical version are given in Fig. 14*a* and *b*. At low cathode temperatures the current will be small and the measurement can be carried out by applying a sufficiently high d.c. voltage between cathode and anode to assure saturated emission. The disadvantage

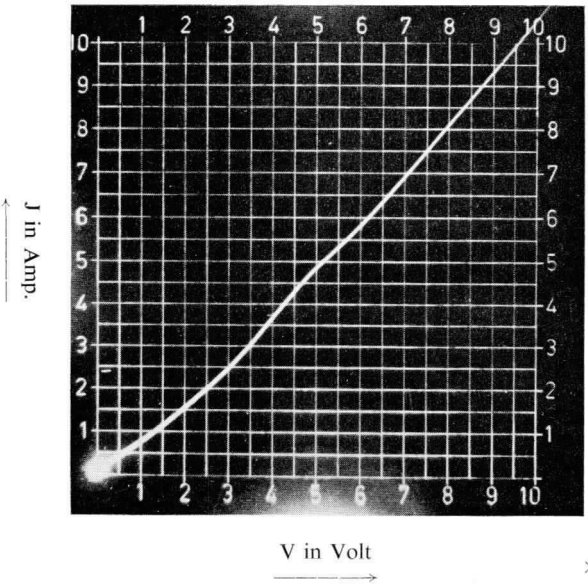

FIG. 15(*a*) The space charge characteristic of a diode measured with pulses from a discharging capacitor with $RC = 10^{-4}$s. Repetition frequency 40 c/s. The so-called 10-volt effect, due to secondary electrons from the anode, is clearly visible. Full horizontal scale 20 V, full vertical scale 4.10^{-2} A.

$\times 6.25 \times 10^{-2}$

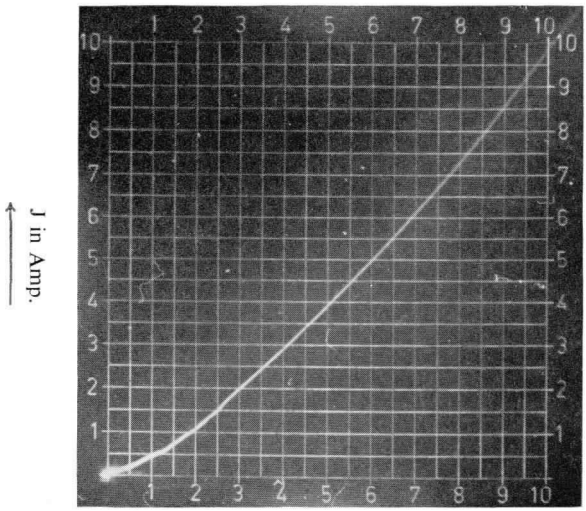

FIG. 15(*b*) The space charge characteristic of a diode measured under the same electrical conditions as given in the subscript to Fig. 15(*a*). Full horizontal scale 100 V, full vertical scale 0.625 A.

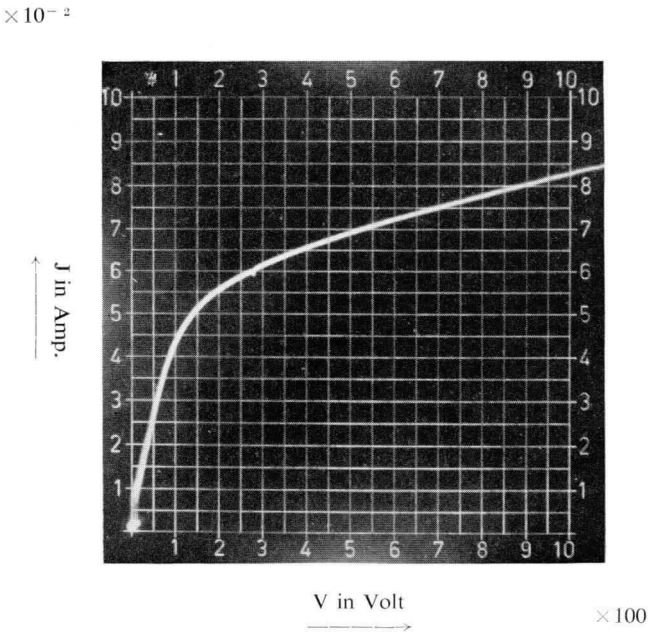

FIG. 15(*c*) The transition from space charge limited current to saturated current in a diode. Conditions as in Fig. 15(*a*). Full horizontal scale 1000 V, full vertical scale 0.1 A. The temperature has been decreased in order to obtain saturation at the highest applied voltage.

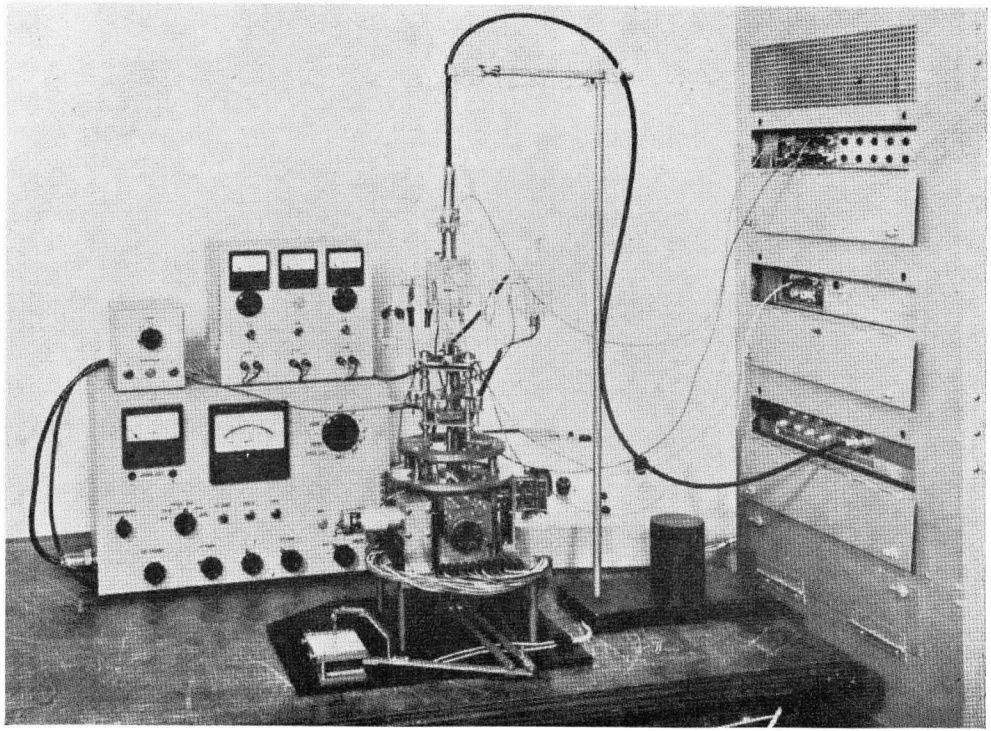

FIG. 16. The apparatus used for the measurement of the current distribution of a cathode. The upper part of the tube contains the anode with a hole and a collector, the lower part contains the cathode which is moved automatically in a zig-zag fashion.

of this method is the high probability of cathode contamination due to products released from the anode. At the normal operating cathode temperatures it may happen that the heat generated in the anode during current flow is excessive. In this case the applied voltage must be pulsed with a sufficiently low duty cycle. It may be advantageous to use pulses obtained from discharging a condenser, so that the voltage decreases during the pulse. A display of the I–V_a characteristic on the oscilloscope screen can then easily be obtained and it can be seen whether or not saturation has been reached. See Fig. 15*a*, *b* and *c*.

The Schottky effect tends to increase the saturated current. Measurements at a few values of the voltage in the saturated region permit the extrapolation to zero field according to the formulae (17) valid for the plane-parallel configuration. It is not always easy, however, to ascertain when saturated emission has been reached. At a patchy surface the transition from the space charge region may be very indistinct. The transition region is not only due to the difference in field strength necessary to saturate the emission from different patches but also to the cancellation of the field, caused by the mutual interaction of the individual patches. The exact Schottky line may only be expected when this patch field has become sufficiently small compared to the applied field. The dimensions of the patches and their work function differences determine the extent of the transition region. If the theoretical slope of the Schottky line has not been reached it is properly speaking not permissible to extrapolate the $\ln J_{\text{sat}}$ versus $V_a^{\frac{1}{2}}$ curve to zero voltage and to use the $(J_{\text{sat}})_0$ so obtained. Even the statement of the proportionality factor between the experimentally determined slope and the theoretical slope, calculated from the macroscopic geometry, is insufficient, as this factor is not a constant over the range of applied voltages. It is better then to state the field strength at the cathode as calculated from the macroscopic geometry and the applied voltage.

The other important property of the electrons, their energy distribution, will usually be determined in the same structure, Fig. 14*a* and *b*. In the cylindrical case the applied voltage is only indirectly a measure of the energy. In this case the tangential component of the velocity contributes to the measured current. A suitable displacement of the $\ln I$ versus V_a curve is necessary[43].

It has been mentioned already that only at sufficiently high negative anode voltage is the $\ln I$–V_a relationship represented by

a straight line, the slope of which can be used for the calculation of the cathode temperature. There is no reason to believe that this behaviour will not be found. However, if the anode voltage is not low enough, so that the emission from the highest work function patches becomes saturated, the electrons coming from these patches gain energy in the existing field. The energy distribution will start to deviate from the Maxwellian distribution and the $\ln I$–V_a relationship is no longer represented by a straight line. The character of this curve will be determined completely by the configuration of the patchy surface. It may be that a certain part of the curve will be almost straight, but the slope will in general not correspond with the cathode temperature. Under practical conditions the electrons emitted by the cathode are accelerated towards another electrode. If the energy distribution under these conditions must be determined another technique must be used. This technique, which is of great importance for porous composite surfaces, will be described in section 2*d*.

Knowledge of the inhomogeneity of the emission of polycrystalline surfaces is necessary to explain the observed currents in a more quantitative way. Experiments with the electron emission microscope have given information about the distribution of the current over the surface. This information is, however, mainly of a qualitative nature. The observed picture is not always easy to interpret. In the usual design no measurement can be made of the current coming from any given small area. See, however, the design of Schenk[43a]. It is of course of fundamental importance to be able to study the cathode in almost the same environment as in actual practice, but the vacuum conditions in the usual emission microscopes are certainly not the same as they are in radio valves. The instrument must be constructed in such a way that the field at the cathode surface is sufficiently high, so that at the normal operating temperature the electron trajectories are practically unhindered by space charge. The microscope described by Popov and Druzhinin[44] seems to fulfil the requirements better than the older designs. Instruments of this kind will be of great value in the further study of the patchy surfaces characteristic of practical cathodes[44a].

Some approximate information can be obtained from the transition of space charge current into saturated current about the work function differences and the dimensions of the patches[45]. From the transition of the retarding field current into space charge

current it is also possible to obtain some knowledge of the patchy structure[46]. Recently another method has been used by Jansen, Venema and Weekers[47] which supplies the required information in a more quantitative way, but still with certain limitations. Although the instrument used in these studies has so far mainly been applied to oxide-coated cathodes and dispenser-type cathodes, the principle is of general interest and will be discussed here. See Figs. 16 and 17. The measuring device consists of a flat cathode and parallel anode with a small hole (diameter 10 μm) which is scanned by the cathode. Rectangular pulses are applied to the cathode. A part of the electrons drawn to the anode passes through the hole

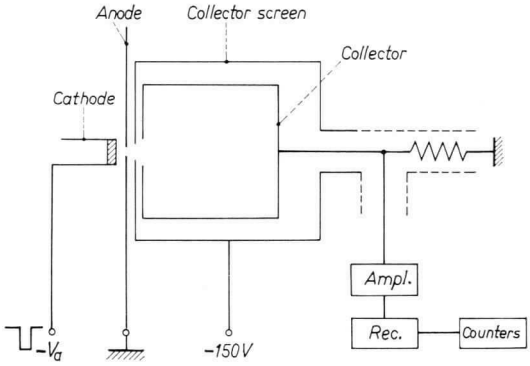

FIG. 17. Electrode system used for the measurement of the current distribution. The hole in the anode had a diameter of 10 μm.

and reaches the collector behind the anode. By changing the position of the cathode with respect to the anode hole a measurement of the current distribution along the cathode surface can be made. In the first experiments, the resolution in surface area was about 25 μm. The advantage of this method, as compared to, e.g., the electron emission microscope, is the rather simple set-up which allows the study of cathodes during life. Although the resolution is not too high with this type of instrument interesting results have already been obtained (see p. 253). It is to be expected that a resolution of a few microns may be reached by the use of a smaller hole and a longitudinal magnetic field. A scanning technique, involving the magnetic collimation of the electron flux from the cathode has recently been used by Stanier and Mee[47a].

(*c*) SINGLE CRYSTAL SEMICONDUCTING CATHODES

Emitters of this type, although of the greatest importance for the understanding of practical cathodes, have hardly been investigated. The work started by Sproull[138] seems to have been finished without providing a final explanation of the mechanism of operation of the alkaline earth oxide-coated cathode. It must be admitted that the technique of making and handling single crystals of barium, strontium and calcium oxide and of mixed crystals is not easy. In addition it may be said that a practical cathode constitutes a structure far removed from the ideal crystal, which has an important bearing on the way it functions.

The fact that the number of charge carriers in a semiconductor is many times less than in a metal results in the phenomenon of internal space charge near the surface under the influence of an external field (see p. 193)[48]. This field, penetrating the crystal, causes the charge carriers to move to or from the surface depending upon their sign and the direction of the applied field. A positive field needed when determining φ, attracts the electrons to the surface, causes the bands to bend downwards and decreases the work function; an increased electron emission must result. It can, however, be shown that the influence of surface states may completely dominate the field effect. If the contribution of the surface states is important the external field does not penetrate into the semiconductor. The problem of the mirror image force can then be treated in the same way as has been done for a metal.

Another effect appears if electrons move in a field in a semiconductor. They will gain energy and their temperature may well be higher than that of the lattice. It is not impossible that such an effect contributes to an increase in the emission current[49]. This current is indeed very sensitive to the electron temperature.

Apart from the emission properties, the conduction properties are also of importance. The phenomenon of bulk conductivity has been considered on p. 192, that of surface conductivity on p. 197. The shape of the crystal and the geometry of the structure used in the measurement determine which type of conduction is predominant. The type of charge carriers which dominate in the conduction mechanism can be determined from the Hall coefficient or from thermoelectric measurements.

Measurements of the emission and the bulk conductivity of barium oxide single crystals have been carried out by Kane[50].

The crystals were activated by a heat treatment up to a temperature of 1400°K (activation, see p. 238). The $I-V_a$t characteristic gave a strong indication of the presence of a patch field. At the various states of activation, the emission and conductivity readings were taken at a temperature of 1000°K, with the surprising result that no correlation could be found between these quantities. A proportionality was to be expected for a Wilson type of semiconductor. Kane concludes from these results that surface states are responsible for the great difference in electron density at the surface and in the interior.

(*d*) POLYCRYSTALLINE COMPOSITE SURFACES

As far as the patchiness of the surface is concerned the picture developed for the inhomogeneously emitting metal cathodes also holds for composite surfaces. The measurement of the emission constant A_R and the work function φ_R follows the same lines with structures as given in Fig. 14*a* and *b*. As the resistance will in general not be too great, the anode voltage required to reach saturated emission will only be slightly higher than that required in the absence of a resistance. However, the resistance usually has such a value that the saturated current, if drawn continuously, would cause an excessive heat production. In this case, therefore, pulse measurements with low duty cycle are necessary. As soon as the space charge potential minimum reaches the cathode at the high work function areas, saturation starts at these places. The patch field helps in establishing this condition. With increasing field strength the whole cathode gradually becomes saturated and the Schottky influence of the field on the work function starts to play a part. This influence will not be very different from the effect observed with metal cathodes. The field inside the semiconductor may also show its influence, but it will be disturbed by the patch field which also penetrates the crystals. A very complicated situation exists which is difficult to survey.

The so-called intersection method, in which the graph representing the retarding field current as a function of the anode voltage on a semi-logarithmic scale is extrapolated towards high values until it intersects the graph representing the saturated current as a function of the anode voltage, results in the determination of a φ value which is about equal to φ_E (see p. 224). Consequently a conclusion about

the actual A_R and φ_R values cannot be obtained by applying this method[51].

The measurement of conductivity is usually done in a plane-parallel structure, the layer under investigation being slightly pressed between parallel metal plates[52]. It is also possible to use a rod of non-conductive material provided with electrodes in the form of two spirals[53,54]. The material which is being investigated is applied to the rod by a spraying or dipping technique. Other designs for measuring the conductivity directly used a probe in the coating, or applied wires coated with alkaline earth oxide and twisted afterwards. It is important for the interpretation of the experimental results to keep the geometry in mind[55]. Eisenstein also applied a different method[56]. His diode structure contained an anode with a hole. The electrons passing the hole are decelerated by a potential difference between the anode and a collector until their energy is almost zero. The retarding potential required to reach this point is the energy gained between cathode surface and anode. By using two different anode voltages, causing different cathode currents and consequently different surface potentials and by determining the shift of the retarding field characteristic, caused by the change in surface potential, the resistance in the cathode can easily be determined. As will be shown later, various cathode properties can be determined by this method. The determination of the surface potential can also be done by means of a measurement with a movable anode and extrapolation to zero distance[57].

The energy distribution of the electrons can be determined in the various ways described under (*a*). It is, however, obvious that the situation is more complicated now, especially in the case of porous emitters. A current emitted by the cathode will cause a potential drop in the coating. In a porous structure, electrons emitted from places at different potential may reach the anode. In this case it is to be expected that the energy distribution will deviate from the Maxwellian. As already explained in (*b*) on p. 226, the inhomogeneously emitting surface promotes this effect. The coating resistance, like the emission, is not homogeneously distributed. Another cause for a difference between cathode temperature and electron temperature may be found in the " heating " effect. The electrons, when passing a potential difference, present in the interior of the grains, may be accelerated to higher velocities than correspond to the temperature of the grains[49]. Under appropriate conditions,

however, the method may be used for cathode temperature measurements[58]. As has been indicated already, it is advantageous to accelerate the electrons first, simulating in this way practical conditions. Resistance effects will then be more pronounced. A structure similar to that proposed by Eisenstein[56] can be used to carry out the analysis. In this way Bulyginskii and Sibir[59] studied L-cathodes and Bulyginskii and Dobretsov[60] investigated oxide cathodes. The structure used by Jansen, Venema and Weekers[61] is shown in Fig. 18. The diameter of the anode hole in this structure is usually 100 μm. Pfetscher and Veith[62] used a design based on the same principle for a study of cylindrical cathodes.

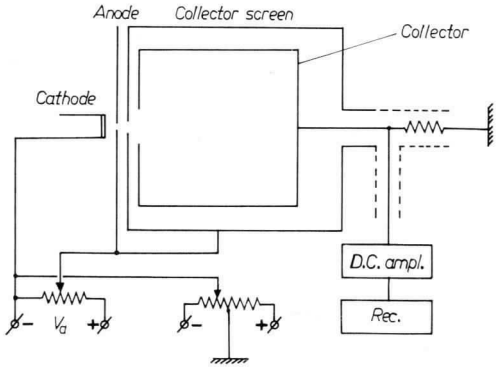

FIG. 18. Schematic picture of the electrode system used for the determination of the energy distribution of the emitted electrons. The d.c. amplifier is practically at earth potential, the cathode potential can be varied by means of a potentiometer while the anode voltage and screen voltage are fixed at different values.

The distribution of the emitted current over the surface can be investigated with the same type of apparatus used by Jansen, Venema and Weekers as described under (*b*).

3. Measurements in practical tubes

In section 2 a description was given of measurements carried out with specially designed apparatus. In this way a particular quantity can be determined under carefully controlled conditions which will generally not be found in actual practice. For a fundamental study any difference between the practical conditions and those used in the

study is probably unimportant for it may be expected that any theory developed with the results obtained in the special apparatus will also largely hold for a cathode used in a practical tube. However, it is certainly necessary to be careful in this respect. When two types of cathodes have to be compared, it is to be expected that the results of measurements carried out in special structures may be applied to practical tubes, particularly if large differences exist between the two types. But reliable measurements of thermionic cathode properties under practical conditions must always be the ultimate aim.

Unfortunately, however, a practical tube does not generally provide a structure suitable for the desired measurements for there is often doubt about the actual surface area of the emitting part of the cathode and about the cathode temperature which may vary considerably along the cathode surface. Thus in general it is impossible to use a practical tube for accurate measurement of the emission capability of the cathode. What is possible, however, is the comparative measurement of various properties in different samples of a particular type of tube, a matter of great importance for tube production.

An intermediate approach has been described by Nottingham[63] who has carefully considered the problem of cathode evaluation, particularly with the aim of applying conditions which approach those used in practice. The basis of his approach is a thorough treatment of the theoretical I–V_a characteristic of a diode in the retarding- and space charge-current region. The voltage values which separate the space charge-current region from the retarding field region and from the saturated current region are given special attention. In order to interpret thoroughly an experimentally determined characteristic a comparison is made with the theoretical curves, which hold for various values of the saturated current. The calculation of these so-called master curves, which are valid for a homogeneously emitting cathode, is made quite easy by the use of a number of tables given by Nottingham. The voltage range which is applied in the evaluation is small and in accordance with the values used in practice. However, to obtain information regarding the saturated emission and hence of the values of the work function and the emission constant, the temperature of the cathode must be kept sufficiently low, far below the normal operating temperature. Apart from the assumption of a uniformly emitting cathode, which is

certainly not true in practice, the use of the low temperatures seems to be rather dangerous. There is no guarantee that the cathode properties at normal temperatures will be deducible from those obtained at low operating temperatures, even if a particular temperature coefficient, based on experimental and theoretical considerations, is taken into account. Furthermore, the gas composition may be different at different temperatures and may influence the cathode properties. Hung's results on oxide cathodes[64], quoted by Nottingham, seem to confirm this. It must be noted further that the temperature measurements have to be made by means of thermocouples, which generally excludes the use of practical tubes for the required measurements.

The comparative merits of various radio tube materials as regards their effect upon the electrical characteristics can best be determined in a standard diode. Such a diode is described in A.S.T.M. Designation F270–56[65]. It has the advantage that it is less complicated than a practical tube but provides a structure comparable to it.

The measurements which will be described here can be carried out not only with standard diodes but with almost any kind of tube.

(*a*) EMISSION MEASUREMENTS

Several methods for checking the emission properties of the cathode in a practical tube have been used. Pulse methods in which multi-electrode valves are operated as diodes, all electrodes except the cathode being connected together, may yield information about the saturated emission. These methods suffer from the risk of damaging the cathode because much greater current densities are drawn than in normal operation. Furthermore the voltage used differs markedly from that applied normally and experience shows that emission characteristics obtained in this way do not always correlate with the emission behaviour found under normal operating conditions. The correlation is much better when the under-heating characteristic is used[66]. With fixed voltages applied to the various electrodes, such as the grids and the anode, the heater power is varied by changing the heater voltage. The anode current then measured is a function of heater input which is directly related to the cathode temperature. At low temperature the saturated emission is drawn and this emission changes very rapidly with temperature. Consequently, as the cathode temperature is raised from a very low level where the current is practically zero, a sharp rise in anode

current is observed at a certain heater voltage. With increasing heater input the rate of rise of current decreases and finally levels off. Under complete space charge conditions the current is quite insensitive to temperature. The point of transition from temperature-limited to space charge-limited emission, known as the knee temperature, serves as a characteristic of the emission properties of the cathode. See Fig. 19. Not only the knee temperature but also the shape of the curve may give information about the cathode, e.g. its homogeneity. It will be evident that this shape is further determined by the geometry of the tube and the applied voltages. The method is therefore suitable for comparative measurements on one particular type of tube.

An alternative method, which is sometimes used to measure the underheating characteristic, is to start from normal operating conditions and then to switch off the heater voltage suddenly. The change of anode current with time is then observed.

(*b*) RESISTANCE MEASUREMENTS

If the cathode resistance has a sufficiently high value it will influence the electrical properties of the tube in which this cathode is used. In practice only space charge-limited currents need be considered. Denoting the cathode current by I_c and the resistance by R_c the potential of the cathode surface is raised by the amount R_cI_c and the potential differences in the tube between the cathode surface and other electrodes change correspondingly. In a diode, the anode voltage which has to be used for the calculation of the current becomes $V_a - I_cR_c$. As R_c will generally be a function of the current and as moreover the cathode emission is quite inhomogeneous, resulting in a combination of more or less space charge-limited emitting areas, the I_c–V_a characteristic may deviate markedly from the theoretically expected behaviour. The contact potential difference and the cathode inhomogeneity, being unknown in practical cases and sometimes the 10 V effect (see Fig. 15*a*), prevent the use of the I_c–V_a characteristic for a determination of R_c, except for large values of R_c. For triodes, tetrodes, etc., the same considerations hold if the I_a–V_g characteristic or its derivative is used. In particular the change in the transconductance $g_m = (\partial I_a/\partial V_{g1})_{V_a}$ can be used to follow changes in resistance during life, if it is assumed that other factors which influence the I_a–V_{g1} characteristic remain constant or can be neglected. With a resistance

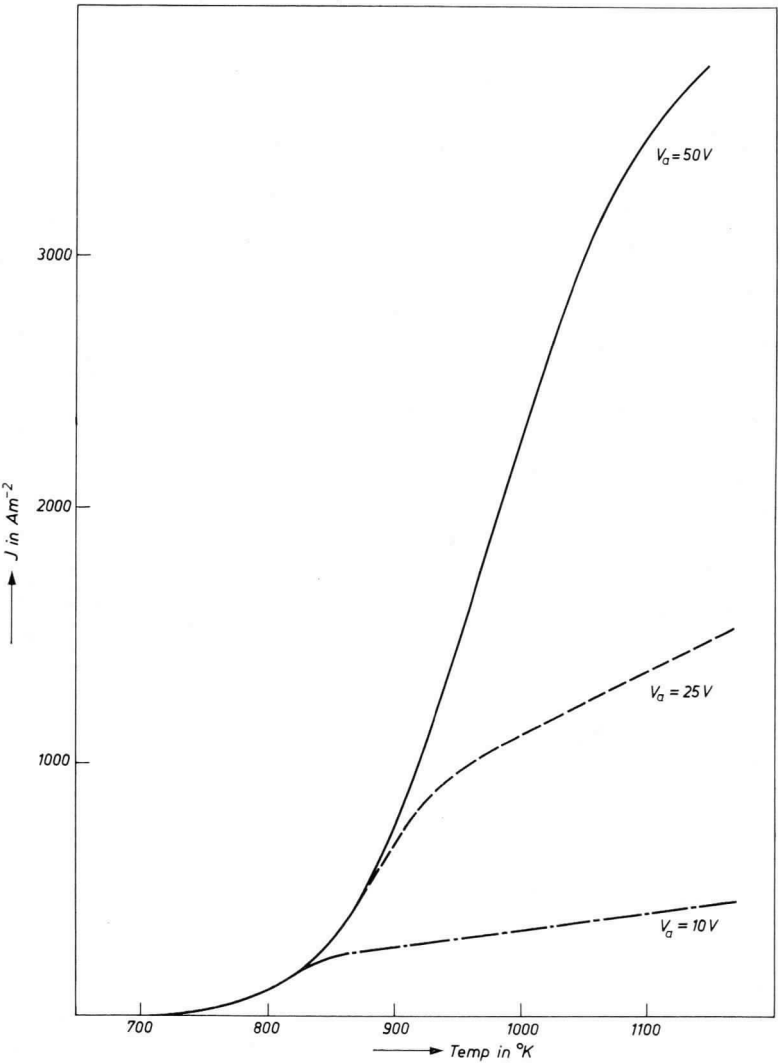

FIG. 19. The underheating characteristic of a cathode for different values of the anode voltage.

R_c the value of g_m becomes:

$$g_m = \frac{g_{m_0}}{1 + \alpha R_c g_{m_0}}$$

$\alpha = I_c/I_a$ and g_{m_0} is the value of g_m for $R_c = 0$.

A different method of determining changes in the cathode resistance has been suggested by Horsfall[67]. In this method the first grid of the tube is at a small positive potential with respect to the cathode via a large resistance (~ 0.1 MΩ). The diode impedance between grid and cathode surface is therefore almost constant, which enables the grid to be used as a probe for the measurement of the cathode surface potential. The application of an alternating voltage to the anode, in addition to the normal d.c. voltage, causes an alternating current in the tube, and due to the cathode resistance an alternating potential of the cathode surface. The grid is now used as a probe and its a.c. potential measured. Another measurement yields the alternating anode current and from these results the cathode resistance can be derived. The analysis shows that the ratio of grid voltage and anode current is not directly the cathode resistance, but that a constant term, depending on the tube parameters, must be subtracted from the calculated resistance. As this term is constant during life the method is applicable to the determination of resistance changes in the course of life. Moreover, this extra term can be determined fairly accurately in the beginning, so that the method is also useful for absolute measurements, although with some restrictions.

The resistance is usually not distributed homogeneously throughout the thickness of the cathode. The so-called interface resistance in oxide-coated cathodes is found in a thin layer near the metal base and is due to badly conducting compounds, formed by the reaction of the alkaline earth oxides and impurities in the base metal. To determine this interface resistance separately, use is made of the rather high capacitance of the interface. The principle of one method[68] for its determination consists of a measurement of g_m at a low (10 kc/s) and at a high frequency (10 Mc/s). At the high frequency the resistance is short-circuited by the capacity of the interface and from the difference in g_m values the resistance can easily be computed. In another method[69] rectangular current pulses are fed through the cathode and the tube, and the voltage across the tube, operating under space charge conditions, is observed. Due

to the resistance R_{ci} and the capacitance C_{ci} of the interface layer, the voltage across the layer builds up according to:

$$V_i = I_c R_{ci} \left\{1 - \exp\left(-\frac{t}{R_{ci}C_{ci}}\right)\right\}$$

in which I_c is the current flowing during the pulse. From the shape of the voltage pulse across the diode, the voltage between cathode surface and anode being constant, the value of R_{ci} is easily determined.

Improvements to the standard techniques, in particular for the determination of smaller resistances, are described by Tamaya[70] and Frost[71]. The first and two other methods are suggested in the A.S.T.M. Test methods for interface impedance, designation F300–57T[72].

(*c*) NOISE MEASUREMENTS

These measurements may be performed with the object of gaining knowledge of the noise phenomenon itself, and with the particular object of obtaining a better understanding of the physics of cathodes, as in the work of Hannam and van der Ziel[73]. Another object may be the use of the shot noise values to check the emission properties of cathodes, particularly in practical tubes. As has been mentioned in section A8, this noise is reduced considerably by space charge. A tube with a cathode that is far from homogeneous, may show an $I_a - V_{g1}$ characteristic which is typical of space charge conditions. However, an area with poor emission may still be present and may contribute to the current. Although its influence in this respect is small, its contribution to the noise level may be quite large because this contribution is not very much decreased by space charge, contrary to the noise from the better emitting areas. So two comparable cathodes may show a negligible difference in current but a large difference in noise level. Thus a noise measurement may provide a better understanding of the patchiness of the cathode surface and may serve as a tool for the study of cathodes processed under different conditions[74].

C. VARIOUS TYPES OF THERMIONIC CATHODES

I. Alkaline earth oxide-coated cathodes

1. INTRODUCTION

Of the various types of thermionic cathodes the alkaline earth oxides are by far the most commonly used, the reason being that this type of cathode shows the lowest work function. Therefore relatively

low temperatures (900–1200°K) can be used so that a good efficiency is obtained. Practical cathodes consist of the double oxide of barium and strontium or of the triple oxide of barium, strontium and calcium. As the oxides are difficult to handle—they are readily attacked by water vapour and carbon dioxide—the cathodes are prepared from compounds. In almost all cases the carbonates are used and are decomposed during the pumping process to leave the oxides. The cathode, in order to be a good emitter, must be subjected to an activation process. During this process the electron emission, which is usually very small after the decomposition and varies considerably from cathode to cathode, increases strongly and reaches a final value which shows generally a much smaller spread than is observed in the beginning. In this activation process the surroundings of the cathode play an important part because the gas composition too must stabilize. The activation is favoured by the presence of reducing elements in the nickel—" activators "—and in addition current flow through the cathode usually has a pronounced effect on the activation. Therefore elements present in the nickel core, such as magnesium, aluminium and silicon, have a beneficial effect on the cathode properties especially at the beginning of life. At every stage in the preparation of the cathode, great care must be taken to prevent contamination. This holds not only for the core and for the carbonates but also for other components in the tube, and for the glass of the envelope. Particularly dangerous are chlorine[75] and sulphur[76].

A great deal of work has been done to arrive at an understanding of the principle of operation of the oxide cathode. After some sixty years of study, which was quite intensive during certain periods, it must be said that a completely satisfactory picture has still not been obtained. This is partly due to the extremely complex circumstances prevailing during normal operation and partly because the oxide cathode was in practical use long before the physical theories necessary to explain its behaviour had been developed. It may be that a full understanding of the mechanism of operation will be reached only after the period during which the oxide cathode has found its widest application.

2. THE CORE METAL

The type of cathode application determines the choice of the core metal. Nickel is favourable in the case of indirectly heated cathodes.

Chemically it is sufficiently stable towards the oxides, and evaporates very slowly at the operating temperature. It can be degassed quite well and has a rather low heat conductivity and thermal emissivity which is of importance for the heat economy of the cathode. Copper has been suggested as a core material because of its low thermal emissivity but the temperature range in which this metal can be used is too small for mass production purposes. For directly heated cathodes the tensile strength of nickel is too low at operating temperatures and certain nickel alloys or tungsten have to be used.

The reducing elements originally put into the nickel to improve the workability have been shown to be of vital importance to the operation of oxide cathodes. At the high temperatures used during processing and in actual operation, these impurities diffuse towards

TABLE 1

ASTM grade no.	Manganese per cent	Carbon per cent	Magnesium per cent	Silicon per cent	Tungsten per cent
		Active alloy type			
3	0.13	0.06	0.04	0.20	—
4	0.07	0.05	0.005	0.19	—
6	0.005	0.04	0.004	0.19	—
7	0.05	0.03	0.03	0.03	3.98
10	0.18	0.09	0.07	0.03	—
11	0.12	0.06	0.04	0.03	—
		Passive alloy type			
21	0.005	0.03	0.005	0.01	—
22	0.005	0.03	0.005	0.01	—

the surface where they react with the oxide. The number of elements present in commercially available nickel alloys, which are reducing and are usually called activators, is rather small. They are listed as follows: carbon, zirconium, magnesium, manganese, aluminium, silicon and perhaps tungsten. The amounts present differ for the different kinds of alloys, as is evident from the figures in Table 1[77]. It should be realized that the normal methods of analysis yield the total amount of a particular element, although it may be present in the alloy in the active or in an inactive state, sometimes referred to as " free " and " combined ". Only the active content of the reducing element is of importance. It is commonly assumed that the

impurity elements are distributed homogeneously through the nickel, but this is certainly not always the case. The process in which the nickel tubing for indirectly heated cathodes is made may influence the active amount of reducing elements originally present. Moreover, in the process of decomposition of the carbonates part of the content of reducing elements may become oxidized. The governing factor in the operation of the cathode is of course the amount of active element left which can reduce the oxides. The total amount of reducing elements is directly proportional to the thickness of the nickel sleeve, which is usually determined by mechanical requirements. Properties such as temperature distribution along the cathode and warming up time are also governed by the thickness of the nickel tube. In practice a value between 0.05 and 0.1 mm is chosen. The sleeve is either made from tube or from sheet which is folded. Folded, lock-seam sleeves are cheaper than tubes and are therefore widely used.

Two aspects of the reducing elements are important: firstly their chemical behaviour towards the alkaline earth oxides, secondly their diffusion through the alloy towards the surface. The chemical aspects of the combination of oxide and activator have been treated by White[78] and by Rittner[79]. Both authors have made thermochemical computations of the equilibrium pressure of barium resulting from the reactions between the alkaline earth oxides and the activators in the alloy; see Appendix I. The *free* elements magnesium, zirconium, aluminium and silicon are very active and the equilibrium pressure at 1000°K equals the pressure above solid barium, which obviously constitutes the highest limit. Carbon yields an equilibrium pressure at 1000°K of 4×10^{-6} torr and tungsten of 2×10^{-9} torr. If these reducing elements are present in the nickel the barium equilibrium pressure will usually be lower due to the formation of solid solutions. The pressure is then a function of the concentration if saturation has not been reached. In a particular case the available data usually allow the " approximate " calculation of the equilibrium pressure.

The diffusion of the active elements in the nickel core is treated mathematically by the introduction of the diffusion constant D, which is a function of temperature and written as:

$$D = D_0 \exp\left(-\frac{E_{\text{diff}}}{RT}\right)$$

Values of D_0 and the activation energy E_{diff} are known for all the elements which have been mentioned and are given in Table 2[80,81].

It is not known how great the equilibrium pressure of barium in a fully activated oxide cathode must be. This pressure is determined not only by the rate of evaporation of barium from the coating but also by the presence of "poisoning" agents, which include chemically active gases and ions of the residual gas bombarding the cathode. Moreover, activation may also be caused by gases such as hydrogen, or methane, found in varying amounts under practical conditions. A calculation (see Appendix II) of the amount of activator arriving at the surface of the core per m^2 and per sec may, however, be carried out for special alloys. Assuming that this amount of activator reacts with barium oxide, the amount of barium produced per m^2 and per sec is also known. This assumption is certainly true for magnesium, silicon, aluminium and zirconium.

TABLE 2

Activator	$D_0(m^2/s)$	$E_{diff}(J/mole)$
Al	1.87×10^{-4}	2.68×10^5
Mn	7.50×10^{-4}	2.81×10^5
Mg	0.44×10^{-4}	2.37×10^5
Si	1.50×10^{-4}	2.58×10^5
W	11.2×10^{-4}	3.10×10^5

In Fig. 20a and b Kern's results of the calculations for several single additive nickel alloys are shown, together with the results of life tests obtained with cathodes made with these nickels[82]. For sufficient emission under these particular circumstances a barium supply rate of 10^{14}–10^{15} barium atoms/m^2 sec corresponding to a barium pressure of 10^{-10}–10^{-9} torr is needed.

The formation of an interfacial layer of a chemical compound between the nickel core and the alkaline earth oxides may hinder the diffusion of the impurities towards the oxides. Also the diffusion coefficient for a particular element as measured in nickel, containing this element as the dominant alloying constituent, may differ from the diffusion coefficient for this element when it is present together with other impurities in comparable amounts[83]. Furthermore, the metallurgical history of the nickel used in cathodes, in particular

its surface state, may influence the diffusion of the activators to the oxides.

So far only the reduction of barium oxide has been discussed, but for practical cathodes it is also necessary to consider the reactions with strontium oxide and calcium oxide, if present. Thermodynamical calculations show that the equilibrium pressure of

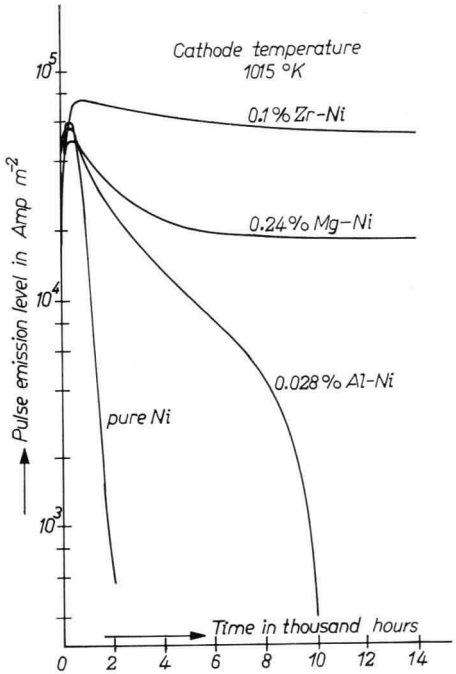

FIG. 20(*a*). The pulse emission of alkaline earth oxide cathodes on single additive nickel alloys as a function of life. From Kern, H. E., *Bell Lab. Rec.* **38**, 451 (1960).

strontium, resulting from the reduction of the oxide, is at least one order of magnitude lower than that of barium, while the calcium pressure may be considered negligible. The reduction of strontium oxide has been followed by means of the radioactive tracer technique and has been correlated with the diffusion of the activators in the nickel on the one side and with the thermionic emission on the other[80].

In practical circumstances the situation with respect to the chemical reactions of activators and oxides is extremely complex. Without sufficient knowledge of this situation calculations of equilibrium pressures are only of very limited value. Whether the nickel itself has an influence on the emission properties of the oxide cathode is a question to which no clear answer has yet been given[84].

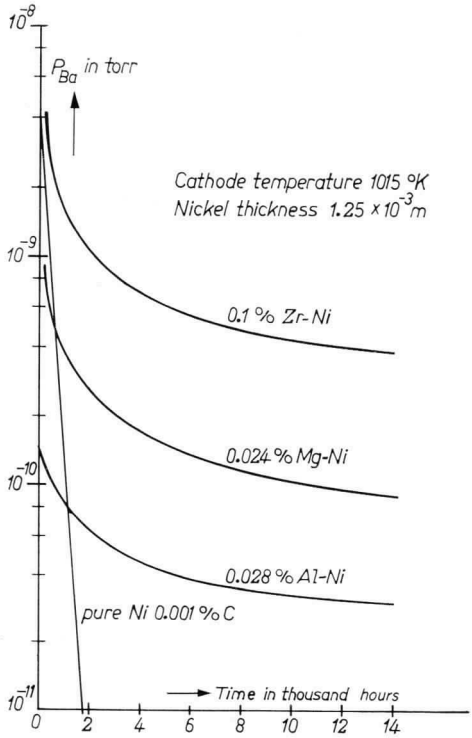

FIG. 20(*b*) The barium pressure, produced by reduction of the oxide cathode on the various single additive nickel alloys also as a function of life (from Kern). The barium pressure must be higher than about 6×10^{-11} torr to obtain a reasonable emission.

3. THE COMPOUNDS USED FOR THE COATING AND THEIR PREPARATION

Nowadays, the only important source of the oxides are the carbonates, the reason being that the carbon dioxide which is produced during decomposition does not react too strongly with the materials

present in the valve. In addition it helps in removing the carbon left over from the binder present in the carbonate paste. The carbonate is made by precipitation from an alkaline earth nitrate solution by means of ammonium or sodium carbonate. The resultant particles may be in the form of spherulites or needles, depending on the temperature, pH and concentration of the solutions. The spherulites are agglomerates of smaller particles. Particles of colloidal size can be obtained under appropriate conditions. The size of the particles used in actual practice varies from a few to several tens of microns. The carbonates are mixed with solvents and usually with a binder, and then stirred or ball-milled to a paste which is applied to the nickel sleeve. Experiments have shown that the mixed crystals of barium and strontium oxide exhibit better electron emission properties than barium oxide, strontium oxide or a mechanical mixture of these, the best composition having a strontium oxide content between about 50 mol per cent and 75 mol per cent [85,101]. The further addition of some calcium oxide is favourable too, the feeling amongst valve makers being that the triple oxide is more resistant to poisoning. The influence of calcium oxide has been attributed to a higher degree of disorder in the oxide crystallites[86,87].

4. APPLICATION OF THE PASTE TO THE BASE

The most common method of applying the paste to the base is spraying, although painting, dipping or dragging are also used. Electrophoresis and centrifuging[88] are other processes which have been employed. After coating, the cathodes are allowed to dry and are stored in an appropriate way. The coating method adopted depends upon the specific requirements. Indirectly heated cathodes are usually sprayed to a thickness ranging from some tens to about a hundred microns. In all cases the layers formed are quite porous although the porosity is not the same for the different coating methods. The pore volume is always above 50 per cent; a dense layer may have a pore volume of 65 per cent, a very loose layer as much as 85 per cent. Usually the layer density is about 1 g/cm^3 corresponding to a pore volume of 75 per cent (density of the solid carbonate = 4 g/cm^3). Loose layers usually provide a higher current density than dense layers, which may be explained by the smaller surface roughness of the latter. Recently the use of an

" emissive tape "—a film of a polymethacrylate binder with alkaline earth carbonate powder—has been described[89]. This tape is printed on to the nickel base.

5. DECOMPOSITION AND ACTIVATION

After being mounted in the assembly and, in the case of indirectly heated constructions, provided with the heater, the cathode is ready for processing. In mass production the tube is pumped on a rotating pumping machine by means of a mechanical rotary pump or a diffusion pump. When the pressure is sufficiently low, e.g. below about 0.1 torr, the heater voltage is applied and the cathode temperature increased in an appropriate way. Under the prevailing conditions a quick process is extremely important and the pumping schedule is therefore as short as possible. The decomposition of the carbonates quickly reaches completion, the carbon dioxide is pumped away and the oxide is left. The temperature must not be chosen too high as otherwise the evaporation of the magnesium from the nickel or of the nickel itself becomes excessive. Also barium may be lost and the layer may sinter too much. A temperature of about 1500°K must be considered to be quite high and may last for only 5 to 10 sec. Heating is usually done as quickly as possible. Before and during the decomposition of the carbonates the binder is cracked, leaving carbon in the coating which, however, is oxidized in the carbon dioxide atmosphere present during decomposition and pumped away as carbon monoxide. Other components in the assembly are heated by eddy-current in order to degas them as far as possible. The whole assembly heats the glass envelope. After the decomposition has come to an end, the pressure drops. At a certain pressure level, the tube is removed from the pump, a barium getter is flashed or a non-evaporated getter is activated, after which the pressure reaches a sufficiently low value, of the order of 10^{-5} torr. Sometimes the getter is appropriately treated before removing the tube from the pump. Voltages are then applied and the activation and ageing of the cathode starts. Usually some current will flow immediately, due to the presence of excess barium already produced by reduction, but this current varies generally from one tube to the other. During the ageing process the cathode stabilizes, usually characterized by a decrease in work function, and reaches its final condition. It must be realized that during the ageing process the cathode is under the influence of a great number of factors. Barium

is produced at the metal base and diffuses through the coating in which carbon dioxide may still be left. This gas is also adsorbed on other components. From these components various gases may still be liberated, especially under the influence of electron bombardment. During the ageing process a quasi-dynamic equilibrium is reached in the valve to which all components, the glass envelope, the cathode, the getter, the mica spacers, the heater, etc., contribute. Knowledge of the gas composition in the tube is evidently of great importance for the understanding of cathode behaviour.

The mechanism of the activation of oxide cathodes by current flow is still a point of discussion. Generally, the influence of a current is very pronounced in the first part of the activation period, the explanation being that the oxides are electrolytically dissociated. According to Kovtunenko and Isarev[90] a positive correlation exists between the barium concentration and the activating current density. In triple oxide the barium concentration is usually found to be much higher than in the double oxide. A higher temperature during current activation increases the amount of barium, but above about 1270°K a decrease is observed, the evaporation of barium becoming more pronounced.

The production of oxygen during activation has been demonstrated by various authors, some of whom detected mass-spectrometrically negative 0_2^- ions while others found 0^- ions. From Shepherd's[91] and Surplice's[92] work it appears that the liberation of singly charged negative oxygen ions is not simply an evaporation but is due to the bombardment by residual gas ions. However, the permanent poisoning of an oxide cathode by oxygen, which is found under certain conditions, is difficult to explain if electrolytic dissociation makes an important contribution to the activation[93].

In their studies on the conductivity of oxide cathodes Metson *et al.* put forward a new explanation of the current influence, in which thermal dissociation of the oxide is promoted by a temperature increase due to the electron bombardment of the grains in the porous oxide layer[94]. Certainly the last word on this matter has not yet been spoken, but it must be realized that the situation in the crystal lattice immediately after decomposition may be quite different from that in a later phase. Furthermore, the high temperature applied in this period, causing variations in composition and lattice disorder, may promote a greater ion mobility. It is common experience that heating to a too high temperature results in a decrease in emission.

This is partly due to sintering, partly to loss of barium by evaporation.

The whole processing schedule depends strongly upon the type of tube. In experimental devices, generally much more care can be bestowed on the decomposition and the degassing of the cathode and on the processing of the other components. MacNair[95] reported that conversion of the carbonates in hydrogen at atmospheric pressure results in a higher emission level and less initial poisoning of the cathode. It is believed that oxidation of various parts surrounding the cathode and of the activators present at the nickel surface is prevented in this procedure.

After decomposition the layer remains porous; some shrinkage is observed, but the structure of the layer does not change fundamentally. During life the layer shows shrinkage due to sintering and recrystallization. The influence of the temperature on the sintering is very pronounced, but it is also affected by other factors such as the crystal size of the carbonates, the presence of impurities, and the density of the layer. The influence of temperature on recrystallization and crystal growth has been studied by Eisenstein[96], both for the carbonates and the oxides, and by Rooksby[97]. Particularly above about 1270°K the barium–strontium oxide crystals grow rapidly. This temperature and even much higher temperatures are usually applied during decomposition with the aim of reducing the time for conversion as much as possible. Different temperature and time schedules for decomposition will generally result in different crystal size of the oxide and may result in different emission behaviour.

The composition of the oxide layer, which is initially homogeneous, changes rapidly. Barium oxide is more volatile than strontium and calcium oxide and evaporates preferentially from the surface, leaving a layer which contains only a fraction of the barium originally present[98]. The presence of the strontium oxide layer has been demonstrated by means of electron diffraction. An X-ray analysis does not show this thin layer, as its thickness is only of the order of several hundreds of atomic layers. This thickness depends upon the life of the cathode. In the case of the barium–strontium oxide cathode the real emitting surface consists mainly of strontium oxide activated by barium, in the case of the triple oxide mainly of strontium–calcium oxide, also activated by barium. Furthermore, at the core-coating interface, a change from the original composition may occur. Due to the reactions taking place between the reducing

elements and the oxides, compounds are formed which have a composition in which the ratio of the alkaline earth metals differs from that present in the oxide layer. Consequently one of these metals will be bound preferentially, resulting in a change in the composition of the oxide[99]. The interfacial layer which consists of compounds formed during the reduction of the alkaline earth oxides, will be discussed later when the problem of resistance is dealt with.

6. PROPERTIES OF OXIDE CATHODES

(*a*) *Emission properties*

It is not surprising that disparities exist in the results obtained by different researchers regarding the apparent emission constant A^* or the Richardson value A_R and the apparent work function φ^* or φ_R of well-activated cathodes. These disparities do not mean necessarily that the saturated emissions at a certain temperature were very different. A high value of φ^* may be combined with a high value of A^* and conversely. The value of φ^* is usually between 0.8 and 1.0 V, the corresponding values of A^* are about 10^{-2} and 10^{-1} A/cm^2 °K^2.†

Some investigators have found a relation between A^* and φ^* during activation of the cathode and also during life[100]. This might be due to a variation in the emission pattern over the surface as suggested by Veenemans[101]. Whether such a variation is found in an emission microscope picture will depend on the resolving power of the instrument used. Typical values of the current density drawn under direct current conditions range from 0.01–1 A/cm^2, whereas under pulse conditions the current density may rise to several tens A/cm^2.

Usually the phenomenon of "decay" is observed with the double or triple oxide[102]. Application of rectangular voltage pulses of sufficient length to the cathode causes the cathode to emit with decreasing current density; during the pulse the emission drops.

† A general remark must be made here about the units used in this part of the survey. In the theoretical treatment the M.K.S.A. system has been used and the values of the fundamental constants, found in the Glossary of Symbols, are expressed in the units of this system. In practical circumstances, however, it is often more convenient to use the centimetre instead of the metre and the gram instead of the kilogram. The author does not consider the disadvantage of using two systems to be very serious, as one system is used for the theoretical calculations and the other for practical considerations.

The emission drop can also be studied by applying short pulses continuously and switching on and off the d.c. anode voltage. The phenomenon may show at least three time constants, one of the order of 10^{-4} sec, the others in the ranges of 10^{-2}–1 sec and of 10^{2}–10^{4} sec. The shortest time constant decay is believed to be due to changes in internal space charge and surface charge[103]. The second one may be related to redistribution of donors under the influence of the applied field[104,105], while the longest decay constant might be related to a change in total number of donors, caused by changes in their distribution in the grains[105]. Ostroukov[106] has discussed the decay from the point of view of a temperature decrease of the emitting areas. Only at appreciable current densities ($>10^{2}$ A/cm^{2}) might a measurable influence be expected. Considering the very inhomogeneously emitting surface (cf. p. 253) the possibility that the decay may be explained by a temperature change must not be disregarded. Campbell and Shepherd[106a] have shown that the anode may play an important role in decay phenomena. For oxide cathodes the Schottky line (cf. p. 225) never shows the theoretical slope. This is due to roughness of the surface, to the influence of the penetrating field and to the redistribution of donors.

(*b*) *Resistance of the oxide cathode*

(α) *Resistance near the surface.* A resistance in the cathode may be found at different places. Under high load, with pulsed voltage, a large potential drop exists in the surface layer of the oxide, which may be interpreted as a high resistance[107]. It is probably due to the exhaustion in the outer porous layer of electrons because of the high electric field. The high potential drop present over a small distance may result in the " sparking " phenomenon. This potential difference will only exist at those places at the cathode where the field at the surface is accelerating. Although this may be found at a patchy surface under practical conditions, even when an $I - V_a$ characteristic typical of space charge operation is observed, these saturated patches do not contribute markedly to the emission current and the mean voltage drop in the surface layer will be small.

(β) *Resistance in the bulk.* The resistance usually found under normal operating conditions is situated in the bulk of the layer. It has been the subject of numerous measurements and theories.

Since the work of Loosjes and Vink[108] it is generally accepted that the porous structure exhibits two main types of electrical conduction, one at low temperature, the other at high temperature. At a low temperature, when the electron density in the pores is extremely small, the current is conducted by the grains and their contact areas. At high temperature the electron density in the pores becomes significant and conduction takes place mainly by the emitted electrons because the mobility of these electrons is much higher than of those in the grain. This is confirmed by measurements of the conductivity and the Hall coefficient[109]. The electron density in the pores is governed by the emission in eq. (12). It is to be expected that the temperature dependence in the high temperature conduction range will be nearly the same as the temperature dependence of the electron emission. This proves indeed to be the case for not too high temperatures ($800°K < T < 1000°K$). It was also found that the resistance in the oxide layer in this temperature range was non-ohmic. The explanation is that the mean free path of the electrons in the pores is such that, during their passage, they gain much more energy than they possess due to their thermal movement. The mean time interval τ during which the electron is under the influence of the electric field is now a function of this field. Denoting the mean free path, determined by the pore size, by $\bar{l}$ the following relationship holds:

$$\bar{l} = \frac{1}{2}\frac{eE}{m}\tau^2 \tag{23}$$

and J is accordingly derived from (4) and (23):

$$J = ne\left(\frac{2e\bar{l}E}{m}\right)^{\frac{1}{2}} \tag{24}$$

So it appears that J is proportional to $E^{\frac{1}{2}}$, a behaviour which is actually observed.

The low temperature conduction ($T < 800°K$) is found to be less sensitive to temperature than the high temperature conduction. If the high temperature conductivity is derived from the measurement at a certain small voltage, different from zero, the experiments show that the two conductivities, acting in parallel, can be described by a relationship:

$$\sigma = \sigma_0 \exp\left(-\frac{eE_c}{kT}\right)$$

The value of the activation energy E_c for the high temperature range is of the order of 1 V, about equal to the work function, the value of E_c at low temperature is 0.1–0.3 V, dependent on the state of activation of the cathode, as is always the case with the work function. The low temperature conductivity is usually explained as a bulk process in the grains of the oxides but, as has been mentioned already, surface conduction in this very porous structure composed of small particles is certainly possible. This latter type of conduction has been postulated by various authors[110]. If surface conduction were responsible for the passage of electrons through the coating at low temperature the activation energy E_c would be determined by the position of the Fermi level with respect to the conduction band at the surface. As has been explained in section A4 this energy difference generally has a different value at the surface of the crystal from that in the interior, owing to the presence of surface states of the electrons. Therefore no conclusions can be drawn from this activation energy with respect to the usual band scheme valid for the bulk of the semiconductor.

Owing to the presence in the coating of various grains of different composition and different crystal planes, the resistance of the cathode is not distributed homogeneously. The resistance may be expected to vary, if measured below a particular point at the cathode surface, not only along the direction parallel to the surface but also in the perpendicular direction. Usually some mean value will be determined, but using the arrangement of Jansen, Venema and Weekers, described in section B2(*b*), the resistance can be measured as a function of the position at the surface. In this way values which differ by a factor of 40 have been determined. A characteristic mean value for a well-activated cathode is a few Ωcm^2 at 1000°K for a layer thickness of 50–100 μm.

(γ) *Interface resistance.* The so-called interface resistance may be found in the interfacial layer formed by the reaction of reducing elements from the nickel and the alkaline earth oxides. The most dangerous element is silicon because it forms a barium orthosilicate layer[56]. The resistance value does not correlate with the thickness of the orthosilicate layer observed during life. The thickness is usually seen to increase steadily during about the first thousand hours after which it becomes constant[111]. This can be due to exhaustion of the silicon in the nickel or to a reduced diffusion rate through the layer. The thickness of the interface layer, when it has

become constant, is of the order of a few μm for a practical cathode nickel, containing about 0.1 per cent of silicon. Whether the layer will show an interface resistance which increases during life depends on various factors. If a resistance is observed, its temperature dependence is characteristic of a semiconducting material. It may thus be expected that other impurities found in the nickel can have a fairly marked influence in the conductivity[112]. It is therefore not surprising that great variations in the growth of the resistance may occur with different batches of nickel showing small differences in impurity content.

Current flow activates the interface compound and leads to a smaller resistance[112]. Tubes which have been running for several thousands of hours under cut-off conditions, so that no current flowed, showed resistances of 40–1000 ohms measured at 940°K, whereas similar tubes which had run for the same period with a current of 60 mA/cm^2 did not show a measurable resistance.

The temperature is found to have a marked influence on the growth of the resistance, a higher temperature favouring the rate of resistance increase. Typical maximum values of the interface resistance range from several tens to several hundreds of ohms for an area of 1 cm^2.

Besides the phenomenon of resistance, the interfacial layer present between the well-conducting oxide layer and the nickel also exhibits the character of a capacitor. The capacitance, which is usually almost independent of the temperature but changes during life, has typical values of the order of a few hundredths of a μF for 1 cm^2.

The problems of interface resistance, which was formerly a very disturbing factor in tubes operating under pulse conditions, in long life tubes[113] and in tubes run under cut-off conditions, have been completely overcome by the use of cathode nickel with a very low silicon content. A silicon content of less than 0.01 per cent is now being recommended. A 96–4 per cent nickel–tungsten alloy is often used for cathodes which are operated for long periods with current cut-off. In directly heated cathodes with a tungsten filament a resistance due to the tungstates presents no difficulties. Nickel alloy filaments, however, sometimes give trouble due to the presence of aluminium.

Bad adhesion of the oxide layer can cause a so-called vacuum interface resistance. It is usually due to a dirty nickel surface, to bad spraying or to an unfortunate choice of a particular kind of nickel.

It has been indicated that, in particular, too much aluminium in the nickel leads to difficulties in this respect[114]. Finally, the interface resistance may cause sparking if the cathode is forced to deliver high current densities.

(*c*) *The current distribution*

The distribution of current over the surface has been studied mainly by electron-optical[115] means. A common drawback of this method is the difficulty of obtaining satisfactory pictures at the operating temperature, owing to the formation of space charge which blurs the picture of the surface underneath. Moreover, no facilities for the actual measurement of the current distribution exist in most cases. The magnification is often rather small, up to about 100 times. Although this technique has clearly revealed the existence of patches, no detailed study has been made regarding the current density distribution. Qualitative information on this distribution has been obtained by using the difference between the experimentally determined slope of the retarding field current and the theoretical one[46]. At high negative values of the anode voltage, the whole area is in the retarding field region, but on increasing the anode voltage the high work function areas cease to give the linear ln J versus V_a relationship. These areas pass into the saturation region.

Using the apparatus described on p. 227, Jansen, Venema and Weekers[47] obtained a pattern of the current distribution along one line drawn over the surface as given in Fig. 21. The whole surface of a 3-mm planar cathode was scanned in this way and the current was recorded. About 15,000 current measurements, taken at equal distances along the zig-zag scanning lines, were used to produce the current distribution curve. The result is shown in Fig. 22. As it would have been very complicated to make a Richardson plot for each chosen area, it has been assumed that such an area was emitting homogeneously. Taking the reflection coefficient as zero and the theoretical A value, the effective work function (see p. 223) could be calculated for these areas[116]. The work function distribution determined in this way is also shown in Fig. 22. The spread in work function is much greater than has been reported before. The given curves are typical for oxide cathodes after some hours. For the whole cathode the values of A_R and φ_R were respectively 3.2 A/cm^2 °K^2 and 1.26 V. The resolving power of the apparatus was about 25 μm. From the curve giving the current as a function of the

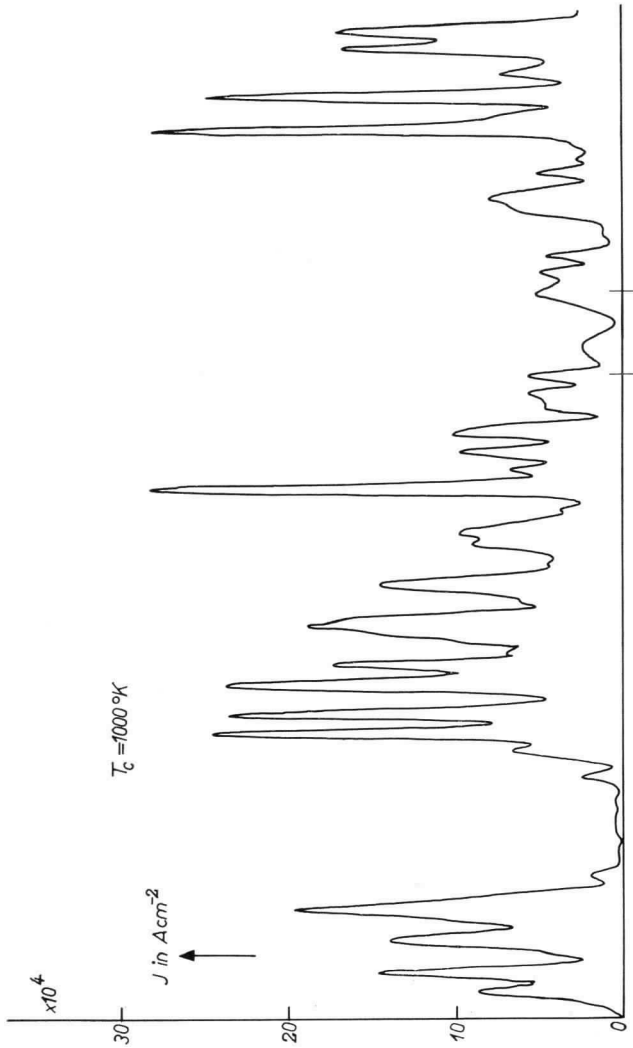

FIG. 21. The current distribution along a line drawn over the surface of a barium–strontium oxide cathode. The Richardson value of the work function for this cathode was $\varphi_R = 1.26$ V, the value of A_R was 3.2 A/cm^2 °K^2.

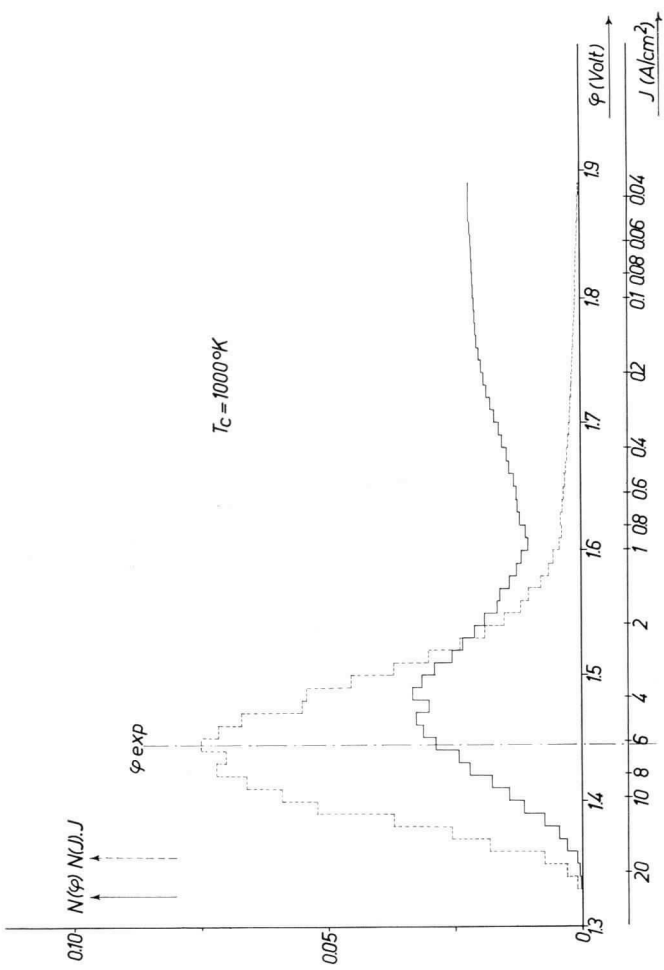

FIG. 22. The current contribution $N(J)\cdot J$ of a barium–strontium oxide cathode after some hours of life for the different values of the current density J (dotted curve) and the effective work function distribution $N(\varphi)$ for the different values of the effective work function φ (drawn curve). $N(J) = N(\varphi)/J_c$. J_c = current density of the total cathode.

place it can be concluded that this resolving power is not sufficient to obtain emission just from one single homogeneously emitting spot. This is in agreement with other observations. Further experiments[47] with a projection type of microscope, similar in design to

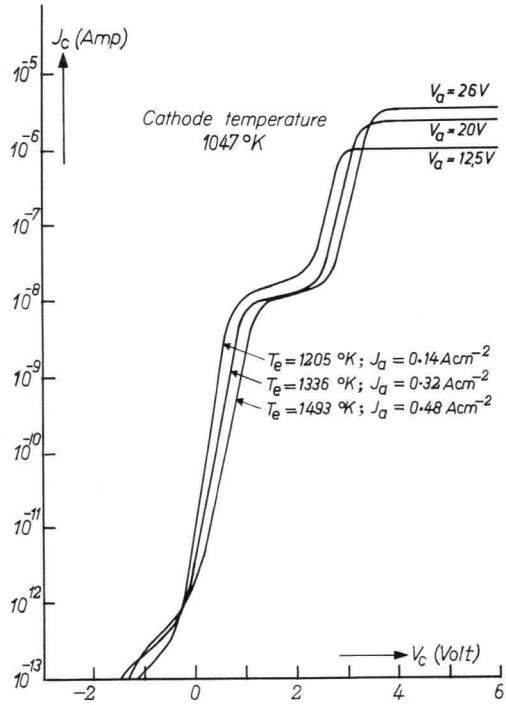

FIG. 23. The retarding field curve of the electrons emitted by a barium oxide cathode after acceleration to 12.5 V, 20 V and 26 V respectively, as measured with the apparatus given in Fig. 18. The cathode temperature was 1047°K and the current densities drawn from the cathode were 0.14 A/cm^2, 0.32 A/cm^2 and 0.48 A/cm^2.

the field emission microscope but with a thermionically emitting oxide cathode, revealed that the size of the best emitting areas was of the order of 1 μm. A resolving power considerably in excess of this value is needed to study the oxide surface thoroughly.

(*d*) *The energy distribution of the emitted electrons*

This distribution is usually measured by means of the retarding field technique, as described in section B2(*d*). A good geometry

is an indispensable condition and the measurement must not change the condition of the cathode. The results obtained with electron current in a diode under space charge conditions are of particular interest and of great technical importance. The apparatus given in Figs. 15 and 16 is suitable for the investigation. The results obtained by Bulyginskii and Dobretsov[60], showing an electron temperature which is higher than the cathode temperature, were confirmed by Jansen *et al.*[61] whose results obtained under different conditions are shown in Fig. 23. It appears that only with small currents is there a good agreement between the two temperatures. At current densities of the order of 0.5 A/cm^2 the difference may amount to 450°C and the interpretation of the retarding field characteristic becomes difficult. Although a full explanation of the shape of the curves cannot as yet be given, the curves suggest the existence of a group of electrons emitted from a low work function area and another group emitted from an area with a considerably higher mean work function, the ratio of the areas being of the order of 0.02. This is in agreement with the results obtained by a different technique, as discussed before, which measured the emission distribution along the surface (see section 6(*c*)). The resistance in the porous oxide layer reduces the slope of the retarding field, as electrons from places at different potential may reach the anode. Therefore the energy distribution becomes broader, simulating a higher cathode temperature.

7. DISPENSER OXIDE CATHODES

Although various types of practical cathodes may be considered to be dispenser cathodes[151] it is customary to use this expression only for those cathodes where a deliberate separation is made between the emitting portion and the part which supplies the alkaline earth element needed for activation. By designing an oxide cathode in which this principle was realized, Lemmens and Zalm[117] were able to incorporate several new features in the oxide cathode, resulting in a better performance, in particular at a high load. In this cathode, the emitting oxide layer of a few tens of microns thickness is deposited on to a gauze of pure nickel wire (see Fig. 24). This gauze constitutes the cover of a small cavity which is part of a nickel sleeve and is filled with a mixture that supplies the barium used for activating the actual emitting oxide layer. The resistance of this layer is small because of its small thickness and the absence

of an interface resistance. Consequently, less heat is generated in the layer, ensuring stable performance at high current density.

A strontium oxide layer or the double oxide of strontium and calcium can be used instead of the usual barium–strontium oxide. The emission properties, when activated by barium, are very similar but the sintering is diminished. The mixture in the cavity can be chosen in such a way that it supplies the proper amount of barium, depending on the particular application. Cathodes of this type show excellent behaviour at a load of 1.5 A/cm^2 for more than 5000 hr. Imai[118] described cathodes based on the same principle.

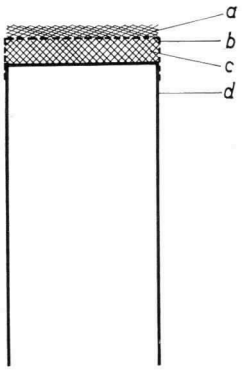

FIG. 24. Schematic picture of a dispenser oxide cathode. *a* is the actual emitting oxide layer, *b* is a gauze of pure nickel, *c* is the compound delivering the appropriate amount of barium, *d* is the nickel sleeve.

8. THE INFLUENCE OF GASES

A thermionic cathode can be treated theoretically without regard to the ambient gas molecules and ions, but in a practical tube the cathode is subject to the influence of its surroundings. The influence of different gases on the oxide-coated cathode has been studied by various authors[119], most recently with the help of an omegatron for the analysis of the gas mixture present in the system[120]. The use of a mass spectrometer is advisable because even if a particular test gas is introduced into a continuously pumped system by means of an adjustable leak or a capillary, the residual gas composition may change due to reactions of the gas which has been introduced.

General agreement exists about the role of oxygen and carbon dioxide. These gases poison the cathode markedly even at pressures below 10^{-6} torr. The action of hydrogen is also clear: on well-activated cathodes it has no influence, but it has a favourable effect on cathodes which are not fully activated. The role of water vapour is uncertain. Various authors have reported a poisoning[121], but others have observed an activating action (Wagener[119]). It may be that the presence of other gases, e.g. hydrogen, interfered in these investigations.

Similar controversial results have been reported for carbon monoxide. Wagener found in this case an influence of the base material: with nickel cores poisoning occurred, whereas with platinum cores activation was found. Cathodes with a low state of activation are reported to activate, whereas well-activated cathodes show poisoning[122]. Here also the residual pressure of carbon dioxide must be taken into account.

Methane is reported to activate at pressures below a value between 10^{-4} and 10^{-5} torr, but to poison at pressures above this value. At the high temperature cathode surface, methane is chemically unstable and dissociates into hydrogen and carbon, which may reduce the barium oxide to yield carbon monoxide and barium[123]. The carbon monoxide pressure in the system, together with the rates of the various reactions involved, determines whether carbon will remain at the surface. At 1000°K the critical carbon monoxide pressure, calculated thermodynamically, is between 10^{-6} and 10^{-5} torr.

Chlorine is well known to have a detrimental effect on an oxide cathode[75], but the situation here is also probably more complicated, as Zykov and Nakhodkin[119] indicate.

9. THE EVAPORATION OF OXIDE-COATED CATHODES

From what has been said before it will be evident that various elements and compounds may evaporate from oxide cathodes. At the operating temperature the evaporation of the alkaline earth oxides and the nickel is of minor importance, although in certain parts of the processing schedule the temperature may reach a sufficiently high value to cause measurable evaporation of these materials. Of the various activators present in the nickel, magnesium in particular may give trouble, as this element is very volatile.

Insulation defects in practical tubes are often due to an excessive amount of magnesium in the base.

Of the alkaline earth metals, produced by reduction, barium is the most important. The rate of barium evaporation is closely related to the amount and nature of the activators. With a pure nickel base hardly any barium evaporation is detectable. In this respect the nature of the grid and anode material must also be taken into account, because reducing elements present in these parts and evaporated during processing of the tube, may activate the cathode and increase the rate of barium evaporation. In a very thorough investigation Wooten, Ruehle and Moore[135] were not able to detect a correlation between the rate of barium evaporation and electron emission, neither could any influence on the space charge current be detected. From this it must be concluded that during life an electrolytic dissociation of barium oxide does not contribute markedly to the production of free barium. If the residual gas contributes to the reduction of the alkaline earth oxides, as is the case for hydrogen and hydrocarbons, it is not certain that the equilibrium pressures of the various metals, calculated thermodynamically, are a direct measure of the amount of evaporated alkaline earth metals. Here the kinetics of the reactions involved are of great importance, and the probability that a strontium atom will be liberated from a barium-strontium oxide cathode may even be greater than the probability that a barium atom will be liberated especially because the surface is rich in strontium.

Cathode material is usually not only transported to the surroundings by evaporation, but may also disappear from the cathode by sputtering, especially if high voltages are applied. The ambient gas, generally hydrogen, nitrogen, methane and carbon monoxide, is ionized during the operation of the tube and the positive ions are driven to the cathode. In the sputtering process too, the strontium contribution may be considerable. It is therefore not surprising that in actual valve practice the total amounts of strontium and strontium oxide, found at electrodes in the neighbourhood of the cathodes, are not very different from the amounts of barium and barium oxide. A thorough study, by means of the radioactive tracer technique, of the amounts of barium and strontium, found on various parts of practical tubes, more particularly of the influence of the anode material on these amounts, have been made by Fränz[123a].

10. THEORIES OF THE MECHANISM OF OPERATION OF THE ALKALINE EARTH OXIDE CATHODE

The theories proposed for the mechanism of operation of the oxide cathode kept pace to a large extent with the general insight gained into the electrical behaviour of solids, in particular of semiconductors. Around 1930, before the development of semiconductor theory, the mechanism was thought to be similar to the thermionic emission of metals which had adsorbed an electropositive element. The excess barium was thought to be present either as small islands of barium[124] or adsorbed as a monolayer. The first view was soon abandoned but the theory of adsorbed barium, proposed by Koller[125] and Becker[126], stood firm and is still accepted by many specialists. Also J. H. de Boer[127], stressing the dominating influence of adsorption on electron emission phenomena in general, attributed a prominent part to the barium atoms adsorbed on the barium and strontium oxide. In de Boer's theory the ionization energy of the adsorbed atoms constitutes the energy to remove an electron from the oxide to infinity; this equals therefore the product of the work function and the electronic charge.

Although the concept of a fundamental contribution by the adsorbed barium—a typical surface phenomenon—has never been either proved or rejected completely, in particular to explain the behaviour at normal operating temperature, later work has mainly been devoted to describing the behaviour of oxide cathodes by means of a semiconductor, in which the unique part played by the surface, in particular for phenomena such as the electron emission, has not been given much attention. It is likely that this simplification is not permissible since several well-established experimental facts cannot be explained by considering bulk properties alone, whereas the introduction of adsorption as a fundamental concept might explain them easily.

The oxide cathode is activated by a reduction process, by which the number of free electrons is increased and the Fermi level shifts towards the conduction band. The simplest model which can be made is the Wilson model in which a donor level is assumed at a sufficiently small distance from the conduction band. This model, which has been used extensively by many authors, was also accepted by Nottingham[128] in his interpretation of Hung's results[64], obtained in a temperature range from about 400–550°K. Although the emission can be explained by assuming a donor level at

a depth of 0.7 eV below the conduction band and a donor density of 2.4×10^{21} per m^3, an extrapolation to normal operating temperatures leads to difficulties, the work function attaining too high a value. Nor is the temperature dependence of the conductivity, which would follow from this picture, in agreement with the observations.

It has often been taken for granted that this donor level is an oxygen vacancy (F-centre) or an excess barium atom. Plumlee[129] has drawn attention to the fact that other donors may exist in the oxide and will contribute to the concentration of free electrons if their ionization energy is sufficiently low. If this were the case to a sufficient extent, the quantity of free barium per unit volume, which plays an important part in most of the theories on oxide cathodes as it is equated with the donor concentration, is of minor importance. The problem of the amount of free barium is difficult, not only from the theoretical but from the practical point of view. Its determination has been carried out by the reaction of barium with water vapour at room temperature to give hydrogen, which is measured volumetrically. The results obtained by various investigators show considerable variations, the amount of excess barium ranging from about 10^{-4} to 6 mole per cent. The method has been studied very carefully by Wooten, Moore and Guldner[130] who showed that extreme care must be taken to ensure that the amount of excess barium is determined and not of any other reducing element. It is therefore not surprising that the figures determined under the most refined circumstances are lower than those measured previously. Indeed the surprising result obtained by Moore, Wooten and Morrison[131] was that no correlation existed between the emission properties of their barium–strontium oxide cathodes, which varied considerably, and the amount of excess barium present in these cathodes. Their conclusion was that if excess barium is of major importance for the thermionic performance of practical cathodes, any correlation must lie below the sensitivity, which was about 10^{-4} per cent by weight or 1 barium atom in 10^6 molecules of oxide. From the observation that many cathodes showed low emission and a relatively high barium content it must be concluded that factors other than excess barium are decisive in practical cathodes.

These results supported Plumlee's view that another donor species than excess barium is responsible for the electrical behaviour.

Considering the various possibilities, Plumlee suggested[129,134], taking into account his own results of the interaction of water vapour and oxide cathodes, that this donor is the (OH^-, e) group, i.e. a double charged hydroxyl group, with one electron very loosely bound. The part played by water vapour is not very clear: Wagener[119] reports an activating action below 10^{-5} torr and poisoning above several times 10^{-5} torr. Plumlee himself observed instantaneous correlation of water vapour pressure and emission. However, in a measuring equipment the presence of water vapour is accompanied by the presence of hydrogen, which is certainly an activating agent. So far there is no experimental evidence against or for Plumlee's donor hypothesis.

The hydroxyl group, suggested as the important donor, will probably show a great mobility. The proton is expected to move rather readily from one oxygen ion to the other. This behaviour fits in very well with the mobile donor hypothesis put forward by Nergaard[105] to explain several peculiarities observed with oxide cathodes, in particular the current decay, observed under pulse conditions (cf. section 6(*a*), p. 248). If current flows through the coating, a potential drop must exist across the oxide layer, and ionized donors, having a positive charge, may move under the influence of the field. The concentration of these donors will decrease at the emitting surface and increase in the region near the metal base. In equilibrium this electrolytic flow is balanced by a diffusion due to the concentration gradient built up in the layer. The decrease in donor concentration at the surface causes a decrease in electron density and consequently a fall in emission. Although the mobile donor hypothesis can explain qualitatively the observed behaviour under current flow, it remains to be proved whether it accounts quantitatively for the results. So far this proof has not been given. Nergaard made some rough estimations, Frost and Kane gave a more elaborate treatment, but the calculated figures do not agree with the experimental results[50,102,132]. More work is needed to prove that the mobile donors contribute noticeably to the emission properties of oxide cathodes. Okumura and Hensley[132a] ascribe an important role to mobile acceptors, which they believe to be barium vacancies.

In the Wilson model a proportionality must exist between the emission density and the conductivity, measured at the same temperature but for different states of activation. This follows immedi-

ately from the formulae (5), (6) and (13). However, band bending, due to surface states, which causes the distance between the Fermi level and the bottom of the conduction band at the surface to be changed, does not alter this conclusion necessarily as the emission is determined by this distance at the surface and so may be the conductivity. The required proportionality has been demonstrated by various investigators[54,133]. Moreover, at a sufficiently high temperature a proportionality must exist according to the Loosjes–Vink picture of the conductivity.

The identification of the amount of excess barium per unit volume with the donor concentration leads to difficulties with regard to the rate of barium evaporation and hence with the life of the oxide cathode[79]. The vapour pressure of barium above the oxide on the assumption of an ideal solution of about 10^{-4} per cent, would amount to about 10^{-7} torr, much in excess of the observed quantity[134]. This was also considered by Plumlee as an indication that excess barium could not be responsible for the electrical behaviour.

Wooten, Ruehle and Moore[135] measured the rate of barium evaporation of active oxide cathodes and obtained a value corresponding to a barium vapour pressure of the order of 10^{-12} torr. In an ideal solution, this would correspond to a mole fraction of barium of 10^{-11}–10^{-12}. Using a Wilson model with barium as a donor it is evident that this amount cannot explain the observed properties[134]. The suggestion of barium adsorbed on the oxide surface seemed again attractive as a possible escape from this dilemma[79].

The idea of surface conductivity is encountered at various places in the literature to explain certain experimental results. Surface conductivity must be related with band bending, the surface states, as caused by adsorbed species, being responsible for the curvature of the bands near the surface. The suggestion of adsorbed barium seems quite natural. Recently, Zalm[136] has tried to explain the behaviour of the oxide cathode on the assumption of adsorbed barium, using the calculation which Krusemeyer and Thomas[137] made for zinc oxide. The results are promising but much more work is needed, particularly on single crystals.

Sproull *et al.*[138] studied various properties of single crystals of barium oxide. Although this work yielded important information, e.g. on the solubility of barium in the oxide and on the band structure

of barium oxide, it has not resulted in a generally accepted theory of the oxide cathode. No work on single crystals of mixed barium–strontium oxide or of strontium oxide has been published. In view of the constitution of the surface layer of the barium–strontium oxide cathode, more information on these oxides seems desirable.

So far the inhomogeneity of the cathode surface has not been taken into account in the theories which have been developed. The results described in section 6(*c*) indicate that only a small part of the cathode emits very well, a large area showing moderate to bad emission. It is at present too early to explain this behaviour but it is most probably related to the various crystal orientations present at the surface. As the small area with low work function contributes very markedly to the total emission, it is to be expected that the A value, calculated on the assumption that the emitting area equals the geometrical area, will be low. Also, the amount of excess barium responsible for the emission of the small area is very small and may not show a correlation with the total amount, especially if the barium is not distributed homogeneously. The high current density at these low work function areas influences the location of the space charge minimum* and may also be responsible for decay effects. It is evident that more information on the emission distribution is highly desirable.

II. Tungsten and thin film emitters, based on tungsten

1. PURE TUNGSTEN

Extensive studies have been made of the thermionic properties of this element which is still in use as an electron emitter in rather special applications, e.g. in X-ray tubes, and in some large transmitting tubes, where high voltages are applied. Tungsten is mainly used in the form of polycrystalline wire or ribbon and heated directly by current flow. Due to its high melting point it can be thoroughly outgassed and the spread in values of the apparent emission constant and the apparent work function as determined by various investigators is not excessive. A value of 4.54 V for φ^* and an A^* value of 60 A/cm^2 °K^2 are probably the most reliable values. The variation of φ^* and A^* with the crystallographic orientation of this element have also been carefully determined. Table 3

* This argument was pointed out to the author by H. Danker and K. Hirsch.

shows the values of these quantities as determined by different investigators[39,40]. The orientation [110] emits very weakly and the determination of the work function is difficult. Field emission data for this orientation indicate a value of about 6.0 V[139].

2. THORIATED TUNGSTEN

This material, an early type of practical emitter, is extensively used in transmitting tubes. It has been studied in much detail since it provides a good example of cathodes which, owing to the presence of a thin layer of a foreign element, show a relatively low work function. The thorium, which was originally added as thoria (about 1 per cent) to the tungsten to improve the life of the filaments by keeping the crystals small at the high operating temperatures, was

TABLE 3

Direction	Nichols		Smith	
	φ^* V	A^* A/cm^{-2} °K^{-2}	φ^* V	A^* A/cm^{-2} °K^{-2}
[111]	4.39	35	4.38	52
[112]	4.69	125	4.65	120
[116]	4.39	53	4.29	40
[100]	4.56	117	4.52	105

found to enhance the electron emission quite considerably if the thoriated wire were treated in a special way[140]. This treatment consists in heating the filament to a temperature above 2600°K for a certain period dependent on the applied temperature, followed by an activation period at a temperature between about 2000 and 2250°K. During the first part of the treatment, which might be for about three minutes at 2800°K, the thoria is believed to be reduced to give thorium partly as small crystalline inclusions and partly dissolved in the tungsten. Traces of carbon seem to play a decisive role in this part of the process[141]. During the activation the thorium atoms diffuse from the interior to the outside mainly by migration along the grain boundaries. Having reached the outside the thorium atoms migrate along the surface and cover it with a monolayer[142]. The use of temperatures above 2250°K causes a deactivation which can be repaired by keeping the filament at a

lower temperature in the activating temperature range of 2000–2250°K. The explanation of the deactivation phenomenon is the evaporation of thorium adatoms from the surface. The rate of evaporation in the operating temperature range of about 1800–2000°K, is so small that it is negligible.

For large filaments the reduction by heat treatment may be insufficient and in this case the wire is carburized by glowing in a low pressure of hydrocarbon (e.g. acetylene). Tungsten carbide then forms and the reduction of thorium oxide proceeds more easily. An activation procedure similar to the one described above, results in an emitter which has the same thermionic properties as pure tungsten activated by thorium. However, at the higher operating temperatures the easier replenishment of thorium makes the carburized thoriated tungsten emitter more stable against residual gas and ion bombardment than the thoriated tungsten cathode[143,144]. The evaporation of thorium from either is about the same[145]. The thermionic constants are given by Dushman and Ewald[146] as: $A^* = 3.0$ A/cm^2 °K^2 and $\varphi^* = 2.63$ V.

3. CAESIUM ON TUNGSTEN

In the presence of caesium vapour a tungsten filament shows an appreciable emission at a low temperature. This phenomenon, described first by Kingdon and Langmuir[147], is explained by the adsorption of caesium ions to the tungsten surface, resulting in the formation of a dipole layer which decreases the work function. The amount of adsorbed caesium depends both on the caesium pressure and the temperature of the filament. In the presence of free caesium metal, the caesium pressure is determined by the lowest temperature in the tube. If the emission of this cathode is determined as a function of its temperature it is found that at low temperatures (several hundred degrees absolute, depending upon the caesium pressure) the emission increases according to the Richardson type of equation. The apparent work function φ^* is then about 1.4 V and the apparent A^* about 3.0 A/cm^2 °K^2. Above a particular temperature, which depends on the caesium pressure, the emission starts to increase more slowly and finally reaches a maximum; then it decreases with increasing temperature. In this part of the characteristic the caesium coverage decreases until the tungsten surface is completely clean. In the final phase of this process the emission starts to increase again with increasing temperature, but

at a much lower level than before. When a pure surface is obtained the Richardson law is obeyed again, but with the φ^* and A^* values of tungsten. See Fig. 25 and ref. (148).

At elevated temperature it is observed that positive caesium ions evaporate as well as electrons, the number being proportional to

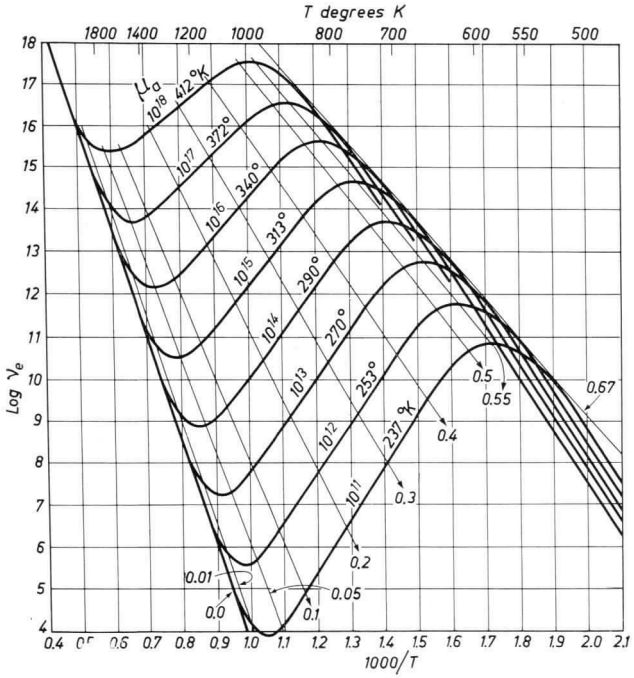

FIG. 25. The number of electrons V_a emitted per cm^2 and per second by a tungsten filament at temperature T in equilibrium with caesium vapour. μ_a = arrival rate (per cm^2 and per second) of caesium atoms. The caesium pressure is determined by the lowest temperature in the tube, which is also indicated. The diagonal straight lines refer to the fraction of the surface covered with caesium atoms. From Taylor, J. B. and Langmuir, I., *Phys. Rev.* **44**, 432 (1933).

the caesium pressure. This phenomenon is understandable if it is realized that the work function of tungsten is greater than the ionization energy of caesium (3.88 eV). It is therefore energetically most favourable for an electron to leave the caesium atom when it is quite close to the tungsten surface and to enter the metal. A

positive caesium ion is thus formed and is adsorbed for only a very short time at this high temperature after which it evaporates. The ratio of the number of ions and the number of atoms evaporated from the tungsten filament may be calculated by means of the Langmuir–Saha equation[9]:

$$\frac{n_2}{n_1} = \frac{1}{2} \exp\left(\frac{e\varphi - E_i}{kT}\right)$$

in which n_2 = number of ions per unit volume in equilibrium
n_1 = number of atoms per unit volume in equilibrium
φ = work function
E_i = ionization energy of the caesium atom.

With decreasing temperature the number of adsorbed ions increases, the work function is reduced accordingly and the electron emission increases. However, the number of positive ions evaporating becomes less, because as the work function decreases it becomes increasingly less favourable for an electron to enter the metal. At a constant caesium pressure it is obvious that the number of evaporated atoms will now increase. In the first part of the adsorption process, in which the coverage is up to about 0.15 monolayers, the reduction in work function is proportional to the number of adsorbed ions (cf. p. 194). The lowest work function is obtained if the coverage is 0.67 of a monolayer. At a higher coverage the work function increases slightly. The work function of an oxidized tungsten surface covered with caesium is even lower at a particular temperature and with a particular caesium pressure than that of a tungsten–caesium surface[147].

The main importance of the investigations on caesium-covered tungsten has been the better understanding they have provided of the properties of the combination of metal and adsorbed films[127,128]. For vacuum tube applications the caesium pressure must be chosen too high in order to obtain acceptable current densities, and for gas-filled tubes the cathode temperature is usually too high. Recently, however, the interest has increased due to the advent of thermionic energy converters. For the conversion of heat—obtained for instance from nuclear sources —to electricity, thermionic emission is expected to be of great importance. Calculations have already revealed a promising efficiency and a great deal of work has been started in this direction. One of the problems encountered in using thermionic

emission for this purpose is the formation of space charge which strongly reduces the available current. Various ways of counteracting the space charge limitation have been suggested, but two ways of approach have been given special attention. The first consists in the use of a close-spaced diode[149], in which the cathode–anode spacing is made so small that no space charge minimum can be developed; the second consists in the neutralization of the negative charge by positive ions[150]. For this purpose caesium has already been investigated in much detail. The use of caesium is attractive because of its low ionization potential and its ability to decrease strongly the work function of the anode to which it is adsorbed.

4. TUNGSTEN–BARIUM DISPENSER CATHODES

(*a*) *Introduction*

Although Nergaard's statement[151] that every practical cathode is a dispenser cathode may be true to a certain extent, it has been customary to use the expression dispenser cathode only for a particular type. This type is characterized by a metallic or semiconducting cathode body, the surface of which is activated by barium or barium oxide or both which are supplied by "dispensing" from a compound present in the body. This dispensing action was first applied in cathodes for gas discharge applications. The L-cathode was the first dispenser cathode to come into use for vacuum tube applications[152]. Three different types of tungsten–barium dispenser cathodes have been described: the L-cathode, sometimes referred to as metal-capillary cathode[153], the impregnated cathode[154] and the pressed and sintered type[155]. The feature of these cathodes is the very high current density which they can deliver; for instance a continuous load of 21.5 A/cm^2 has been reported for an L-cathode in actual tube practice[156]. The absence of any disturbing cathode resistance is responsible for this behaviour. Other attractive properties are the great mechanical strength of the emitting surface, which can withstand high electrical field strength and ion bombardment, and the well-defined nature of this surface which can be shaped to close tolerances. Ion bombardment can spoil the emission but due to a continuous supply of activating material the emission is restored after cessation of the bombardment. The same is true for chemical poisoning. The life of these cathodes

is usually only determined by the amount of activating material present in the cathode and by the rate at which it is consumed. At 1400°K the life of an L-cathode is now more than 10,000 hr.

Cathodes which show a great similarity to the L-cathode, some differing in base or activating material, have been described by Katz[153].

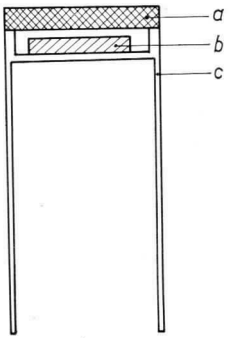

FIG. 26(*a*). Schematic picture of a planar L-cathode.
a is the porous tungsten plug.
b is the pellet delivering the barium.
c is the molybdenum sleeve.

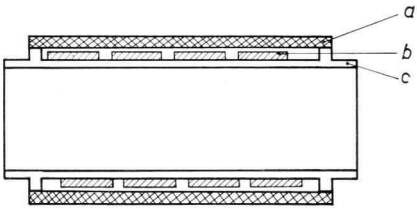

FIG. 26(*b*). Schematic picture of a cylindrical L-cathode.
a is the porous tungsten.
b are the pellets delivering barium.
c is the molybdenum sleeve.

(*b*) *The L-cathode type*

The electron-emitting part of this cathode is the surface of a porous tungsten body which is welded to a solid molybdenum sleeve. See Fig. 26a and b. Behind this porous body is a cavity which contains a suitable compound delivering barium and barium oxide at an appropriate rate. The products pass through the porous

tungsten where they may possibly undergo reactions and cover the outer surface by migration. The molybdenum sleeve contains the heater, which must provide the L-cathode with a temperature in the range from about 1300°K to about 1500°K. The apparent work function of the tungsten surface of 4.54 V is lowered by barium activation to a value of 1.67 V[157].

The L-cathode can be made in a great variety of shapes and dimensions. Planar cathodes with a diameter of 0.6 mm and cylindrical ones with a diameter of 0.8 mm have been used. The density of the tungsten body is usually chosen to be between 16.4 g/cm^3 and 13.5 g/cm^3 or between 85 and 70 per cent of the value for compact tungsten. Within certain limits the rate of supply of activating material and its rate of evaporation can be controlled by this density; a greater variation is obtained, however, by appropriate choice of the compound in the cavity.

Originally the material which was put into the cavity during manufacture of the cathode was barium–strontium carbonate, which was converted to barium–strontium oxide during processing. The carbon dioxide escaped through the porous tungsten, which became oxidized during this part of the process. This resulted in a rather long activation period. An improvement can be obtained by using a compound containing a much smaller amount of gas. There was a further reason why the early L-cathode was not always satisfactory. Rittner[157] showed that the rate of supply of activating material to the cathode surface was much greater than is needed to keep the surface in an active state, provided that the poisoning from the environment was negligible. This meant that a great deal of this material was lost by evaporation without any benefit. A control of the rate of evaporation is an important factor in some applications, especially in those where an electrode is situated very close to the cathode, so a search was made for a compound producing no oxidizing gas and showing a smaller rate of barium supply. A very satisfactory answer was found in a mixture of barium aluminate ($5BaO2{\cdot}Al_2O_3$) and tungsten[158]. Cathodes with this mixture in the cavity show a very small gas evolution and fast activation. The rate of evaporation is about a factor of twenty less than that of the original L-cathode and is very reproducible and constant. This is in contradiction to the early L-cathode, which showed great variations in evaporation from one cathode to another. These variations were caused by the partial blocking of the pores of the plug at the interior

due to the reactions between the tungsten and the oxides, enhanced by the oxidation in the first phase of cathode processing. Even under practical conditions this smaller rate of barium supply does not lead to problems with the ambient gas. The most important properties of this L-cathode are summarized in Table 4.

The emission density is not distributed homogeneously along the surface. Figure 27 shows the current distribution measured by the apparatus used by Jansen *et al.*[47] and described in section B2(*b*). Assuming a constant emission density over the small area from which emission is drawn through the hole in the anode and assuming an emission constant $A = 120$ A/cm^2 °K^2 for each area, the effective work function distribution shown in Fig. 28 has been derived. The emission distribution has also been studied by means of the electron microscope[158a].

TABLE 4. PROPERTIES OF THE L-CATHODE WITH BARIUM ALUMINATE FILLING

Temp. in °K	Pulse emission measured at 1000 V, cathode–anode distance: 1 mm in A/cm^2	Rate of evaporation in μg/cm^{2}hr Density of tungsten: 75%
1400	18	0.17
1450	35	0.46
1500	57	1.2

In attempting to explain the mechanism of operation of the L-cathode three main questions have to be answered:

(1) What is the nature of the emitting surface?
(2) What is the activating agent transported through the porous plug?
(3) What is the mechanism of this transportation?

The experiments carried out to answer these questions were mainly done with L-cathodes which contained barium oxide in the cavity. These cathodes showed the same emission properties as the early L-cathodes with barium–strontium oxide. The strontium oxide served chiefly to prevent melting of the barium oxide–barium carbonate compound during decomposition.

Schaeffer and White[159] concluded from their experiments that the cathode surface consists of tungsten partially covered with barium. Rittner, Ahlert and Rutledge[157] on the contrary concluded that the surface is completely covered with a monolayer of

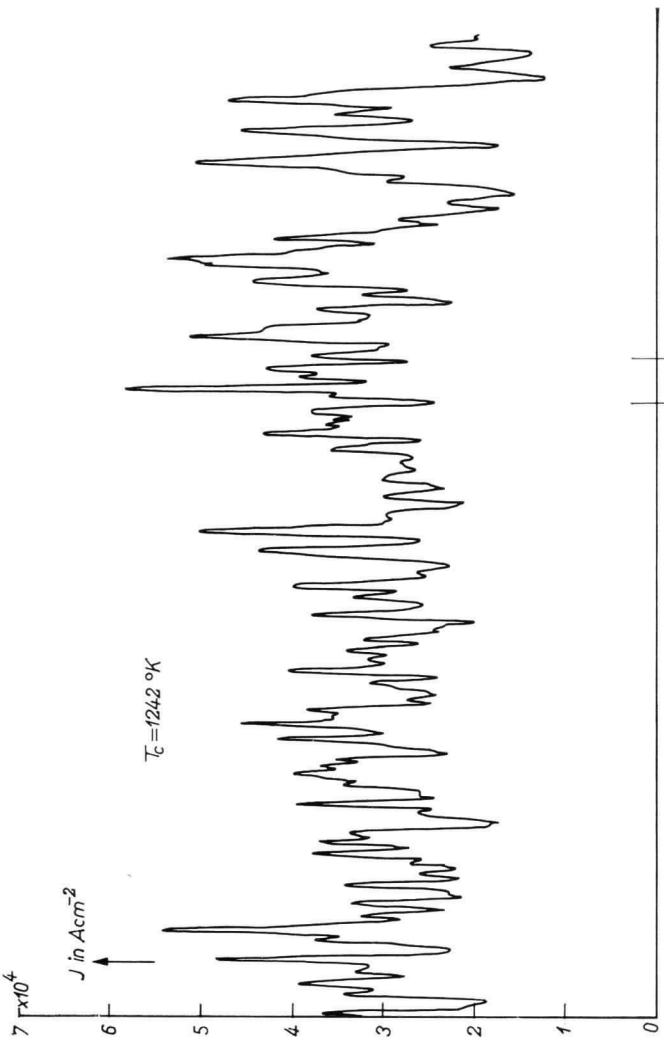

FIG. 27. The current distribution of an L-cathode, measured along a line drawn over the cathode in the beginning of life. Richardson value of the work function of the whole cathode: $\varphi_R = 1.81$ V, with $A_R = 35.6$ A/cm^2 °K^2.

barium and also with an oxygen layer which is nearly monoatomic. The presence of oxygen leads to a better emission and a greater sticking time of the barium. Morgulis[160] showed the presence of

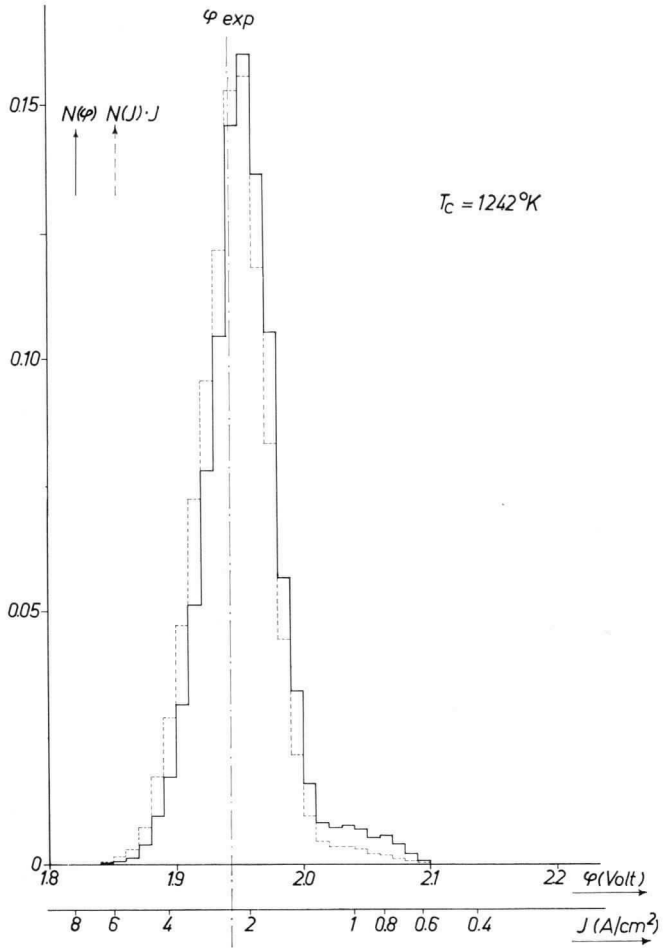

FIG. 28. The current contribution $N(J)\cdot J$ of an L-cathode (dotted curve) and the effective work function distribution (solid line). Note that the effective work function distribution is much more narrow than is found for an oxide cathode.

barium tungstate, which itself is a good thermionic emitter[161], on the surface of a cathode which originally contained barium carbonate. Bulyginskii and Sibir[59] derived from the measurement of the energy

distribution of the electrons the temperature coefficient of a resistance which they assumed on the surface. Jansen[162], in a very thorough investigation of the energy distribution, was able to detect a small resistance (0.9 Ω per cm^2 at 1300°K) on a cathode which originally contained barium–strontium carbonate. Cathodes containing the aluminate showed no resistance, even after 11000 hr. The presence of the tungstate, found under particular conditions, is not surprising, for Rittner *et al.*[157] found it already on the interior of the plug.

It is probable that the pressures of the various constituents in the cavity reach their equilibrium values, and can therefore be calculated thermodynamically. The reaction between barium oxide and tungsten taking place at the interior of the tungsten plug is given by:

$$6BaO + W \rightleftharpoons Ba_3WO_6 + 3Ba \qquad (25)$$

A corresponding equation can be written for the reaction between strontium oxide and tungsten. In the case of the aluminate, the mixture equivalent to $5BaO{\cdot}2Al_2O_3$ actually consists of a mixture of $3BaO{\cdot}Al_2O_3$ and $BaO{\cdot}Al_2O_3$. The first compound reacts readily with tungsten, yielding barium but with a pressure which is a factor of about 160 less than that resulting from the reaction (25). The $BaO{\cdot}Al_2O_3$ compound reacts with tungsten only slightly, the equilibrium pressure of barium being several orders of magnitude less than of the tribarium aluminate. The calculation shows that both the barium and the strontium pressure exceed the pressure of the corresponding oxides by several orders of magnitude. Consequently, it is mainly metal vapour which flows through the plug. The reason for the amounts of metal and oxide being about equal in the evaporant is, according to Rittner, to be found in the relatively large amount of oxygen present in the tungsten plug. This would mean in any case that the nature of the material which flows through the plug varies during its passage from the interior to the outside.

The barium and strontium can be transported through the plug in two ways: they may flow as a vapour through the pores, or they may migrate along the pore walls during the time they are adsorbed. Both phenomena will occur simultaneously but one may be dominant. Schaeffer and White[159] attribute the transportation to surface migration, while Rittner *et al.*[157] and Brodie and Jenkins[163] consider vapour flow or Knudsen flow to be the main mechanism. The investigations by Zingerman and Morozovskii[164] on the transport of barium, and by Ptushinskii and Chuikov[165] on the

transport of strontium, showed that under normal operating conditions surface migration is the dominating process. From a measurement of the rate of flow of barium through porous tungsten carried out in a mass spectrometer, the present author arrived at the conclusion, that migration is certainly not to be neglected. A special cathode, the cavity of which contained in this case barium metal, was shaped in such a way that a large temperature difference could be adjusted between the hottest top part, which included the porous tungsten disc, and the bottom which had the lowest temperature. Both temperatures could be chosen within rather wide limits so that the barium pressure in the cavity could be varied over several orders of magnitude and the transport could be studied at different temperatures of the porous tungsten disc. The rate of flow was very clearly temperature-dependent with an activation energy of 1.7 eV. The residual atmosphere in the spectrometer also had a marked effect on the rate of flow. After being left at room temperature for 15 hr, barium transport was substantially less at the beginning of a new experiment but rose to its previous value in a matter of minutes after reaching normal operating temperature. With Knudsen flow this phenomenon would not be explicable but it is easily understood in terms of surface migration. The value of the transmission coefficient, i.e. the ratio of the pressures at both sides during barium flow through a tungsten disc with a density of 75 per cent was about 2×10^{-3} at 1400°K (compare Zingerman and Morozovskii[164] who found for a density of 70 per cent a value of 2.3×10^{-3} at 1400°K).

(*c*) *The impregnated cathode*

In this type of cathode developed by Levi[154,166], the pores of the porous tungsten body are filled with a suitable compound by heating it above its melting point in contact with the tungsten. The liquid phase is readily taken up by the porous metal. The density of the tungsten is usually chosen to be rather high, between 80 and 85 per cent. The compounds that have given the best results are barium aluminate $5BaO{\cdot}2Al_2O$, a mixture of the compounds $BaO{\cdot}Al_2O_3$ and $3BaO{\cdot}Al_2O_3$ of which the second is the most active one, and barium–calcium aluminate, $5BaO{\cdot}2Al_2O_3{\cdot}3CaO$. The tungsten disc or cylinder is usually welded to the molybdenum cathode part which contains the heater. The porous tungsten body

can be made in a variety of shapes by using a special technique, also developed by Levi[167], which is applicable to the tungsten body of the L-cathode, too. It consists in impregnating the tungsten in its final sintered state with copper or gold, machining it, and then evaporating the copper or gold.

For a number of applications the impregnated cathode is easier to fabricate than the L-cathode as it is less complicated[168]. The processing of this cathode is fast and so is the activation, as the activator is close to the surface in the beginning of life. A disadvantage may be the rather rapid evaporation, especially at the start, although in applications where a strong poisoning exists during this part of life the rapid initial production of barium may even be advantageous. The rate of evaporation is not constant because the barium, in order to reach the cathode surface, has to

TABLE 5. PROPERTIES OF IMPREGNATED CATHODES
IMPREGNANT: BARIUM–CALCIUM ALUMINATE $5BaO{\cdot}3CaO{\cdot}2Al_2O_3$

Temp. in °K	Pulse emission measured at 1000 V, cathode–anode distance: 0.4 mm in A/cm²	Rate of evaporation $dm/dt = Ct^{-\frac{1}{2}}$ $t < 3000$ hr C in $\mu g/cm^2\ hr^{\frac{1}{2}}$
1300	3	24
1400	11.8	62

pass a layer depleted of barium the thickness of which continuously increases. The barium is produced in the cathode by the reduction of the tribarium aluminate by tungsten. Calculation shows that a rate of evaporation is to be excepted which is inversely proportional to the square root of time, and experiments confirm this behaviour[169]. Table 5 summarizes the various important properties of impregnated cathodes. With such cathodes the emission density again varies along the cathode surface[47,169a]. Figure 29 shows the result of measurements of the effective work function distribution at full activation. In this state reached after some hours at 1450°K, the distribution curve is sharpest after which it flattens off in the course of time, although the total current still increases.

The mechanism of operation of the impregnated cathode is in principle the same as that of the L-cathode, although the role of calcium is not completely clear. Brodie and Jenkins[170] attribute the better emission properties to adsorbed calcium. Beck and

Ahmed[170a] have studied the impregnated cathode by means of the secondary electron emission microscope and have obtained very valuable information about the cathode surface structure.

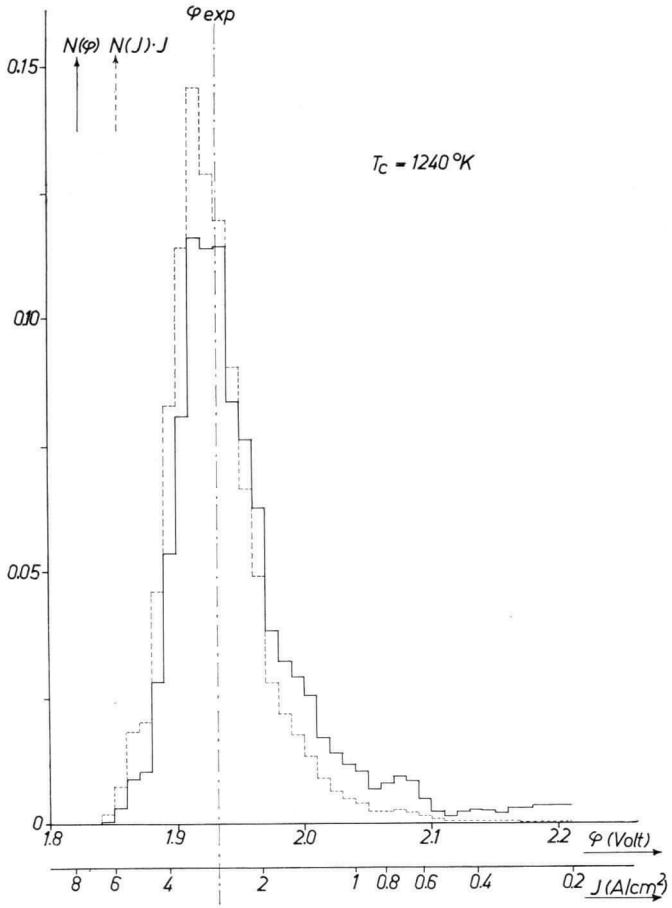

FIG. 29. The current contribution $N(J)\cdot J$ (dotted curve) and the effective work function distribution (solid line) of an impregnated cathode immediately after activation.

(*d*) *The pressed and sintered cathode*

This type of cathode is made by pressing together tungsten or a tungsten–molybdenum alloy with a suitable compound which afterwards delivers the required amount of barium. If necessary an

additional reducing agent is incorporated. Hughes and Coppola[155] worked mainly with the tungsten–molybdenum alloy and the barium aluminate or the barium–calcium aluminate. Huber and Freytag[171] used, amongst many different versions, in particular two combinations, one being a mixture of tungsten, the basic tungstate Ba_3WO_6 and aluminium, the other being a mixture of tungsten, the basic tungstate and tungsten carbide WC. Melnikov *et al.*[172] found that the barium–calcium tungstate is to be preferred to barium tungstate. After pressing the mixture into the desired shape, preferably immediately into the holder (pressure usually 10–20 tons/cm^2) the assembly is heated in vacuum, or better in hydrogen, and sintered. During this process gases which were occluded during pressing are removed.

The emission properties of the various types of pressed cathodes are similar. Hughes and Coppola gave a value for A^* of 2.4 A/cm^2 °K^2 with a φ^* value of 1.7 V for the barium–calcium aluminate compound, which corresponds to a saturated current density of 6 A/cm^2 at 1400°K. Similar values were reported by Huber and Freytag and Melnikov *et al.*

Information on the rate of evaporation of these cathodes is limited. Only Hughes and Coppola deal with it and show the importance of the addition of molybdenum. This metal, being less active than tungsten, can be added to diminish the rate of evaporation of barium and barium oxide and to increase the life of the pressed cathode. The evaporation rate is not likely to remain constant during life, as has been demonstrated in the case of the impregnated cathode.

(*e*) *Influence of gases on tungsten–barium dispenser cathodes*

The effects of various gases on impregnated and L-cathodes have mainly been studied by Jenkins and Trodden[173]. Nitrogen, hydrogen, the rare gases and also carbon monoxide are harmless up to pressures of 10^{-3} torr, whereas oxygen, water vapour and carbon dioxide have a poisoning effect. A critical pressure exists for each of these gases, below which no poisoning is found. This critical pressure increases with the temperature of the cathode, and for impregnated cathodes with a porosity of 20 per cent at 1375°K is about 10^{-7} torr for oxygen, about 3×10^{-7} torr for water vapour and about 10^{-6} torr for carbon dioxide. A formula describing the poisoning phenomena could be derived and it showed agreement with the experimental facts. It contains the arrival rate and the

probability of adsorption of the gas molecules, the barium supply rate and the probability that a barium atom which arrives at the surface removes the adsorbed contamination.

III. Miscellaneous cathodes

1. NICKEL–BARIUM DISPENSER CATHODES

A special type of cathode, related to the oxide-coated cathodes on the one hand and to the dispenser cathodes on the other, is formed when a combination of nickel and the alkaline earth compounds is made. Usually these cathodes are manufactured by pressing nickel powder together with the carbonates, but for relatively small percentages of nickel the nickel powder is simply added to the carbonate paste. An activator may either be present in the nickel or added separately. The aim is the production of a metallic cathode with the emission characteristics of oxide cathodes having the advantage of a low resistance and, if a pressing technique is used, of a well-defined geometrical surface, which can withstand bombardment better than the oxide cathode. In general it can be said that these three objects can be realized reasonably and that, although the operating temperatures for these cathodes have proved to be somewhat higher than for an oxide cathode, they are certainly lower than is needed for the L- or impregnated cathodes. The rate of evaporation of nickel is no longer negligible at the higher operating temperatures.

The " molded " cathode, described by MacNair *et al.*[174] was made by pressing 70 per cent by weight of nickel powder and 30 per cent of barium–strontium carbonate. A current density of 1 A/cm^2 at 1070°K under continuous operation was reported. The results were preliminary. The cathode described by Beck *et al.*[175] is also made by pressing together about 30 per cent by weight of co-precipitated barium–strontium carbonate and about 70 per cent carbonyl nickel powder, but about 1 per cent of a reducing agent—preferably zirconium—is added in the form of zirconium hydride. Decomposition is either done in the tube in which the cathode is mounted or in advance, and is followed by an activation procedure. Outgassing lasts somewhat longer than for an oxide cathode and activation and ageing takes about 24 hr. In normal operation the temperature of this cathode is about 100° higher than that of an oxide cathode giving the same emission.

The temperature for 1 A/cm^2 saturated emission is about 1200°K. At 1270°K and 1 A/cm^2 lives of 5000 hr are reported, whereas at 1340°K and 3 A/cm^2 even 3000 hr of lives have been obtained. The cathodes are also attractive for demountable vacuum systems as they are resistant to poisoning and reactivate easily after exposure to air.

The apparent work function of this cathode is given as $\varphi^* = 1.78$ V, and the apparent emission constant calculated from the figures is $A^* = 23$ A/cm^2 °K^2. The work function is not homogeneous along the surface, its mean value averaged over the surface area being 2.8 V.

A different technique was used by Balas *et al.*[176] who impregnated a porous nickel body (porosity 30–50 per cent) with a solution of barium–strontium acetate and precipitated the alkaline earth carbonates by the addition of ammonium carbonate solution. After drying, the carbonate is present in the pores and in a small amount at the surface. These cathodes show an apparent work function $\varphi^* = 1.02$ V. At about 1080°K the saturated emission with a correction applied for the Schottky effect is 1 A/cm^2.

Fane[177] pressed carbonyl nickel with triple carbonate and boron as a reducing agent. The cathodes were sintered in hydrogen. The apparent work function is given as $\varphi^* = 1.07$ V, but a fairly wide spread is observed in this value. Continuous emission currents of 1 A/cm^2 at 1110°K and 2.5 A/cm^2 at 1170°K in life tests are quoted. The emission is inhomogeneous and originates partly from the oxide in the pores, and partly from the nickel surface, which, however, shows a greatly reduced work function. The cathodes can be exposed to air without serious deterioration, as has been mentioned before. Other preliminary results are reported in the literature[178]. Poisoning of these cathodes is discussed by Jenkins and Trodden[178a].

The general conclusions about this type of cathode, which contains of the order of 70 per cent by weight of nickel, must be that a continuous load of 1–3 A/cm^2 seems possible and that under pulse conditions even greater densities can be obtained. The temperature must be chosen higher than for normal oxide cathodes, roughly 100–150°C. The emission must be expected to be rather inhomogeneous. The cathodes are more resistant to sputtering than oxide cathodes.

2. HEXABORIDES

The thermionic properties of the borides of a number of alkaline earth and rare earth metals were first studied by Lafferty[179]. These MB_6 compounds seem to be attractive as thermionic emitters for various reasons: they show a high electrical conductivity and a good thermal and chemical stability. Their crystal structure consists of a framework of boron atoms with the metal atoms embedded in the interlattice space. At high temperature metal atoms evaporate from the structure, but the surface is immediately replenished by metal atoms which diffuse from the interior and an active surface is constantly maintained, an attractive feature for practical cathodes. According to Lafferty the lanthanum hexaboride proved to be the best thermionic emitter of the various borides which were investigated. At a temperature of 1700°K somewhat more than 1 A/cm^2 current density was obtained, making the material in this respect superior to thorium oxide or a thoriated tungsten emitter. Difficulties were encountered with the base metal due to the inward diffusion of boron, but a good solution was found by using tantalum coated with tantalum carbide. Adhesion is usually rather bad, but with special mechanical constructions the borides may be locked in the surface. Solid cathodes in the form of discs or rods can be made by pressing the powder in the desired shape and then sintering.

Activation of lanthanum hexaboride cathodes is fast, especially when heated to 1870°K for a few minutes. They are resistant to poisoning by atmospheric air at room temperature if they are subsequently heated to 1770–1870°K. The rate of evaporation of these cathodes is rather high. In general it may be said that these cathodes can be useful for special application, as e.g. in ionization gauges, if the high temperature is acceptable. From the Richardson curve the values

$$\varphi^* = 2.66 \text{ V}$$
$$A^* = 29 \text{ A/cm}^2 \text{ °K}^2$$

are reported.

The hexaborides of gadolinium and yttrium, not investigated by Lafferty, are reported to show even better emission than the lanthanum hexaboride[180].

3. THORIUM OXIDE CATHODES

Thorium oxide cathodes[181] are sometimes used in rather special applications where conditions are too severe for alkaline earth

oxide cathodes or where the use of tungsten, which requires a very high temperature, is impracticable. The thoria is applied to the base, which may be tungsten, molybdenum, tantalum or a suitable platinum metal, by one of the usual coating techniques or it may be pressed and sintered in the desired shape, for instance as a cylinder for use in a magnetron. When the pressing technique is applied a mixture of tungsten or molybdenum and thoria is sometimes used in order to increase the electrical conductivity at low temperature. The cathode can then be heated directly by resistance heating. To obtain sufficient and stable emission, an activation process is necessary, as is the case with alkaline earth oxide cathodes. Usually, however, the cathode will be outgassed at a few hundred degrees above the normal operating temperature, and this process is generally sufficient to reach a stable emission. A temperature of about 2100°K is required for this process. When measured with pulses the apparent work function reaches a value of about 2.5 V with an apparent A value of about 2.5 A/cm^2 °K^2. This means that under this condition a current density of about 5 A/cm^2 is obtained at 2000°K. When current is drawn continuously, decay effects are observed with time constants which are rather long, one being of the order of 0.1–1 sec, another even of several minutes. The current drops considerably but anode effects may be very pronounced. A recovery of the emission is observed after cessation of current flow. Complete recovery can be obtained if the period without current flow is chosen sufficiently long, but with shorter periods the recovery is only partial.

When flashed to about 2800–2900°K, an enhanced state of activation is observed in which the current densities may be a factor of 2 or 3 higher than after normal activation. This state of increased emission cannot be maintained at normal operating temperatures. The emission drops to the value observed after the usual activation procedure, in a period which depends strongly on the ambient gas pressure.

The life of the cathodes is determined by various factors. Under the best possible conditions the complete evaporation of the cathode material may give the end of life, but under practical circumstances sputtering by ions from the ambient gas or electrolysis may be predominant.

Applications of this cathode are to be found in tubes where the current density is fairly large and where a high anode voltage is

applied, i.e. in magnetrons, and also in ionization gauges. In this last application, particularly if the gauge is operated under rather rough conditions, where exposure to air of the hot cathode is not exceptional, the use of thoria deposited on to an iridium filament may be advantageous.

4. THERMIONIC CATHODES FOR GAS DISCHARGE APPLICATIONS

The heated cathodes in a gas discharge emit electrons through various mechanisms:

(*a*) thermionic emission
(*b*) electron emission under ion bombardment
(*c*) photoelectric emission, due to photons generated in the discharge.

The discussion in this section will be confined to thermionic emission and it will deal with the demands made upon cathodes operating only under these special conditions. The gas discharge gives rise to the sources of electrons (*b*) and (*c*); of these (*b*) may be accompanied by sputtering of the cathode material which becomes apparent above a particular ion energy. For the discharge to be stable, a particular current must flow in the discharge and through the cathode. If the contribution (*a*) to this current is predominant, the sputtering due to (*b*) will be small. The amount of (*a*) is, however, limited for it cannot exceed the saturated value determined by the area, the work function φ, the emission constant A and the temperature. If the discharge current is increased, the contributions (*a*), (*b*) and probably (*c*) will increase, resulting in a higher sputtering rate, which starts to increase very strongly if the thermionic emission approaches saturation. Contribution (*b*) is then forced to take over, with a catastrophic effect on the cathode. The same will happen if the cathode temperature is decreased.

For a low pressure discharge (p of the order of 10^{-2}–10^{-1} torr) where sputtering is most dangerous, the best results will be obtained when the current is a fraction of the saturated thermionic current. Therefore relatively small current densities are used (<0.5 A/cm^2) so that for large currents a large emitting area is needed. This is unattractive for normal cathodes in view of the heat economy requirement. The multicellular cathode (Hull), which contains a large area of emitting surface in the form of radial vanes effectively shielded against radiation, constitutes a very good solution. Dispenser cathodes derive from this multicellular cathode.

At higher pressures ($p \sim 1$ torr) where sputtering is less, due to the ambient gas, the current density can be increased without leading to rapid destruction of the cathode. The current may now approach the saturated thermionic current, which is economically desirable. Current densities are now several A/cm^2. The ion bombardment together with the current flow in the cathode resistance causes additional heating of the cathode, resulting in a higher temperature which further increases the thermionic emission. Due to the gas pressure, however, the evaporation of the cathode material is greatly decreased and is not detrimental. Sometimes the ion bombardment together with the Joule heating is sufficient to keep the temperature in the working region. In the situation so far described normal alkaline earth oxide cathodes on nickel base are commonly used because of their favourable heat economy. At still higher pressures (several torr) the discharge begins to concentrate on a small cathode area, which is consequently strongly heated, and this makes much higher demands with respect to sputtering. Nickel is therefore replaced in the cathode by tungsten and often a dispenser or storage type is used. In this type of cathode the compound delivering barium or thorium is substantially shielded from the ion bombardment, but supplies these metals to the bare tungsten body. Other compounds such as silica or thoria are added if higher cathode temperatures appear. The cathode for fluorescent lamps consists of a tungsten spiral coated with a mixture containing the alkaline earth oxides and a small percentage of zirconium oxide or hafnium oxide[182]. The high-pressure lamp and the photoflash lamp usually contain a storage type or a pressed type of cathode.

It is not easy to judge the thermionic emission properties of a cathode in a gas discharge, but sometimes the I–V characteristic may yield valuable information[183].

5. HOLLOW CATHODES

A particular type of thermionic cathode—the hollow cathode—has been studied recently in view of the promising results with respect to attainable current density and its particular current-voltage characteristic. The cathode structure contains a cavity, the walls being the electron emitting surfaces, equipped with a hole through which the electrons escape and are drawn to the outside. The problem of the I–V characteristic has been treated theoretically by Brunn[184], whereas for instance Babcock *et al.*[185], Poole[186]

and Fincke[187] gave experimental results and practical solutions. For a well-chosen geometry, e.g. a closed sphere, the voltage distribution and the electron density in the interior can be calculated by means of Poisson's equation and the Maxwell–Boltzmann distribution of the electron energies. The influence of a hole facing an outside anode in the presence of an electric field which penetrates the interior is generally difficult to examine, but with simplifying assumptions, as for instance the use of the potential at the inner surface as deduced in the absence of a space charge, a satisfactory conclusion can be derived about the I–V characteristic to be expected. At sufficiently high negative anode voltage the current is characteristic of a retarding field. With increasing voltage, in the neighbourhood of zero voltage, the current becomes space charge-limited and with a sufficiently high positive anode voltage the area adjacent to the hole starts to deliver an emission which is temperature-limited. With increasing voltage this area increases too, depending upon the particular geometry.

The I–V_a characteristic deviates considerably from the $I = CV^{3/2}$ law; in some cases almost a rectilinear relationship between I and V_a is found and even a curve which is concave towards the V-axis. With hollow cathodes, internally coated with alkaline earth oxide, current densities in pulse operation of up to 100 A/cm^2 at 900°C have been reported. It has been observed that emission may not only originate from the hole itself but also from the edge of the aperture or from the outside area adjacent to it. Special versions of hollow cathodes were given by Nakamura and Sugata[188] and Eichenbaum[189]. The last author used caesium ions to neutralize the interior space charge.

6. EMISSION-INHIBITING MATERIALS

Although one is usually interested in obtaining higher current densities from thermionic cathodes, if possible without increasing the temperature, in some cases a need exists for materials which show the least emission at the highest possible temperature. This is particularly the case where materials are concerned on to which barium, barium oxide or thorium from an external source are evaporated, as in the important case of grids.

Firstly the problems related to the deposition of alkaline earth metals and oxides will be considered. Depending upon the temperature of the electrode from which the emission must be suppressed,

which will usually be different for oxide cathodes and the various types of dispenser cathode, different solutions are possible. Gold plating is advisible for not too high temperatures (500–550°C)[190]. Difficulties arise at higher grid temperature owing to diffusion of the gold to the interior of certain grid materials or to evaporation and subsequent poisoning of the cathode. The explanation of the favourable behaviour of the gold surface when continuously supplied with barium is to be found in the formation of an intermetallic compound with a sufficiently high work function (3.3 V)[191]. For higher temperatures (about 1000–1200°K) pure titanium can be used[192,193], but again evaporation and cathode poisoning limit the operating temperature. On the titanium surface barium atoms have a short sticking time, whereas barium oxide is reduced and the resultant barium evaporates. In the case of a dispenser cathode surface in contact with molybdenum or tungsten parts, it may be desirable to prevent electron emission from these parts. The temperature is high, about equal to the cathode temperature, and the application of titanium is impossible. A solution in this case has been found in the carburization of the molybdenum and tungsten surfaces[194]. For the thoriated tungsten cathodes, from which thorium evaporates, grid emission has been prevented by coating the grid with platinum or titanium[192,195].

APPENDIX I

THERMOCHEMICAL CALCULATIONS

The Gibbs function, also called the Gibbs free energy, or thermodynamic potential is given by the expression:

$$G = U - TS + pV$$

The expression $H = U + pV$ is called the heat function or enthalpy. Consequently:

$$G = H - TS$$

A chemical reaction taking place at a certain temperature T is accompanied by a change in Gibbs function ΔG, given by:

$$\Delta G = \Delta H - T\Delta S$$

where ΔH is difference in heat content of the reactants and the products and ΔS is the difference of the entropies of reactants and products.

The heat content of one mole, i.e. the heat of formation from the elements, is known for many compounds and is tabulated for a certain standard temperature T_0, usually 298°K[196]. Also, the heats of transformation, fusion and evaporation, and the entropies of the compounds and elements are tabulated at 298°K. From these tables the change $\Delta G(T_0)$ accompanying a particular reaction can easily be calculated at 298°K. For other temperatures a correction must be made with the help of the heat capacity, the molar specific heat at constant pressure, C_p. Often this correction can be omitted because of uncertainties in the data of the heat content and the entropy.

It can be shown that a relation exists between the equilibrium constant K of a chemical reaction and the change in Gibbs function ΔG. If the gas pressures are expressed as partial pressures of one atmosphere the change in Gibbs function is written as ΔG^0, the standard Gibbs function change, and the relation between K and ΔG^0 is:

$$\Delta G^0 = -RT \ln K$$

The equilibrium constant K is given by:

$$K = p_1^{\nu_1} \times p_2^{\nu_2} \times p_3^{\nu_3} \times \ldots$$

where the pressures p_1, p_2, etc. are expressed in atmospheres and ν_1, ν_2, etc. denote the number of moles of the various gaseous components appearing in the reaction equation. For the reactants ν is negative, for the products it is positive.

If only one gaseous product is involved in the reaction, $K = p$ and if heat capacity terms are neglected, the pressure of the gas is given by the equation:

$$\log p \text{ (torr)} = 0.2185 \left\{ -\frac{\Delta H^0(T_0)}{T} + \Delta S^0(T_0) \right\} + 2.88$$

APPENDIX II

DIFFUSION OF THE ACTIVATOR IN THE NICKEL

It is assumed that the diffusion takes place in a solid bounded by a pair of parallel planes at $x = 0$ and $x = 1$. Two cases can be considered which are treated mathematically in practically the same way. Either the concentration at the two boundaries is taken to be zero for all times except $t = 0$, which applies to a volatile activator

such as magnesium, or the concentration is zero at one boundary and no loss exists at the other, which is found for instance with silicon.

The diffusion is described by the equation:

$$\frac{\partial C}{\partial t} = D \frac{\partial^2 C}{\partial x^2} \tag{A1}$$

where C represents the concentration and D the diffusion coefficient. At $t = 0$ the concentration is assumed to be constant $C(x, 0) = C_0$.

In the first case the boundary conditions are:

$$\begin{aligned} C(x, 0) &= C_0 \qquad 0 \leqslant x \leqslant l \\ C(0, t) &= 0 \qquad t > 0 \\ C(l, t) &= 0 \qquad t > 0 \end{aligned} \tag{A2}$$

In the second case $(\partial C/\partial x)_{x=0} = 0$ for $t > 0$ instead of $C(0,t) = 0$. This condition applies also in the first case at $x = \frac{1}{2}l$, so that the solution for the second case can be obtained from that for the first case by replacing 1 by 21.

The solution of (A1), which satisfies (A2), is[197]:

$$C(x, t) = \frac{4C_0}{\pi} \sum_0^\infty \frac{1}{2n+1} \sin \frac{(2n+1)\pi x}{l} \exp\{-(2n+1)^2 \pi^2 Dt/l^2\}$$

The average concentration is:

$$\overline{C(x, t)} = \frac{8C_0}{\pi^2} \sum_0^\infty \frac{1}{(2n+1)^2} \exp\{-(2n+1)^2 \pi^2 Dt/l^2\}$$

and the flux at $x = l$

$$-D\left(\frac{\partial C}{\partial x}\right)_{x=l} = \frac{4C_0 D}{l} \sum_0^\infty \exp\{-(2n+1)^2 \pi^2 Dt/l^2\}$$

For relatively long times $t > l^2/2\pi^2 D$ the first term of the series gives a satisfactory approximation:

$$-D\left(\frac{\partial C}{\partial x}\right)_{x=l} = \frac{4C_0 D}{l} \exp\left(-\frac{\pi^2 Dt}{l^2}\right)$$

For relatively short times $t < l^2/2\pi^2 D$ a good approximation is:

$$-D\left(\frac{\partial C}{\partial x}\right)_{x=l} = C_0\left(\frac{D}{\pi t}\right)^{\frac{1}{2}}$$

which is the solution for the flux at the surface of an infinite solid. This expression is usually applied in the calculation of the barium production at the nickel alkaline earth oxide interface.

LITERATURE

COMPREHENSIVE ARTICLES AND BOOKS DEALING WITH THERMIONIC CATHODES WHICH HAVE APPEARED SINCE 1945:

A. S. EISENSTEIN: Oxide Coated Cathodes, in *Advances in Electronics*, vol. 1 (Edited by L. Marton), Academic Press, New York, 1948.

H. FRIEDENSTEIN, S. L. MARTIN and G. L. MUNDAY: The mechanism of the thermionic emission from oxide coated cathodes, in *Reports on Progress in Physics*, vol. 11, 1948.

C. HERRING and M. H. NICHOLS: Thermionic Emission, in *Reviews of Modern Physics*, vol. 21, No. 2, April 1949.

G. HERMANN and S. WAGENER: *The Oxide-coated Cathode*, vols. 1 and 2, Chapman and Hall, London, 1951.

L. N. DOBRETZOV: *Elektronen und Ionenemission*, V.E.B. Verlag Technik, Berlin 1954 (in German).

G. H. METSON: On the electrical life of an oxide-cathode receiving tube, in *Advances in Electronics and Electron Physics* (Edited by L. Marton), Academic Press, New York, 1956.

W. B. NOTTINGHAM: Thermionic Emission, in *Handbuch der Physik*, vol. 21 (Herausgegeben von S. Flügge), Springer Verlag, Berlin, Göttingen, Heidelberg, 1956.

LITERATURE ON SOLID STATE PHYSICS IN GENERAL:

CH. KITTEL: *Introduction to Solid State Physics*, Wiley, New York; Chapman and Hall, London, 1956.

A. J. DEKKER: *Solid State Physics*, Prentice-Hall, Englewood Cliffs, 1960.

LITERATURE ON NOISE IN GENERAL:

A. VAN DER ZIEL: *Noise*, Prentice-Hall, New York, 1954.

D. A. BELL: *Electrical Noise*, D. VAN NOSTRAND, London, 1960.

W. R. BENNETT: *Electrical Noise*, McGraw-Hill, New York, 1960.

REFERENCES*

1. HUTNER, R. A., RITTNER, E. S. and PRÉ, F. K. DU, *Philips Res. Rep.* **5**, 188 (1950).
2. WILSON, A. H., *Proc. Roy. Soc.* A**133**, 458 (1931).
3. PELL, E. M., *Phys. Rev.* **87**, 457 (1952).
4. FORMAN, R., *Phys. Rev.* **96**, 1479 (1954).
5. TAMM, I., *Physik Z. Sovjetunion* **1**, 733 (1932); FOWLER, R. H., *Proc. Roy. Soc.* A**141**, 56 (1933); SHOCKLEY, W., *Phys. Rev.* **56**, 317 (1939).
6. BARDEEN, J., *Phys. Rev.* **71**, 717 (1947).
7. SCHOTTKY, W., *Z. Physik* **113**, 367 (1939); SCHOTTKY, W., *ibid.* **118**, 539 (1942); SCHOTTKY, W. and SPENKE, E., *Wiss. Veröffentl. Siemens-werke* **18**, 3, 1 (1939); MOTT, N. F., *Proc. Roy. Soc.* A**171**, 27 (1939); GARRETT, C. G. B. and BRATTAIN, W. H., *Phys. Rev.* **99**, 376 (1955).
8. SCHOTTKY, W., *Physik. Z.* **15**, 872 (1914).
9. LANGMUIR, I. and KINGDON, K. H., *Proc. Phys. Soc.* A**107**, 61 (1925).
10. HERRING, C. and NICHOLS, M. H., *Rev. Mod. Phys.* **21**, 185 (1949).
11. W.B.N., p. 17.
12. LEWIS, T. J., *Proc. Phys. Soc.* B**67**, 187 (1954).
13. MORANT, M. J. and HOUSE, H., *Proc. Phys. Soc.* B**69**, 14 (1956).
14. OLLENDORF, F., *Archiv. f. Elektrot.* **44**, 177 (1959).
15. FOWLER, R. H., *Statistical Mechanics*, 2nd ed. p. 402, Cambridge Univ. Press (1936).
16. See for instance HERRING, C. and NICHOLS, M. H., *Rev. Mod. Phys.* **21**, 245 (1949).
17. NOTTINGHAM, W. B., *Phys. Rev.* **49**, 78 (1939). W.B.N., pp. 23, 104.
18. HUTSON, A. R., *Phys. Rev.* **98**, 889 (1955).
19. HERRING, C. and NICHOLS, M. H., *Rev. Mod. Phys.* **21**, 224 (1949).
20. SMITH, G. F., *Phys. Rev.* **100**, 1115 (1955).
21. EPSTEIN, P. S., *Verh. Dtsch. Phys. Ges.* **21**, 85 (1919).
22. FRY, T. C., *Phys. Rev.* **17**, 441 (1921); *ibid.* **22**, 445 (1923).
23. LANGMUIR, I., *Phys. Rev.* **21**, 419 (1923).
24. KLEYNEN, P. H. J. A., *Philips Res. Rep.* **1**, 81 (1946).
25. RITTNER, E. S., *J. Appl. Phys.* **31**, 1065 (1960).
26. CHILD, C. D., *Phys. Rev.* **32**, 492 (1911).
27. FERRIS, W. R., *R.C.A. Rev.* **10**, 134 (1949).
    W.B.N., p. 34.
28. SEIFERT, R. L. E. and PHIPPS, T. E., *Phys. Rev.* **53**, 493 (1938); *ibid.* **56**, 652 (1939).
29. MOTT-SMITH, H. M., *Phys. Rev.* **56**, 668 (1939); GUTH, E. and MULLIN, C. J., *Phys. Rev.* **59**, 575 (1941); GUTH, E. and MULLIN, C. J., *ibid.* **61**, 339 (1942); BELFORD, G. G., KUPPERMANN, A. and PHIPPS, T. E., *Phys. Rev.* **128**, 524 (1962).
30. LANGMUIR, I. and BLODGETT, K. B., *Phys. Rev.* **22**, 347 (1923); PAGE, L. and ADAMS, N. I., *ibid.* **68**, 126 (1945); PAGE, L. and ADAMS, N. I., *ibid.* **76**, 381 (1949); W.B.N., p. 67.

* In the references W.B.N. refers to W. B. Nottingham's publication mentioned in Literature.

30a. BECKER, J. A., *Rev. Mod. Phys.* **7**, 95 (1935).
31. SCHOTTKY, W., *Ann. Phys.* **57**, 541 (1918).
32. JOHNSON, J. B., *Phys. Rev.* **32**, 97 (1928).
33. VAN DER ZIEL, A., Low-frequency noise in vacuum tubes (flicker effect) in *Noise in Electron Devices* (Edited by L. D. SMULLIN and H. A. HAUS), Chapman and Hall, London (1959).
34. SOMMER, H., THOMAS, H. A. and HIPPLE, J. A., *Phys. Rev.* **82**, 697 (1951).
35. SHELTON, H., *Phys. Rev.* **107**, 1553 (1957).
36. GREENBURG, J., *Phys. Rev.* **112**, 1898 (1958).
37. HOBSON, J. P., *Can. J. Phys.* **34**, 1089 (1956).
38. W.B.N., p. 107.
39. NICHOLS, M. H., *Phys. Rev.* **57**, 297 (1940).
40. SMITH, G. F., *Phys. Rev.* **94**, 295 (1954).
41. W.B.N., p. 10.
42. HENSLEY, E. B., *J. Appl. Phys.* **32**, 301 (1961).
43. SCHOTTKY, W., *Ann. Phys.* **44**, 1011 (1914); W.B.N., p. 67; HEINZE, W. and HASS, W., *Z. Techn. Phys.* **19**, 166 (1938).
43a. SCHENK, D., *Ann. Phys.* **23**, 240 (1935).
44. POPOV, B. N. and DRUZHININ, A. V., *Radiotekh. i Elektron.* **3** (8), 1084 (1958); *Radio Eng. and Electronics* (U.S.S.R.) (English translation) **3** (8), 160 (1958).
44a. SANDOR, A., *Adv. in Electron Tube Techn.*, p. 77, Pergamon Press, 1961; *J. Electron. and Control* **13**, 401 (1962).
45. LINFORD, L. B., *Rev. Mod. Phys.* **5**, 47 (1933).
46. BULYGINSKII, D. G., and DOBRETSOV, L. N., *Zh. tek. h Fiz.* **26**, 1141 (1956); *Soviet Phys. Techn. Phys.* **1**, 1115 (1956).
47. JANSEN, C. G. J., VENEMA, A. and WEEKERS, TH. H., to be published in *J. Appl. Phys.*, April (1966).
47a. STANIER, B. J. and MEE, C. H. B., *J. Electron. and Control* **16**, 545 (1964).
48. MORGULIS, N. D., *J. Exp. Theoret. Phys.* (U.S.S.R.) **16**, 959 (1946); LEHOVEC, K., *Phys. Rev.* **96**, 921 (1954); TOLPYGO, K. B., *Radiotekh. i Elektron.* **3** (8), 980 (1958); *Radio Eng. and Electronics* (U.S.S.R.) (English translation) **3** (8), 2 (1958).
49. LEVITIN, S. M., *Zh. tekh. Fiz.* (U.S.S.R.) **23**, 1700 (1953); DYKMAN, I. M. and TOMCHUK, P. M., *Fiz. Tverdogo Tela* **2**, 2228 (1960); *Soviet Phys. Solid St.* **2**, 1988 (1961).
50. KANE, E. O., Technical Report 3, Contr. no. Non r-401 (08), Department of Physics, Cornell Univ., Dec. 31 (1954).
51. HEINZE, W. and WAGENER, S., *Z. Physik* **110**, 164 (1938); HUBER, H., Thesis, Berlin University, 1941.
52. VINK, H. J., Thesis, Leiden, 1948; LOOSJES, R. and VINK, H. J., *Philips Res. Rep.* **4**, 449 (1949); METSON, G. H., *Proc. I.E.E.*, part C, monograph 221 R (1957).
53. EISENSTEIN, A. S., Oxide-coated cathodes in *Advances in Electronics*, vol. 1, p. 15, 1948.
54. HANNAY, N. B., MACNAIR, D. and WHITE, A. H., *J. Appl. Phys.* **20**, 669 (1949).
55. RUDOLPH, J., PAULISCH, A., *Tech. Wiss. Abh. Osram Ges.* **7**, 103 (1958); PAULISCH, A., *Halbleiter und Phosphore* 1956 Coll. Vieweg 1958, p. 386.
56. EISENSTEIN, A., *J. Appl. Phys.* **20**, 776 (1949).
57. LOOSJES, R. and VINK, H. J., *Philips Res. Rep.* **2**, 190 (1947).
58. COPPOLA, P. P., *Rev. Sci. Instr.* **31**, 137 (1960); AFFLECK, J. H., *Electronics* **33** (16), 80 (1960).

59. BULYGINSKII, D. G., and SIBIR, E. E., *Fiz. Tverdogo Tela* **1**, 467; *Soviet Phys. Solid St.* **1**, 421 (1959).
60. BULYGINSKII, D. G. and DOBRETSOV, L. N., *Zh. tekh. Fiz.* **26**, 977 (1956); *Soviet Phys. Tech. Phys.* **1**, 957 (1956).
61. JANSEN, C. G. J., VENEMA, A. and WEEKERS, TH. A. In press.
62. PFETSCHER, O. and VEITH, W., *Le Vide*, no. 52–53, 181 (1954).
63. W.B.N., p. 45.
64. HUNG, C. S., *J. Appl. Phys.* **21**, 37 (1950).
65. Standard method of test for relative thermionic emissive properties of materials used in electron tubes, A.S.T.M. designation F270-56, American Society for Testing Materials, Philadelphia.
66. HERMANN, G. and WAGENER, S., *The Oxide-Coated Cathode*, vol. 1, p. 90, Chapman and Hall, London (1951).
67. HORSFALL, J. P., private communication.
68. RAUDORF, W., *Wireless Engineer* **26**, 331 (1949).
69. WAYMOUTH, J. F., *J. Appl. Phys.* **22**, 80 (1951).
70. TAMAYA, J., *Rev. Sci. Instr.* **31**, 696 (1960).
71. FROST, H. B., *I.R.E. Trans El Div.* ED6-7, 315 (1959).
72. A.S.T.M. standards on electron-tube materials, Dec. 1957, American Society for Testing Materials, Philadelphia.
73. HANNAM, H. J. and VAN DER ZIEL, A., *J. Appl. Phys.* **29**, 1702 (1958).
74. DAHLKE, W. and DLOUHY, F., *Proc. I.R.E.* **46**, 1639 (1958).
75. HAMAKER, H. C., BRUINING, H. and ATEN, A. H. W., *Philips Res. Rep.* **2**, 171 (1947).
76. HIGGINSON, G. S., *Br. J. Appl. Phys.* **8**, 148 (1957); SURPLICE, N. A., *Br. J. Appl. Phys.* **10**, 359 (1959).
77. Specification for nickel alloy cathode sleeves for electronic devices, A.S.T.M. Designation F239-57 T, American Society for Testing Materials, Philadelphia.
78. WHITE, A. H., *J. Appl. Phys.* **20**, 856 (1949).
79. RITTNER, E. S., *Philips Res. Rep.* **8**, 184 (1953).
80. PETERSON, R. W., ANDERSON, D. E. and SHEPHERD, W. G., *J. Appl. Phys.* **28**, 22 (1957).
81. ALLISON, H. W. and MOORE, G. E., *J. Appl. Phys.* **29**, 842 (1958).
82. KERN, H. E., *Bell Lab. Rec.* **38**, 451 (1960).
83. MIZUNO, H., *J. Phys. Soc. Japan* **12**, 1315 (1957).
84. MOORE, G. E. and ALLISON, H. W., *J. Appl. Phys.* **27**, 1316 (1956).
85. BENJAMIN, M. and ROOKSBY, H. P., *Phil. Mag.* **15**, 810 (1933); *ibid.* **16**, 519 (1933); HUBER, H., Thesis, Berlin University, 1941.
86. WRIGHT, D. A., *Le Vide* no. 51, 58 (1954).
87. TERADA, J., *J. Phys. Soc. Japan* **19**, 555 (1955).
88. HUBER, H. and FREYTAG, J. P., *Le Vide* **15**, 234 (1960).
89. VARADI, P. F., DOOLITTLE, H. D. and ETTRE, K., *Advances in Electron Tube Techniques*, Proc. 5th U.S. National Conf., p. 114, Pergamon Press, 1961.
90. KOVTUNENKO, P. V. and ISAREV, B. M., *Radiotekh. i Elektron.* **4**, 866 (1959); *Radio Eng. and Electronics* (U.S.S.R.) (English translation) **4** (5), 190 (1959).
91. SHEPHERD, A. A., *Nature* **170**, 839 (1952).
92. SURPLICE, N. A., *Br. J. Appl. Phys.* **11**, 430 (1960).
93. METSON, G. H., *Vacuum* **1**, 283 (1951).
94. METSON, G. H. and MACARTNEY, E., *Proc. I.E.E.*, part C, monograph 357 E, Febr. 1960.

95. MacNair, D., Report XXI Ann. Conf. Physical Electronics M.I.T. 1961, p. 1.
96. Eisenstein, A., *J. Appl. Phys.* **17**, 434 (1946).
97. Rooksby, H. P., *Br. J. Appl. Phys.* **6**, 272 (1955).
98. Gärtner, H., *Phil. Mag.* **19**, 82 (1935); Darbyshire, J. A., *Proc. Phys. Soc.* **50**, 635 (1938); Huber, H. and Wagener, S., *Z. Techn. Physik* **23**, 1 (1942).
99. Harwood, M. G. and Fry, N., *Br. J. Appl. Phys.* **6**, 62 (1955).
100. Detels, F., *Jb d. drahtl. Telegr. a Teleph.* **30**, 10, 52 (1927); Kniepkamp, H. and Nebel, C., *Wiss. Veröff. Siemens-Konzern* **11**, II, 75 (1932).
101. Veenemans, C. F., *Nederl. Tijdschr. Natuurk.* **10**, 1 (1943).
102. Sproull, R. L., *Phys. Rev.* **67**, 166 (1945); Matheson, R. M. and Nergaard, L. S., *J. Appl. Phys.* **23**, 869 (1952); Frost, H. B., Thesis M.I.T. (1954); Haas, G. A., *J. Appl. Phys.* **28**, 1486 (1957).
103. Ostroukov, A. A., *Fiz. Tverdogo Tela* **3**, 3 (1961); *Soviet Phys. Solid St.* **3**, 1, 3 (1961).
104. Krusemeyer, H. J. and Pursley, M. V., *J. Appl. Phys.* **27**, 1537 (1956).
105. Nergaard, L. S., *R.C.A. Rev.* **13**, 464 (1952).
106. Ostroukov, A. A., *Radiotekh. i Elektron.* **6**, 2063 (1961); *Radio Eng. and Electronics* (U.S.S.R.) (English translation) **6**, 1850 (1961).
106a. Campbell, D. A. and Shepherd, W. G., *J. Appl. Phys.* **34**, 2473 (1963).
107. Loosjes, R. and Vink, H. J., *Philips Res. Rep.* **2**, 190 (1947); Loosjes, R. and Vink, H. J., *Le Vide* **5**, 731 (1950); Loosjes, R., Vink, H. J. and Jansen, C. G. J., *J. Appl. Phys.* **21**, 350 (1950); Jansen, C. G. J., Loosjes, R. and Compaan, K., *Le Vide*, no. 52–53, 129 (1954).
108. Loosjes, R. and Vink, H. J., *Philips Res. Rep.* **4**, 449 (1949).
109. Forman, R., *Phys. Rev.* **96**, 1479 (1954); Yabumoto, T., *J. Phys. Soc. Japan* **14**, 134 (1959).
110. Higginson, G. S., *Br. J. Appl. Phys.* **9**, 106 (1958); Metson, G. H. and Macartney, E., *Proc. I.E.E.*, part C, monograph 347 E (Oct. 1959).
111. Eaglesfield, C. C., *Elect. Comm.* **28**, 95 (1951).
112. Waymouth, J. F., *J. Appl. Phys.* **22**, 80 (1951).
113. Metson, G. H., Wagener, S., Holmes, M. F. and Child, M. R., *Proc. I.E.E.* **99**, III, 69 (1952).
114. Frost, H. B., *Bell Lab. Rec.* **39**, 18 (1961).
115. Heinze, W. and Wagener, S., *Z. Techn. Phys.* **20**, 16 (1939).
116. Jansen, C. G. J. and Loosjes, R., *Philips Res. Rep.* **8**, 81 (1953).
117. Lemmens, H. J. and Zalm, P., *Philips Techn. Rev.* **23**, 19 (1961).
118. Imai, T., *J. Phys. Soc. Japan* **12**, 831 (1957).
119. Hermann, G. and Krieg, O., *Ann. Phys.* **4**, 441 (1949); Wagener, S., *Proc. Phys. Soc.* B**67**, 369 (1954); Zykov, G. A. and Nakhodkin, N. G., *Radiotekh i Elektron.* **3**, no. 8, 1031 (1958); *Radio Eng. and Electronics*. U.S.S.R.) (English translation) **3** (2), no. 8, 79 (1958).
120. See e.g. Garbe, S. in Supplemento al Nuovo Cimento **1**, 810 (1963).
121. Jacobs, H. and Wolk, B., *Proc. I.R.E.* **37**, 1247 (1949).
122. Garbe, S., private communication.
123. Rittner, E. S., *Philips Res. Rep.* **8**, 227 (1953).
123a. Fränz, J., *Telefunken Röhre* **41**, 167 (1962).
124. Espe, W., *Wiss. Veröff. Siemens-Konzern* **5**, III, 29, 46 (1927); Rothe, H., *Z. Physik* **36**, 737 (1926); Detels, F., *Jahrb. d. Drahtl. Telegr. und Teleph.* **30**, 10, 52 (1927).
125. Koller, L. R., *Phys. Rev.* **25**, 671 (1925).

126. BECKER, J. A., *Phys. Rev.* **34**, 1323 (1929); BECKER, J. A. and SEARS, R. W., *Phys. Rev.* **38**, 2193 (1931).
127. BOER, J. H. DE, *Electron Emission and Adsorption Phenomena*, Cambridge University Press, 1935; *Elektronen emission und Adsorptionserscheinungen*, Barth, Leipzig, 1937.
128. W.B.N., p. 128.
129. PLUMLEE, R. H., *J. Appl. Phys.* **27**, 659 (1956).
130. WOOTEN, L. A., MOORE, G. E. and GULDNER, W. G., *J. Appl. Phys.* **26**, 937 (1955).
131. MOORE, G. E., WOOTEN, L. A. and MORRISON, J., *J. Appl. Phys.* **26**, 943 (1955).
132. NERGAARD, L. S., *Halbleiterprobleme*, vol. 3, p. 154, Vieweg, 1956.
132a. OKUMURA, K. and HENSLEY, E. B., *J. Appl. Phys.* **34**, 519 (1963).
133. NISHIBORI, E. and KAWAMURA, H., *Proc. Phys. Math. Soc. Japan*, **22**, 378 (1940).
134. PLUMLEE, R. H., *R.C.A. Rev.* **17**, 231 (1956).
135. WOOTEN, L. A., RUEHLE, A. E. and MOORE, G. E., *J. Appl. Phys.* **26**, 44 (1955).
136. ZALM, P., Rep. 21st Ann. Conf. Phys. El. M.I.T., 1961.
137. KRUSEMEYER, H. J. and THOMAS, D. G., *J. Phys. and Chem. Solids* **4**, 78 (1958).
138. TYLER, W. W. and SPROULL, R. L., *Phys. Rev.* **83**, 548 (1950); KANE, E. O., *J. Appl. Phys.* **22**, 1214 (1954); SPROULL, R. L., BEVER, R. S. and LIBOWITZ, G., *Phys. Rev.* **92**, 77 (1953); TIMMER, C., *J. Appl. Phys.* **28**, 495 (1957).
139. MÜLLER, E. W., *J. Appl. Phys.* **26**, 732 (1955).
140. LANGMUIR, I., *Phys. Rev.* **22**, 357 (1923).
141. JENKINS, R. O. and TRODDEN, W. G., *J. Electronics* **12**, 1 (1962).
142. DANFORTH, W. E. and GOLDWATER, D. L., *J. Appl. Phys.* **31**, 1715 (1960).
143. SCHNEIDER, P., *J. Chem. Phys.* **28**, 675 (1958).
144. SEIFFARTH, W., *Siemens Z.*, **35**, 670 (1961).
145. JENKINS, R. O. and TRODDEN, W. G., *Br. J. Appl. Phys.* **10**, 10 (1959).
146. DUSHMAN, S. and EWALD, J. W., *Phys. Rev.* **29**, 857 (1927).
147. LANGMUIR, I. and KINGDON, K. H., *Science* **57**, 58 (1923); *Phys. Rev.* **21**, 380 (1923); *Phys. Rev.* **23**, 112 (1924).
148. TAYLOR, J. B. and LANGMUIR, I., *Phys. Rev.* **44**, 432 (1933).
149. HATSOPOULOS, G. N. and KAYE, J., *Proc. I.R.E.* **46**, 1574 (1958).
150. HERNQUIST, K. G., KANEFSKY and NORMAN, *R.C.A. Rev.* **19**, 244 (1958); WILSON, V. C., *J. Appl. Phys.* **30**, 475 (1959); WEBSTER, H. F., *J. Appl. Phys.* **30**, 488 (1959); HOUSTON, J. M., *J. Appl. Phys.* **30**, 481 (1959).
151. NERGAARD, L. S., *R.C.A. Rev.* **18**, 186 (1958).
152. LEMMENS, H. J., JANSEN, M. J. and LOOSJES, R., *Philips Techn. Rev.* **11**, 341 (1950).
153. KATZ, H., *Siemens and Halske A.G. Research Bulletin* II, 123 (1951); *J. Appl. Phys.* **24**, 597 (1953).
154. LEVI, R., *J. Appl. Phys.* **24**, 233 (1953); *ibid.* **26**, 639 (1955).
155. COPPOLA, P. P. and HUGHES, R. C., *Proc. I.R.E.* **44**, 351 (1956); *Philips Techn. Rev.* **19**, 179 (1957/58).
156. HASKER, J., private communication.
157. RITTNER, E. S., AHLERT, R. H. and RUTLEDGE, W. C., *J. Appl. Phys.* **28**, 156 (1957); RUTLEDGE, W. C. and RITTNER, E. S., *J. Appl. Phys.* **28**, 167 (1957).

158. BROEK, C. A. M. VAN DEN and VENEMA, A., unpublished work.
158a. DRUZHININ, A. V., *Iz. Akad. Nauk SSSR Ser. Fiz* **25**, no. 6, 730 (1961).
159. SCHAEFFER, D. L. and WHITE, J. E., *J. Appl. Phys.* **23**, 669 (1952).
160. MORGULIS, N. D., *Zh. Tech. Fiz.* (*U.S.S.R.*) **26**, 536 (1956); *Soviet Phys. Techn. Phys.* **1**, 517 (1956).
161. MELNIKOV, A. I., MOROSOV, A. V., SOBOLEVSKAYA, R. B. and SHULMAN, A. R., *Fiz Tverdogo Tela* **2**, 704 (1960); *Sov. Phys. Solid St.* **2**, 650 (1960/61).
BONDARENKO, B. V., OSTAPCHENKO, E. P. and TSAREV, B. M., *Radiotekh. i Elektron.* **5**, 1246 (1960); *Radio Eng. and Electron.* (U.S.S.R.) (English translation) **5**, (8), 77 (1960).
KAPITSA, M. L., MELNIKOV, A. I., MOROSOV, A. V., POPOV, B. N., SOBOLEVSKAYA, R. B., TSAREV, B. M. and SHULMAN, A. R., *Radiotekh. i Elektron.* **3**, 1010 (1958); *Radio Eng. and Electron.* (U.S.S.R.) (English translation) **3**, no. 8, 47 (1958).
162. JANSEN, C. G. J., private communication.
163. BRODIE, I. and JENKINS, R. O., *J. Electronics* **2**, 33 (1956/57).
164. ZINGERMAN, YA. P. and MOROZOVSKII, V. A., *Radiotekh. i Elektron.* **3**, 1017 (1958); *Radio Eng. and Electron.* (U.S.S.R.) (English translation) **3**, no. 8, 56 (1958).
165. PTUSHINSKII, YI. G. and CHUIKOV, B. A., *Radiotekh. i Elektron.* **2**, 1530 (1957); *Radio Eng. and Electron.* (U.S.S.R.) (English translation) **2**, no. 12, 90 (1957).
166. LEVI, R., *J. Appl. Phys.* **26**, 639 (1955).
167. LEVI, R., *Philips Techn. Rev.* **17**, 97 (1955).
168. LEVI, R., *Le Vide* **54**, 284 (1954).
169. RITTNER, E. S., RUTLEDGE, W. C. and AHLERT, R. H., *J. Appl. Phys.* **28**, 1468 (1957).
169a. DRUZHININ, A. V., *Radiotekh. i Elektron.* **7**, 1547 (1962); *Radio Eng. and Electron.* (U.S.S.R.) (English translation) **7**, 1446 (1962).
170. BRODIE, J. and JENKINS, R. O., *Proc. Phys. Soc.* **B69**, 1343 (1956).
170a. BECK, A. H. W. and AHMED, H., *J. Electron. and Control* **14**, 623 (1963); *J. Appl. Phys.* **34**, 997 (1963).
171. HUBER, H. and FREYTAG, J., *Le Vide* **54**, 310 (1954).
172. MELNIKOV, A. I., MOROZOV, A. V., POPOV, B. N. and MAKLALOV, A. A., *Bull. Acad. Sci. U.S.S.R.* **22** (5), 610 (1958).
173. JENKINS, R. O. and TRODDEN, W. G., *J. Electron. and Control* **7**, 393 (1959).
174. MACNAIR, D., LYNCH, R. T. and HANNAY, N. B., *J. Appl. Phys.* **24**, 1335 (1953).
175. BECK, A. H. W., BRISBANE, A. D., CUTTING, A. B. and KING, G., *Le Vide* **54**, 302 (1954).
176. BALAS, W., DEMPSEY, J. and REXER, E. F., *J. Appl. Phys.* **26**, 1163 (1955).
177. FANE, R. W., *Br. J. Appl. Phys.* **9**, 149 (1958); *ibid.* **11**, 513 (1960).
178. See for instance: MESNARD, G. and UZAN, R., *Le Vide* **50**, 1492 (1954); UZAN, R., *Le Vide* **54**, 290 (1954); THIEN-CHI N. and DUSSAUSSOY, P., *Le Vide* **54**, 297 (1954); RICHARDSON, J. F., *Br. J. Appl. Phys.* **8**, 361 (1957); ARSHANSKAIA, N. G., PARKHOMENKA, V. S. and RASKINA, N. I., *Radiotekh. i Elektron.* **3**, 1058 (1958); *Radio Eng. and Electron.* (U.S.S.R.) (English translation) **3** (8), 118 (1958); BOONE, E. M., *Proc. I.R.E.* **47**, 1650 (1959).
178a. JENKINS, R. O. and TRODDEN, W. G., *J. Electron. and Control* **10**, 81 (1961).
179. LAFFERTY, J. M., *J. Appl. Phys.* **22**, 299 (1951).
180. KUDINTSEV, G. A. and TSAREV, B. M., *Radiotekh. i Elektron.* **3**, 428 (1958); *Radio Eng. and Electron.* (U.S.S.R.) (English translation) **3** (3), 182 (1958).

181. DANFORTH, W. E., *Advances in Electronics* **5**, 169 (1953); GOLDWATER, D. L., *J. Franklin Inst.* **261**, 1 (1956).
182. LOWRY, E. F., MAYER, E. L. and HOMER, H. H., *Sylvania Techn.* **3**,1 (1950).
183. See for instance: PENGELLY, A. E. and WRIGHT, D. A., *Br. J. Appl. Phys.* **5**, 391 (1954); CAYLESS, M. A., *Br. J. Appl. Phys.* **8**, 331 (1957).
184. BRUNN, K. R., Technical Rep. 3, Contr. no. Nonr 1834/08/Project no. 373–162. Scientific Rep. 10 Control no. AF 19(604)–524, Electrical Engineering Res. Lab., University of Illinois (Apr. 15, 1957).
185. BABCOCK, M. L., HOLSHOUSER, D. F. and VON FOERSTER, H. M., *Phys. Rev.* **91**, 755 (1953).
186. POOLE, K. M., *J. Appl. Phys.* **26**, 1176 (1955).
187. FINCKE, G. C., *Advances in Electron Tube Techniques, Proc.* 5th U.S. National Conference 1960, p. 120, Pergamon Press, 1961.
188. NAMAKURA, S. and SUGATA, E., *Techn. Rep. Osaka Univ.* **8**, 261 (1958).
189. EICHENBAUM, A. L., *R.C.A. Rev.* **23**, 230 (1962).
190. BAKER, B. O., *Br. J. Appl. Phys.* **4**, 311 (1953).
191. SHISHKIN, YU. G. and SOKOL'SKAYA, I. L., *Radiotekh. i Elektron.* **5**, 1218 (1960); *Radio Eng. and Electron.* (U.S.S.R.) (English translation) **5** (8), 32 (1960).
192. ESPERSEN, G. A. and ROGERS, J. W., *Trans. I.R.E.* ED**3**, 100 (1956); *Philips Techn. Rev.* **20**, 269 (1958/59).
193. CHAMPION, J. A., *Br. J. Appl. Phys.* **9**, 491 (1958).
194. RITTNER, E. S. and LEVI, R., *J. Appl. Phys.* **33**, 2336 (1962).
195. CHAMPION, J. A., *Br. J. Appl. Phys.* **10**, 71 (1959).
196. See for example: KUBASCHEWSKI, O. and EVANS, E. L., *Metallurgical Thermochemistry*, Pergamon Press, London, 1956.
197. CARSLAW, H. S. and JAEGER, J. C., *Conduction of Heat in Solids*, Oxford University Press, 1959.

ACKNOWLEDGEMENTS

The preparation of the manuscript would have been impossible without the help of many colleagues. Much information collected by the author in several years' work on thermionic emission has been obtained in numerous discussions. The author is indebted to the researchers who contributed to his knowledge on this subject, but he cannot mention them all explicitly. Several exceptions must be made, however. His sincere thanks go to Mr. C. G. J. Jansen and Dr. P. Zalm with whom the author co-operated very closely during several years and who gave valuable criticism to the manuscript, to Mr. C. H. R. Gentry who contributed not only with valuable technical information, but also supplied the assistance indispensable for the linguistic problems which arose in writing the manuscript, and to Dr. H. Bienfait for his continuous general interest. The author is further indebted to Mr. J. v. Laar, Dr. H. J. G. Meijer and Dr. P. G. van Zanten for valuable suggestions. Thanks are due to Mr. Th. A. Weekers for his assistance in the preparation of the figures.

~~[illegible]~~

Rhenium polyhedag.

$\varrho = 4,92$ $A = 360$

5 P. 221 105
223

A p2 202

A_T p 221

A_R p 223

is $A_R = A_T$

A^* p 224